Real-time implementation for Grid Forming Control of Type-4 Wind turbine to mitigate voltage and frequency instabilities in high renewable penetration

MSc Thesis-European Wind Energy Master

Shubham Sethi

TU Delft Delft University of Technology

NTNU Norwegian University of Science and Technology

REAL-TIME IMPLEMENTATION FOR GRID FORMING CONTROL OF TYPE-4 WIND TURBINE TO MITIGATE VOLTAGE AND FREQUENCY INSTABILITIES IN HIGH RENEWABLE PENETRATION

MSC THESIS - EUROPEAN WIND ENERGY MASTER

by

Shubham Sethi

in partial fulfillment of the requirements for the degree of

Master of Science
in Electrical Engineering

at the Delft University of Technology, & the Norwegian Univeristy of Science and Techonology
to be defended publicly on Friday August 30, 2019 at 09:00 AM.

Supervisor:	Dr. ir. Jose Rueda Torres,	TU delft
Thesis committee:	Prof. ir. Mart Van der Meijden,	TU Delft
	Dr. ir. Jose Rueda Torres,	TU delft
	Prof. dr. Irina Oleinikova,	NTNU
	Dr. ir. Thiago Batistia Soeiro,	TU delft

This thesis is confidential and cannot be made public until August 2021.

An electronic version of this thesis is available at http://repository.tudelft.nl/ and https://dataverse.no/dataverse/ntnu.

TU Delft Delft University of Technology

NTNU Norwegian University of Science and Technology

ABSTRACT

The increasing penetration of PE converter interfaced generation units in electrical power systems have given rise to many challenges in the power system operation. Two of the most important challenges are the voltage control and frequency control in the absence of conventional generation units. Furthermore, the PE converters can interact with the power system elements causing the power system to become unstable.

In this thesis, the effect of the wind turbines modified with grid-forming capability is analysed on the transmission networks as well as on the Offshore VSC-HVDC converter station. The dynamic response of the WTs is studied considering the high share of the power electronic converter interfaced generation.

It is shown when the wind turbine power converters are equipped with the implemented control strategy, they can provide voltage and frequency stability to the system and further upgrades can be added to enhance the system response. The control strategy implemented employs the direct voltage control which is upgraded with voltage dependent active current control for improving the transient voltage recovery of the system. The inertial response based on modifying the machine side converter is also added which extracts kinetic energy from the wind turbine rotor that improves the frequency response of the system following load change.

In the end, an offshore wind farm network is modeled which includes the offshore wind park connected to an offshore MMC HVDC converter station for delivering bulk power to the DC source connected via the HVDC cable. The developed wind turbine model is employed for integration in the offshore wind farms which has shown to eliminate the transient overvoltages occurring in the offshore network during the blocking of the HVDC converter.

ACKNOWLEDGEMENT

I feel honoured and grateful to have met and worked with Dr. José Rueda throughout all this time. He has been an inspiration for me to get things successfully done and to keep me thrilled in the Scientific Research Path. His guidance, support and feedback was invaluable for the realisation of this Project. I also want to thank Prof. ir. Mart Van der Meijden for his confidence, supervision and guidance during the scheduled meetings that were part of this Work, and Dr. Thiago Batistia Soeiro for being part of my Thesis Committee and providing me very interesting insights on the operation of MMC during our short meeting. I would also like to thank Prof. dr. Irina Oleinikova who agreed to supervise me during my thesis, despite me being located in a different country. I'm grateful for the flexibility she has offered me during the development of this work alongside helping me fulfill all the requirements from my second degree awarding university, NTNU.

I want to highlight and thank the major share of knowledge of Dr. Abdul Korai, from the Universität Duisburg-Essen, whose work served as in inspiration for development of this work . Further, all my gratitude and acknowledgment to Dr. Zameer Ahmad for his bright counselling and feedback, and to MSc. Arcadio Perilla, Dr. Lian Liu, from TU Delft IEPG Group, for their mastery, advice and teaching.

And of-course, I am forever grateful to my parents who have also supported me and believed in me. I could never have come here without your unconditional love and support. I am also grateful to DeeJayy, my sisters and my cousins who always encouraged me to push my boundaries.

Finally, I feel very happy to have met during these two years all the brilliant people who were my classmates and who are now my friends.

CONTENTS

LIST OF FIGURES

LIST OF TABLES

ABBREVIATIONS

DC . . . . . Direct Current
DSO . . . . . Distribution System Operator
DVC . . . . . Direct Voltage Control
EMT . . . . . Electromagnetic Transients
ENTSOE . . . . . European Network of Transmission System Operators for Electricity
FRT . . . . . Fault-Ride Through
GSC . . . . . Grid-Side Converter Station
HV . . . . . High-Voltage
HVDC . . . . . High-Voltage Direct-Current
Hz . . . . . Herts
IDE . . . . . Point of Common Coupling
LCC . . . . . Line-Commutated Converters
LV . . . . . Low-Voltage
MPPT . . . . . Maximum Power Point Tracker
ms . . . . . mili-second
Mvar . . . . . Reactive Mega-Volt-Ampère
MW . . . . . Mega-Watts
OWF . . . . . Offshore Wind Farms
OWP . . . . . Offshore Wind Parks
p.u. . . . . . Per Unit
PEC . . . . . Power Electronic Converters
PEI . . . . . Power Electronic Interfaces
PI . . . . . Proportional-Integral Control
PLL . . . . . Phase-Locked Loop
PMSG . . . . . Permanent-Magnet Synchronous Generator
PWM . . . . . Pulse-Width Modulation
RES . . . . . Renewable Energy Sources
RTDS . . . . . Real-Time Digital System
SCR . . . . . Short-Circuit Ratio
SDC . . . . . Synchronous Damping Control
SVM . . . . . Space-Vector Modulation
VDACC . . . . . Voltage-Dependent Active Current Control
VDAPR . . . . . Voltage-Dependent Active Power Reduction

1

INTRODUCTION

Following the Paris agreement, global electrical energy production has begun to transition drastically towards renewable energy sources (RES) [21]. Most of these RES are interfaced with the grid through power electronics (PE) converters as represented in figure 1.1. Upon increasing the energy generation from RES, conventional power plants should be accordingly disconnected from the network. Since the conventional power plants are based on electrically excited synchronous generators (figure 1.2) which provide necessary inertia for maintaining the stability of the grid, disconnection of these generators introduces several technical challenges for reliable operation of the electrical power systems by TSOs.

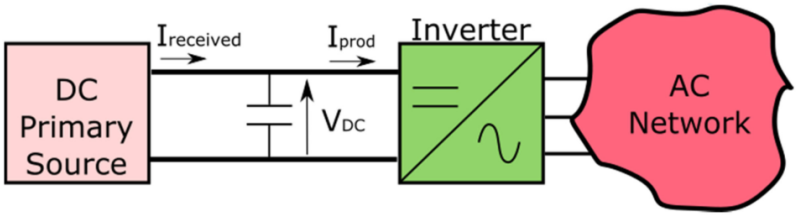

Figure 1.1: PE converter-interfaced renewable energy sources[32]

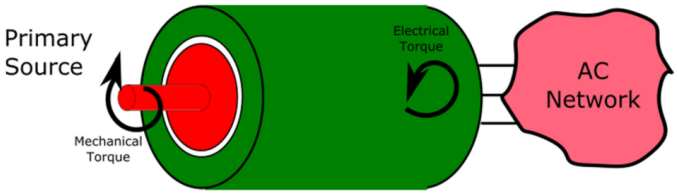

Figure 1.2: Traditional energy conversion systems [32]

The critical challenges under such scenarios are mainly related to the voltage and frequency control by PE converter-interfaced generation units in the absence of conventional generation units. A specific issue pertaining to the voltage instability include the short-term voltage incidents which can cause sustained low voltages in significant portions of the power system. The slow voltage recovery following the disturbances, or fast voltage collapse, can both lead to stalling of induction motor loads in the power system thereby creating a cascading effect which can eventually lead to a collapsed network. The decreasing inertia of the grid also leads to much faster dynamic behaviour of the network, requiring converter controllers to have a faster response time. Moreover, there is an inherent flaw in the proportional and integral (PI) based current control strategies of existing grid-connected converters. These PI controllers can lead to unforeseen interactions under high renewable penetration scenarios which can make the network unstable.

The restoration of the electrical grid by PE converter-based generation units is another major concern for the grid operators. There is enough experience for grid-restoration via conventional generation units; however, the restoration process using PE converter-based generation units is a new challenge as there isn't enough experience nor existing grid and control requirements. The currently applicable network connection rules are clearly not capable of coping with the new emerging challenges, although further revision is underway [46].

Moreover, the increasing distance from the land for the development of new and larger Offshore Wind Parks (OWP) also introduces complex challenges for the network operators. The transmission scheme employed for more significant distance is primarily HVDC rather than HVAC to minimize power loss. The typical connection scheme layout for an Offshore wind park is represented in figure 1.3. Traditionally in the HVDC OWP, only the offshore converter of the HVDC acts as the master grid-forming unit, providing voltage and frequency set-points for the Offshore wind parks to be connected, whereas the wind-turbine converters act in grid-feeding mode. As HVDC technology is still young, there might be scenarios which might be fatal for the operation of OWP if overlooked. One such phenomenon is the transient overvoltages in the offshore network that occur following the blocking of HVDC converters station. Detailed investigation of such a process accompanied by stringent grid codes for the operation of HVDC OWP, therefore, becomes necessary for ensuring the reliability of the offshore as well as the onshore network.

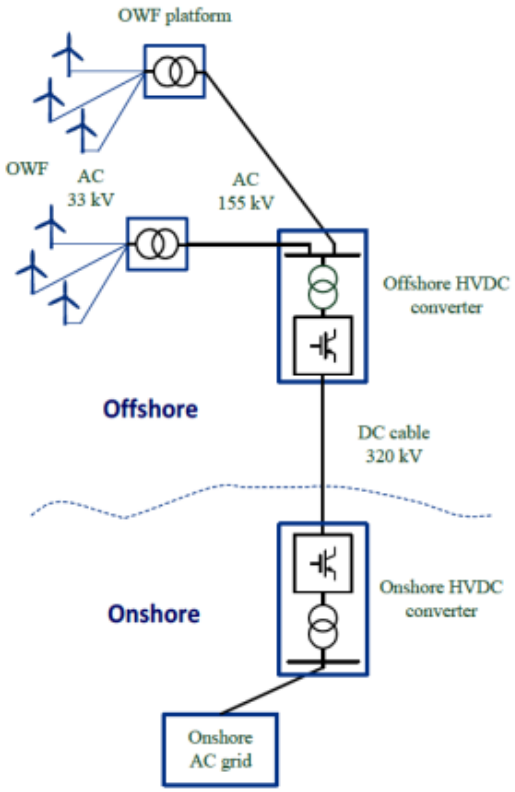

Figure 1.3: Traditional connection scheme of an Offshore Wind Park linked through HVDC to the onshore grid [39]

Full-inverter-interfaced systems are already operational in microgrids for low or medium voltage, however, few studies have been applied on transmission system applications[32]. It is to be expected that the PE converter-based generation currently deployed will influence the dynamic and transient behaviour of the transmission network in the following years (figure1.4). Therefore, proper solutions entailing new and innovative control strategies for PE converter-based generation units that can address such challenges, become highly significant if a conceivable future with 100% RES is to be ever realized. One can argue that

the battery storage, thermal storage and heat to power can be feasible solutions in the absence of conventional generation. However, the high investment costs, lower lifespan and low efficiency of storage devices compared to the control modifications make it economically infeasible to be implemented at an extensive scale in the power systems [85].

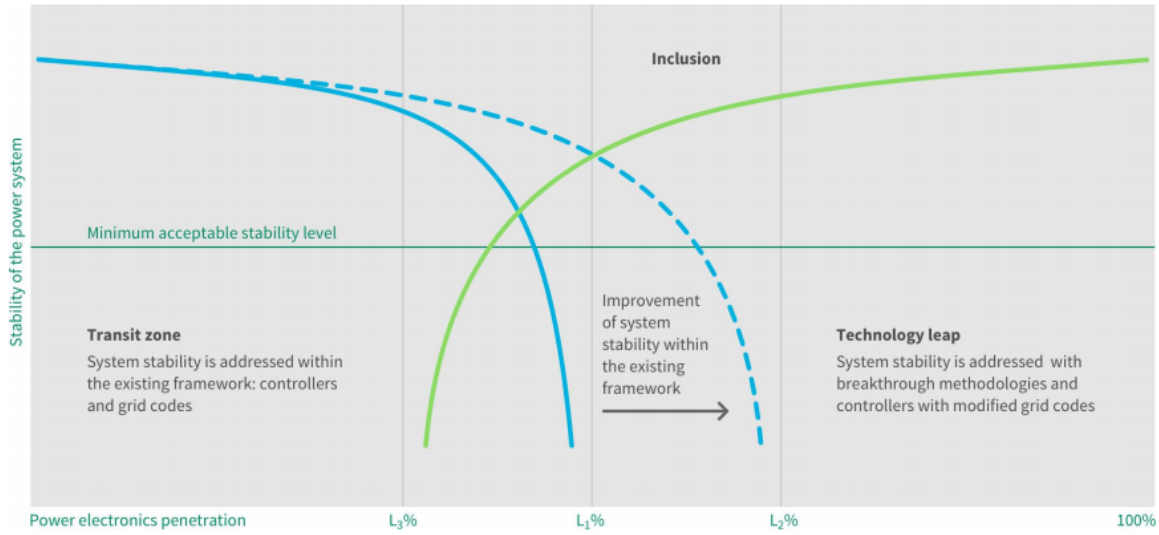

Figure 1.4: Migrate project approach for increasing PE converter-based generation [14]

In view of the challenges mentioned above, several applications need to be addressed by the PE converters, which include enhanced grid forming control accompanied by grid restoration and prevention of adverse controller interactions. The grid forming control should be capable of providing the voltage-var control, frequency stabilization around the nominal frequency and should operate in grid-connected as well as in islanded mode. It should also be capable of limiting the voltage rise following load shedding as well as provide short-term voltage instability mitigation. The new control scheme should be designed in such a way that it adapts automatically to the current depending on the grid conditions by trying to fulfil the main objectives of voltage and frequency control [37]. Therefore, the implementation of new control approach should exhibit superior performance in PE-converter dominated networks. Moreover, the wind-turbine control should be easily adaptable to the offshore wind farms to address the overvoltage phenomena following the converter blocking [39]. This thesis addresses these urgent issues that might be a roadblock towards the development of grids with extensive integration of PE converter-based generation. Several grid-forming control schemes have been extensively studied in many works of literature , but the majority of the knowledge for such control strategies is limited to microgrids. Despite there being several schemes which do not require PLL [33], the work under this thesis employs PLL for synchronization of converters with the grid.

1.1. SCOPE OF PROJECT AND RESEARCH QUESTIONS

Based on the problem definition, review of existing *grid-forming* control strategies, as well as the research and implementation gaps identified in the available literature, the scope of this work has been defined which is explored through the study of following main research questions.

- What are the required modifications in the default RSCAD type-4 wind turbine model to make it work as a grid-forming wind turbine?
- What modifications and additions are required to be done in the identified *grid-forming* control strategy to enable its operation in standalone mode, as well as improve its dynamic performance in the grid-connected mode?

- Can the implemented control strategy help in mitigating voltage and frequency instabilities in power networks having more than 50% share of wind energy (power electronic interfaced) generation?
- Can the implemented control scheme operate in islanded mode of Offshore Wind Farms while the HVDC converter station is blocked and simultaneously prevent overvoltages during the islanded operation?

1.2. OBJECTIVE OF THESIS

The overall objective of this thesis is to develop the detailed wind turbine model for provision of enhanced controls for large size (aggregated) wind power plants that ensures voltage and frequency stability in power system with high penetration level of power electronic converter-based generation units. To achieve this objective, the following specific tasks are pursued:

- Development and implementation of necessary modifications in the detailed type-4 Wind turbine model in the RSCAD library, to make it work as Grid-forming control in standalone operation as well as in grid connected mode.
- Transient voltage stability assessment of power systems with high share of wind energy generation and the impact of wind energy systems in voltage recovery following the fault.
- Identification and execution of the required modifications to further improve the voltage and frequency stability of the power system with high share of wind energy generation. Analysis of provision of frequency support by the inertial response of the wind energy utilizing the stored energy in wind turbine rotors.
- Development and analysis of existing MMC based VSC-HVDC systems in RSCAD for bulk power transfer from (aggregated) Offshore Wind Farms to the HVDC converter station and beyond.
- Analysis of the root cause behind the occurrence of transient overvoltages in the offshore grid after the blocking of the HVDC offshore converter and implementation of the enhanced wind turbine control to eliminate such occurrences.

1.3. SIMULATION TOOL USED

Real-time Digital Simulator (RTDS) is the extensive tool used for the development of this work, which is designed to conduct Electromanetic Transient Simulations (EMT). The simulator can work over a range of frequency from DC (0 Hz) to 3 kHz. The RSCAD software is used for simulating the power systems on RTDS.

1.3.1. RTDS HARDWARE

The RTDS hardware can simulate complex power systems with a typical time step of 20-50μs, and it also allows for small time-step range of 1-4 μs. TU delft has 2 NovaCor cards and others are with PB5 processor cards, with NovaCor being the most advanced processor card developed by RTDS so far.

1.3.2. RSCAD SOFTWARE

To extract maximum benefits out of the RTDS hardware RSCAD software was developed by RTDS technologies. The RSCAD software runs simulation based on two different files, both of which are required to generate desired results. The modelling is done in the "draft file" screen, while the developed model is analyzed for problems and results in the "runtime" screen. The RSCAD software library has almost all the tools which are used by power systems engineers and is further expanding. However, it is not as extensive as Matlab library, and hence it becomes crucial factor in determining the control that is implementable with the given library components.

There are several advantages of using RTDS over other EMT tools such as PSCAD or RMS tools like PowerFactory, which include:

- Because of RTDS being real-time, the simulation runs instantly rather than having to wait for long hours as experienced with PowerFactory and PSCAD.

- RTDS and RSCAD software allows for detailed modelling of the power electronic components. This is a crucial factor in designing control strategies as some strategies that perform exceptionally well with the RMS simulations of PowerFactory, might not give expected results in RSCAD, because PowerFactory models might disregard some system specific details which might occur in practical operation. Therefore, the implementation in RTDS allows for validating the control in real-world scenarios.
- Moreover, the development in RTDS can allow for Hardware-in-loop testing which becomes advantageous as a converter can be tested accurately for the practical-world scenarios without physically being connected to the power systems network.

1.4. OUTLINE OF THESIS

In this section a brief outline of all the chapters of this report is provided.

CHAPTER 1: INTRODUCTION

This chapter provides an overview of the project, detailing about the problems that arise with increasing the power-electronic interfaced generation in the power systems, as well as the urgency of such a project. A more thorough description of the project follows while the objectives of the thesis and the research questions are addressed. Finally, some description of the simulation tool used is provided.

CHAPTER 2: LITERATURE REVIEW

This chapter begins with a general overview of wind energy systems, followed with the specific themes that are necessary for addressing parts of problems encountered during the development of this project. The control strategies for the grid-integration of renewable energy is stressed upon, determining the necessity of grid-forming controls. Eventually, the research and implementation gaps are identified, followed up with the methodology used for addressing those research gaps and fulfilling thesis objective.

CHAPTER 3: ENHANCED GRID FORMING CONTROL

This chapter reviews the identified control strategy [51] [39] for implementation in RSCAD and its short-comings. A method for enabling its standalone operation is included which is based on the microgrid applications of BESS. Having implemented the identified control strategy with the proposed modifications, the controllers performance is investigated in standalone operation as well as its operation with an infinite grid.

CHAPTER 4: CONTROL CHALLENGES IN GRID CONNECTED MODE

This chapter extends the implemented controller in Chapter 3 in the 9-bus system to increase the generation by wind energy systems to upto 88%. Modifications for improving the transient voltage stability based on VDACC [82] [36] as well as frequency stability based on inertial response [55] [59] are implemented in the existing control structure to further enhance the performance of wind turbines.

CHAPTER 5: MMC HVDC BASED OFFSHORE WIND FARMS

In this chapter, a model is developed which allows for bulk transfer of power from the offshore wind farms to the MMC based VSC-HVDC converter station. The possible issues in modelling such a network are addressed. Following the development of the completely functional model, the specific issue of transient overvoltages during blocking of the VSC HVDC are addressed, which are mitigated using the control strategy implemented in Chapters 3 and 4.

CHAPTER 6: CONCLUSIONS AND FUTURE WORK

The most important conclusions obtained through this study are summarized in this chapter. The research questions of the project are answered with references to the corresponding chapters that contain more information relating to each research question. Moreover the research contributions to the IEPG group at TU Delft are listed along with challenged encountered during development of this work. Finally the prospects for extending this work for enabling 98-100% PE interfaced generation as well as Offshore Multi-terminal HVDC networks are reflected upon.

2

LITERATURE REVIEW

The primary reason why the *grid-forming* capability of the PE converter-interfaced RES needs to be developed is because of their predicted use in the upcoming years. The rise in electricity production from RES increased by a staggering 140% from 2015 and will rise at a significantly higher rate until 2050 [54]. Consequently, TSOs are being compelled to make more stringent Grid-code requirements for RES integration. This implies that in the future, wind farms and large-scale PV systems will have to actively manage frequency, voltage/reactive power, support against voltage excursions, flickers, and harmonics. In other words, for a valid power system integration, renewable power plants will have to meet a *grid-forming characteristic*. Although significant efforts are being made to integrate the PE converters of solar-PV and wind turbines with grid-forming capability, this research primarily focuses on wind turbines [49], [10].
The primary reason for choosing wind turbines for development of this work is the total generation capacity

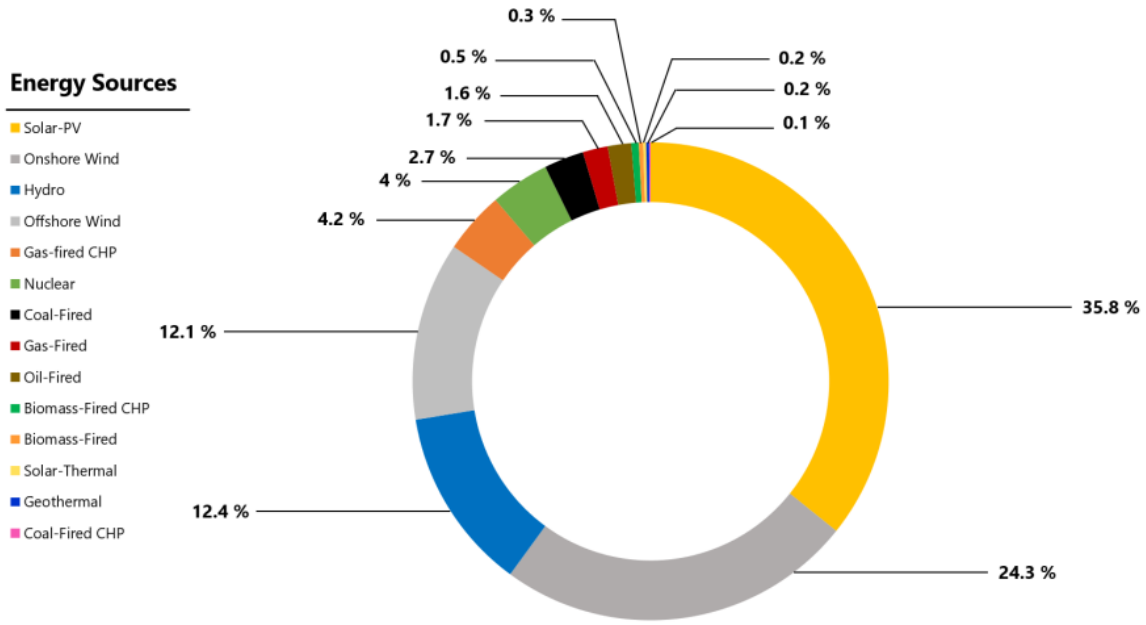

Figure 2.1: Global electricity production in 2050 [54]

from onshore and offshore wind will form a significant share in the future ([37], [91]), as depicted in figure 2.1. Other contributing factors that are enabling wind energy to go mainstream and become the leading renewable energy source are:

- Several government initiatives following the Paris Agreement of 2015 have come into action at the international level. Prominent ones amongst those include the United Nations Framework

Convention on Climate Change (Accord de Paris) [21], the EU H2020 Massive InteGRATion of Power Electronic Devices (MIGRATE) [3], and the EU H2020 PROgress on Meshed HVDC Offshore TransmissiOn Networks (PROMOTiON) [18].

- The likelihood of predominant wind conditions that enable wind turbines and wind farms to provide energy 24 hours is very high in Northern Europe, especially in the North Sea. Consequently, the same geographical conditions which makes wind energy much favourable in Northern Europe is also responsible for the unreliability of solar energy in the region.
- In terms of life cycle assessment based on total CO_2 emitted, wind turbines are cleaner than solar panels and can produce about forty-eight thousand times the energy per kilo-Watt than solar panels. As of 2016, the contribution of wind energy accounted for 4% of world's total electricity whereas solar provided only 0.5% [2], [90].

The initiatives by international governing bodies to increase the growth of renewable energy has lead to improvements in technology and trends and have forced the business models and financial funds to steer towards making renewable energy mainstream. This has enabled significant improvements in the wind energy technology as well. The significant improvements in wind turbine technology include:

- The development and implementation of wind turbines with power levels as high as 12 MW is becoming a norm. Such high power requires significant advancements in material technology as these wind turbines reach as high as 260-meter [15]. This applies to all the elements that builds the wind turbine system (blades, tower, nacelle, hub, new foundation concepts, etc.) Rare earth permanent magnet generators are being used which eliminate the need of heavier coils. Similarly, the improvements in the semiconductor technology has allowed development of converters with higher switching frequencies while reducing the overall size.
- The electrical and mechanical aspects of the wind turbines have improved significantly. The optimization of aerodynamic design of wind turbine blades has lead to developments of blades as high has 107-meter [15]. The permanent magnet direct-drive generators allow for a full control of variable-speed winds extracting maximum available power at every instant.
- Along with hardware implementations, there has been significant improvements in the ICT and software infrastructure which enables smart control of wind turbines as well as intelligent management of wind farms. These innovative control systems (based on Model-Predictive Control or State Vector Modulation techniques) are designed to meet the stringent grid code requirements for frequency and voltage support.

2.1. OVERVIEW OF WIND ENERGY CONVERSION SYSTEMS

The concept of wind energy systems is a combination of several interdisciplinary engineering subjects which include mechanical and electrical technologies accompanied with control theory and network interconnection [11], [91]. Figure 2.2 represents the major components involved in integrating the wind energy conversion systems (WECS) with the electrical grid, which are summarized as follows.

1. **Wind Power**- Power produced by a wind turbine is given by the relation[76]:

$$P_w = \frac{1}{2}\rho\pi R^2 C_p(\lambda,\beta)u_w^3 \tag{2.1}$$

where ρ is the density of air, R is the turbine radius, u_w is the wind speed and C_p is the coefficient of power. C_p is a function of tip speed ratio (given by λ) and pitch angle (β) [45]. Tip speed ratio (λ) is defined as the ratio of tip speed ($=\omega R$) over wind speed (u_w). Based on equation 2.1, a typical Power Vs Wind speed curve is represented in figure 2.3.

2. **Pitch angle control and Power reference**- The main aim of optimal blade design is to capture maximum power available from the wind. However, in case of winds being too strong, the power extraction needs to be limited to protect the wind turbine. The pitch control is used for maneuvering the turbine blades to extract maximum power, and also to limit the power production in case wind speed gets too high, which allows for **Maximum Power Point Tracking (MPPT)**. The aerodynamic

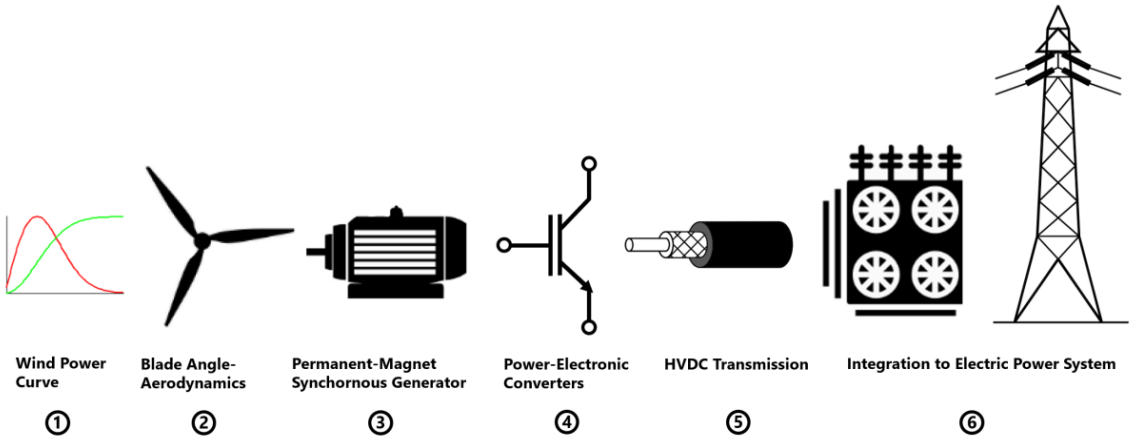

Figure 2.2: Structure of Wind Energy Conversion System [75]

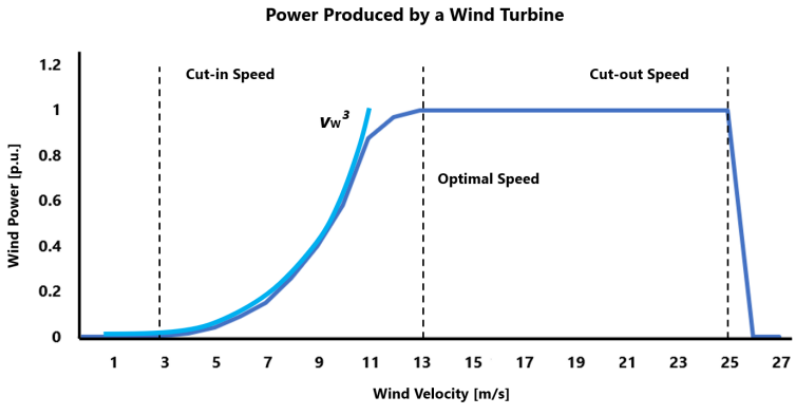

Figure 2.3: Wind turbine power as function of wind speed [86] [73]

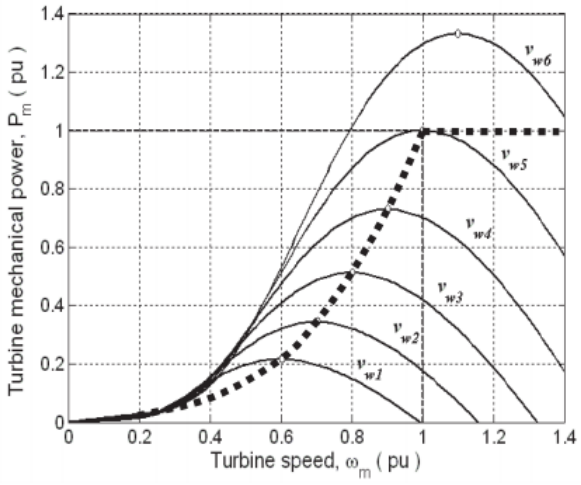

Figure 2.4: Turbine mechanical power as a function of rotor speed for various wind speeds [86] [73]

design of blades, pitch angle control and the wind power characteristics are aimed at maximizing the energy extraction from the wind, as represented by the figure 2.5.

3. **Generator and Shaft** - WT can be composed of different Generator Systems, which are mainly

differentiated between Geared-Drive Systems, Direct-Drive systems, Fixed Speed, Variable Speed, Doubly-Fed Induction Generator (DFIG) and Fully-Rated Converter. Geared-Drive systems are however becoming less frequent because of the maintenance associated with the gearbox as well as its noise, paving the way for direct-drive systems. The direct-drive systems thus comprise of the systems where the generator rotates at a slow speed 30-60 Rotations per Minute (rpm) [75]. For this rotation speed, PMSG with large radius are best suited and hence direct-drive systems are predominantly PMSG and fully scale converter (FSC) based systems. This also exhibits an advantage as for FSC systems, the PMSG (and wind turbine) are completely decoupled from the grid and are thus more immune to grid faults. Further, with PMSG, the flux is assumed to be sinusoidally distributed along the air gap which significantly reduces the excitation losses and torque density of the generators [45], [91]. The rotor magnetic field is always constant in a PMSG because of the Permanent Magnets, and the actual direction of the magnetic field is given by the Electro-magnetic field (emf) of the generator which is induced in the stator by the rotor field [73]. PMSG for the medium voltage type-4 wind energy systems are discussed extensively in section 2.2.

4. **Power Electronic Interface (PEI)**- As the renewable source is intermittent in nature, the voltage and frequency produced as the direct output of these sources is variable. Therefore, power electronic converters become a mandatory part of solar and wind energy conversion systems, as they convert the varying voltage and frequency into constant values. In context of wind turbines, this means that the variation in wind and corresponding mechanical drivetrain is compensated in exchange for the control of these power converters. This controllability allows for the power converters to adapt the voltage and frequency of the supply into the voltage and frequency required by the load and maintaining constant phase angle, therfore *forming the grid* and keeping it operating [39], [72]. Since the control of PEI forms a majority part of this thesis, it is disccused in detail in sections 2.2 and 2.3

5. **HVDC Transmission**- The swiftly evolving concepts and configurations in the HVDC networks have lead to their significant rise around the world, and HVDC grids that overlay the AC network are being seriously considered for future developments [13]. The breakeven distance for using HVDC transmission network is approximately 50 km [13], and the advantages of using HVDC transmission over HVAC are clearly elaborated in [74]. Moreover, there are several configurations proposed in literature for creating Multi-terminal HVDC systems which is a major technology leap in the HVDC transmission. Other than the point-to-point connections (figure 1.3, the so called 'Hub-and-Spoke' arrangements are being proposed for Offshore Wind developments in the North Sea[12].

6. **Integration to Electrical Power System**- The energy transition focused on increasing renewable integration and DERs can also create threats to the reliability of the power system. Therefore, the TSOs are being faced with a challenge to enable energy transition whilst maintaining the security of supply. A recent incident that highlights the urgency and importance of addressing such challenges was encountered in UK, where the Hornsea Offshore park got disconnected, following the disconnection of a gas power plant leading to the biggest power cut in the last decade [19], [24]. Some of the major challenges associated with increasing PE-converter based generation have already been discussed extensively in the first section of Chapter 1, and are dealt with in the development of this work.

2.2. WIND TURBINE GENERATOR AND CONTROL

The wind turbine generator based on permanent magnets rotor has been slightly touched upon in third point (3) of the previous section 2.1. This section elaborates more about the Operation of PMSG and their control in the WECS based on type-4 wind turbines. The configuration of generator and converter system used in wind turbines of several megawatts is shown in figure 2.6, and is typical for the wind turbines operating at medium voltages of 3 kV or 4 kV [53].The connection to the grid is based on the controlling of grid side converter and is discussed extensively in section 2.3 as it forms the major part of this thesis work. The major components of the wind turbine generator and converter model to be discussed in this section include:

- Permanent Magnet Synchronous Generator (PMSG)
- Machine Side Converter (Rectifier)

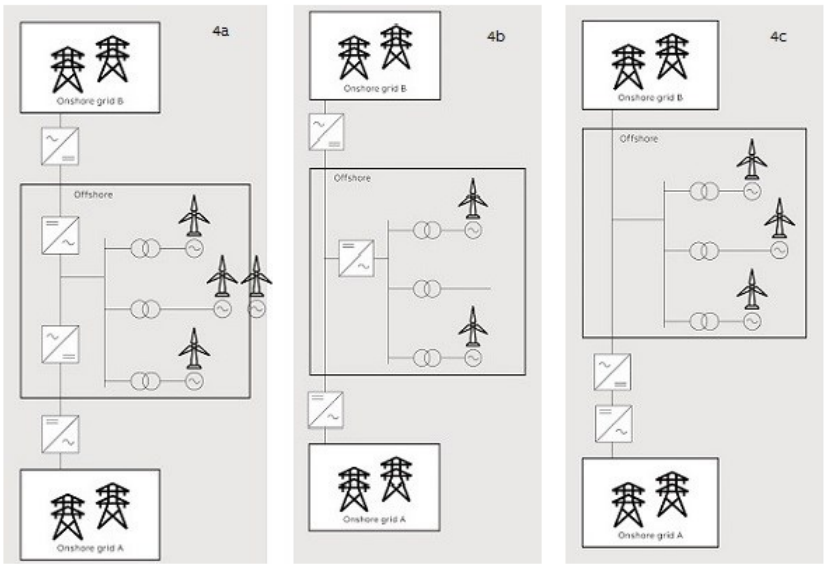

Figure 2.5: (4a) Hub-and-spoke with multiple HVDC links.
(4b) HVDC connection schemes for offshore wind: Hub-and-spoke with multi-terminal HVDC system.
(4c) HVDC connection schemes for offshore wind: Hub-and-spoke with AC links and HVDC back-to-back station as is implemented in, for example, the Kriegers Flak Combined Grid Solution project [12]

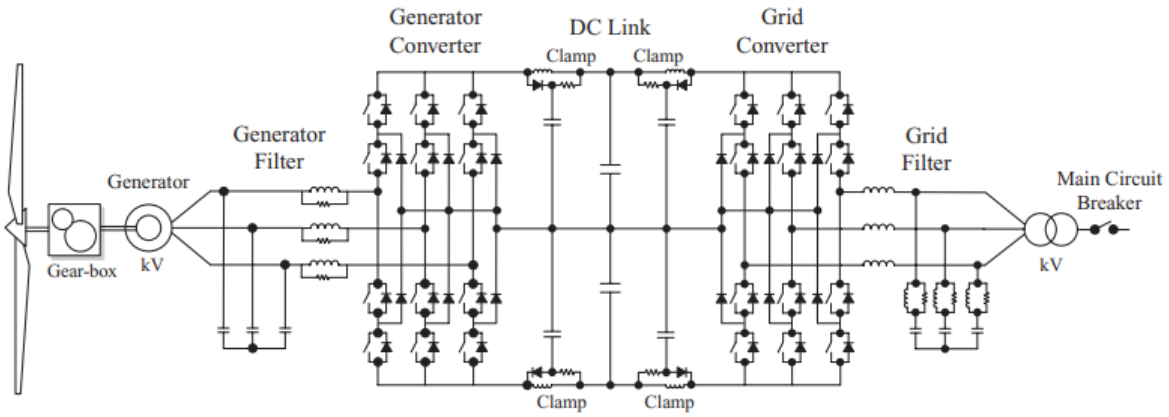

Figure 2.6: Configuration for Type-4 wind energy systems with three-level NPC converters [7]

2.2.1. PERMANENT MAGNET SYNCHRONOUS GENERATOR (PMSG)

Permanent magnet synchronous generators are brushless as the agnetic flux is generated by rotor magnets. The absence of rotor windings lead to high power density, non-existent rotor winding losses and reduced thermal stress on the rotor. The only drawback of using PMSG in wind energy systems lie in the high costs of rare-earth permanent magnets, and their susceptibility to demagnetization. However, as previously discussed, the advantages of using PMSG far outweigh their drawbacks, especially in wind energy systems of several megawatts. Based on how the permanent magnets are mounted on the rotor, the PMSG can be classified into surface mounted and inset PM generators.

SURFACE MOUNTED PMSG

As the name suggests, the permanent magnets are placed on the rotor surface, as shown in figure 2.7. The figure shows evenly mounted magnets (16 in the represented figure), seperated by non-ferrite materials between two adjacent magnets. As the permeability of magnets and non-ferrite material is approximately the same, the effective air gap between the rotor and stator is uniformly distributed around rotor urface.

Such a configuration is known as non-salient pole PMSG. However, these magnets are subject to centrifugal forces that can cause their detachment from rotor and hence their application is limited to low-speed operations.

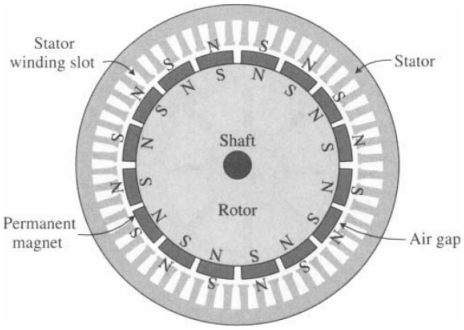

Figure 2.7: Generic representation of Surface-mounted nonsalient PMSG [8]

INSET PMSG

In the inset PMSG, the permanent magnets are inset into the rotor surface as shown in figure 2.8. Since in this configuration, the magnets are not seperated by a non-ferrite material but rather the rotor corematerial, saliency exists. The magnets arranged in this configuration experience less stress due to centrifugal forces in comparision to the surface-mounted PMSG and therefore, inset PMSG can operate at a higher rotor speed.

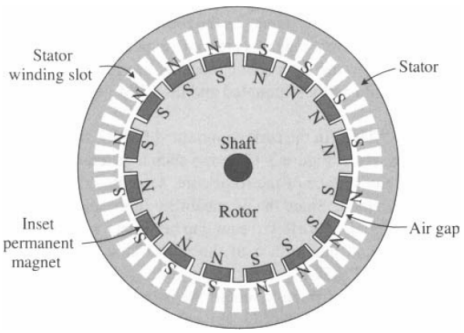

Figure 2.8: Inset PMSG with salient poles [7]

TIME DOMAIN MODELLING OF PMSG

Having discussed the different rotor arrangements it is important realise the voltage equations for the synchronous generator in time-domain modeling that are important for development of control of the wind energy systems. The time-domain modelling is based upon the synchronous rotating reference frame, also called *dqo* coordinate system [80] [34], is used to derive stator voltages. Equations for stator windings are given by equation 2.2:

$$\begin{aligned} v_d &= r_s i_d + \frac{d}{dt}\Psi_d + \omega_r \Psi_d \\ v_d &= r_s i_q + \frac{d}{dt}\Psi_q - \omega_r \Psi_q \end{aligned} \tag{2.2}$$

where r_s is the stator resistance, v_d and v_q are the d and q components of the terminal voltage vector, while i_d and i_q are the d-q components of the stator currents respectively. The stator flux components represented by the Greek letter Ψ are represented by equation 2.3

$$\begin{aligned} \Psi_d &= L_d i_d + L_{md} i_d + \Psi_m \\ \Psi_q &= L_q i_q + L_{mq} i_q \end{aligned} \tag{2.3}$$

As can be observed from the equation 2.3, the stator flux for d and q components is dependent on L_d and L_q, the respective stator inductance components, while the magnetic strength, Ψ_m, represents the flux linkage induced by the rotor magnets on the stator windings. It must also be noted that, for a non-salient pole PMSG (figure 2.7), $L_d = L_q$, whereas for a salient pole PMSG (figure 2.8), $L_d < L_q$. Based on whether the generator is a salient pole or non-salient pole type, the machine side converter control is decided to allow for optimal performance of the wind energy system, as is elaborated in the subsection. 2.2.2.

2.2.2. MACHINE SIDE CONVERTER

Figure 2.6 represents the full scale converter and synchronous generator arrangement for the wind energy system. This section discusses in detail about the NPC converter used and the control of Machine side converter (MSC) for MPPT of the generator. The control of Grid-Side Converter (GSC) is mainly responsible for addressing the challenges with grid integration of PE converter-based generation and is explored further in Section 2.3.

THREE-LEVEL NEUTRAL POINT CLAMPED CONVERTER

The converter employed here (figure 2.6) is a Voltage Source Converter (VSC) and uses the **3-level Neutral Point Clamped (NPC)** topology. For this converter topology, the converter power rating can reach easily 6 MVA, without any series or parallel switching devices or converters [8], [25]. To minimize switching losses, the device switching frequency is normally kept to a few hundred hertz (a value of 900 Hz switching frequency is used in the development of this work).
The difference can be easily understood by the representation used in figure 2.9. The figure depicts the phase to DC-link middle point voltage of the NPC inverter (grid-side converter) in comparision to the two level VSC inverter. As it can be observed, depending upon the switching-pattern, the output phase voltage of the NPC

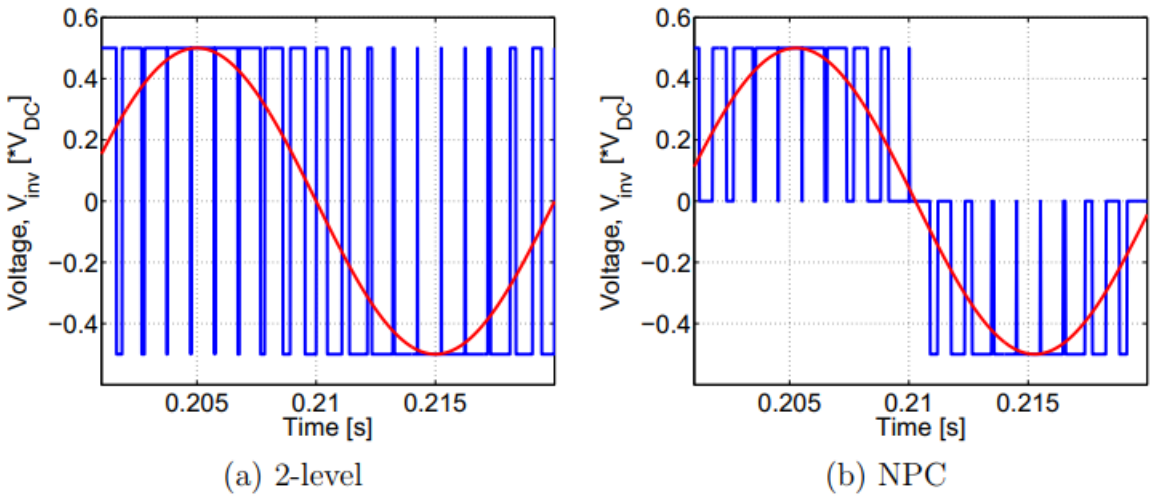

Figure 2.9: Output phase voltage of 3-level NPC converter [42]

topology can get three different values ($+\frac{V_{DC}}{2}$, 0, $-\frac{V_{DC}}{2}$), whereas at the 2-level VSC inverter, only two values can be present ($+\frac{V_{DC}}{2}$, $-\frac{V_{DC}}{2}$) [42]. Hence, the NPC topology is preferred over the 2-level VSC converter used in low voltage level (690 V) WECS as by having more voltage levels the form of sinusoidal signal is reached thereby minimizing the need for an output filter. However, the topology of the converter used does not direct the control algorithms used and therefore, does not impact the grid-studies developed in this work.
In order to simplify the controlling of AC voltages, the d-q transformations are done that makes use of a d-q synchronous rotating reference frame. the d-axis is aligned with the vector of machine flux or the grid voltage at the point of common coupling. This is done so as to simplify the control of voltages and currents. the d-q transformation makes the AC sinusoidal voltages to DC with a rotating reference frame. The overall controlling of wind turbine by the converter control using d-q transformation can be understood from the figure 2.10.

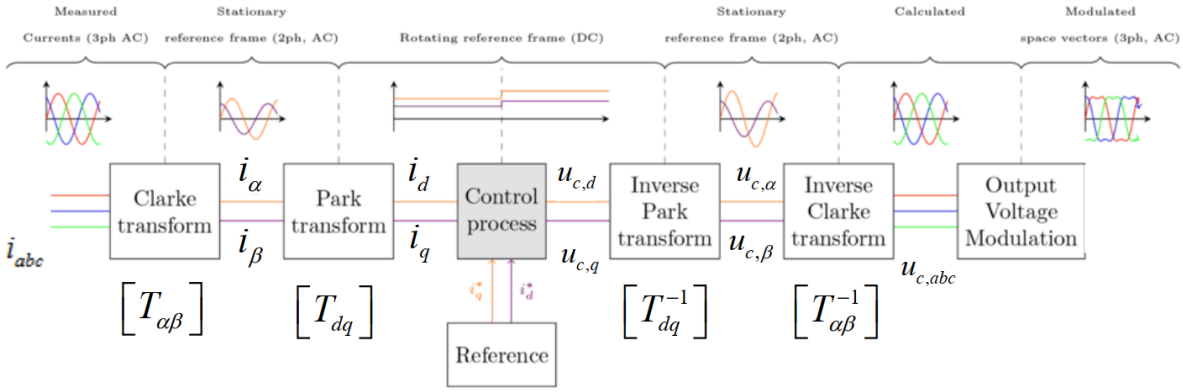

Figure 2.10: Transformation steps that take place in the control of VSC[68]

CONTROL OF MACHINE SIDE CONVERTER

For the control of wind energy system the control generator-side active power control with Maximum Power Point Tracking (MPPT) is an important aspect, along with grid-side reactive power control and DC voltage control. The machine side converter (MSC) is mainly responsible for the MPPT of the PMSG and can be controlled by a number of methods [6], [9] to achieve different objectives. For instance, the $d-$ axis stator current can be set to zero during the operation to achieve a linear relationship between the stator current and the electromagnetic torque. Such control is called **Zero d-Axis Current (ZDC) control** [5]. Alternatively, the generator can be controlled by **Maximum Torque per Ampere (MTPA) control** [5] to produce maximum torque with minimum stator current. Yet another approach is to operate the system with **Unity Power Factor (UPF) control**. [9] provides an in-depth analysis of the mentioned MSC control techniques. An important decision to consider while determining which control to implement is the speed range of the selectd generator. Based on case studies conducted in [9], it was concluded that MTPA control scheme works for full operating range of both salient and non-salient PMSG, whereas ZDC control only works for full operating range of a non-salient PMSG. Table 2.1 provides a summary for the operating range of synchronous generators with different control schemes.

Generator Control Scheme	ZDC	MTPA	UPF
Non-salient PMSG	Full	Full	Partial
Salient pole PMSG	Partial	Full	Partial

Table 2.1: Operating range of PMSG with ZDC, MTPA, and UPF control schemes [9]

The advantages of MTPA control are further extended for application of the wind enrgy systems in weak grids. The work implemented in [84] is very similar to MTPA control with few minor modifications, and evidently leads to a stable performance of the PMSG when the wind turbines are integrated with weak AC grids. The control scheme mentioned in [84] has been used in the development of this work. The model was initially available in the RSCAD library and is represented in the figure 2.11.

After validating the model for its operation in strong grid and weak grid and performing small-signal stability analysis, the tuned controller parameters were obtained in [84], and are reproduced in the Table 2.2. These parameters are used as defined in the implemented RSCAD model. This control is implemented such that

K_{p1}	200 kA^{-1}	K_{p2a}	0.01 kA/rad	K_{i2b}	500 kAs^{-1}
K_{i1}	5000 kAs^{-1}	K_{i2a}	0.55 kAs/rad	K_{d2b}	0.02
K_{d1}	0.02	K_{p2b}	200 kA^{-1}		

Table 2.2: Optimized control parameters [84]

the stator current is 180 degrees out of phase with the stator voltage. This is done to maximize the efficiency of PMSG. Moreover, the quadrature axis component (or torque component) of stator voltage is maintained to match the power requirements of the wind turbine. The real component of the stator control is varied to

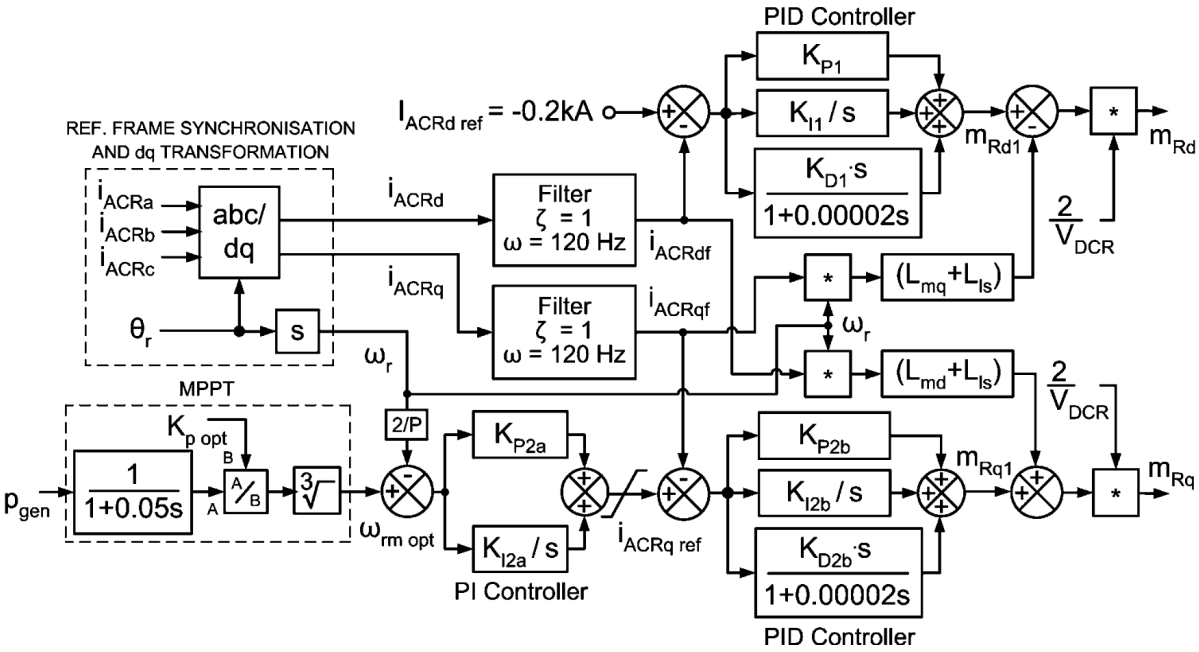

Figure 2.11: Model of machine side controller [84]

keep the reactive power at a minimum as long as the power output of the machine is 1 per unit or less [30]. However, this scheme is suitable for operation of wind turbine in weak grid, it does not support starting of the system and thus cannot provide grid-restoration capability. In order to provide grid-restoration capability to the wind turbine, the controller mentioned in [84] needs to be disabled during the starting mode and a controller based on dc link voltage needs to be activated [51], [72], [73]. The pitch controller is switched back on when the grid is restored. This modification is made because the DC-voltage controller has a fast dynamic response, unlike the pitch controller. However, this switching between two modes depends on the availability of medium voltage. An assumption of constant wind power support being present during the grid restoration and load pickup is made in this scenario[51].

2.3. GRID SIDE CONVERTER CONTROL

The grid side converter which converters DC link Voltage to sinusoidal AC voltage is the key interfacing element of any inverter-based distributed generator. Since grid studies is the focus of this work, the control algorithm governing the inverter operation is the model core, and hence losses calculation or the analysis of switching process of semiconductors is neglected. So far most of the Grid Side converters have been controlled using the grid-feeding technique in which their main funtion has been to deliver the full amount of energy that reaches the DC-link of the inverter. A short overview of grid-feeding inverters is presented followed with the need of grid forming inverters (converters) and the current trends in the grid-forming approach.

2.3.1. GRID FEEDING INVERTERS

In modern power systems, almost all the renewable energy based generators that work with Maximum Power Point Tracking (MPPT) are equipped with a grid-feeding inverter. The concept of MPPT is based on extracting the maximum power availble from renewable resources and grid-feeding converter accompany in delivering that maximum available power to the grid, irrespctive of the power requirements of the network. Accordingly the synchronous generators present in the network adjust their control to keep the power systems in balanced state.

Figure 2.12 shows an averaged value equivalent circuit of a two or three level VSC converter being used in grid feeding mode. It mainly comprises of two control loops. The outer control loops are used for generating reference value of the d- and q- axis reference currents and is based on controlling active and reatcive powers. The inner control loop, represented by the orange box is the current control loop that regulates VSC

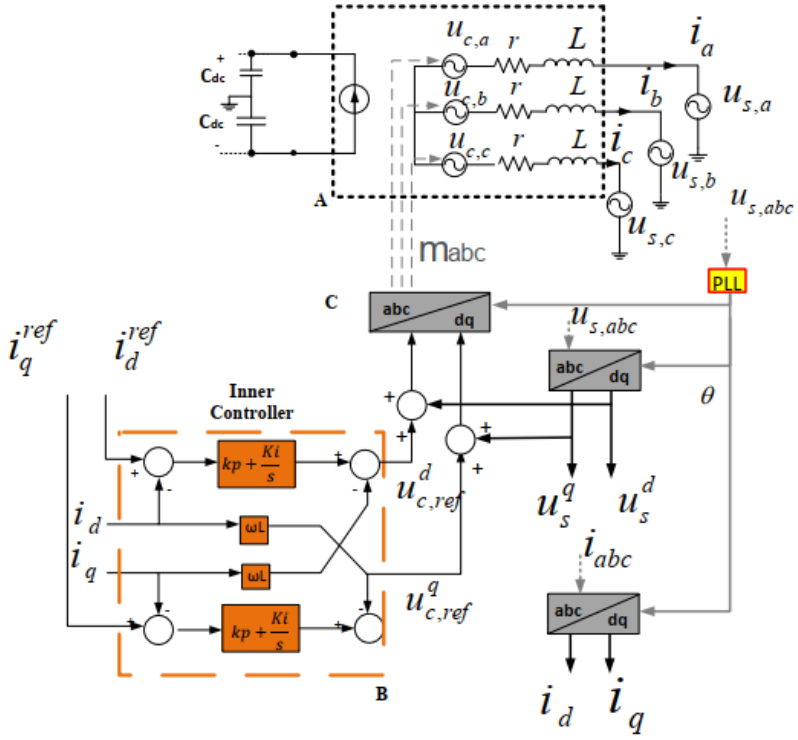

Figure 2.12: Overview of control of the VSC based on grid-feeding approach [68]

current (i) via the internal converter voltage (u_c). It must be noted that for generating the d- and q- axis currents, Park transformation is used that uses the angle based on the voltage angles determined by the Phase Locked Loop (PLL). Based on the outer control loop, the grid feeding wind turbines can provide some support functions to the grid which mainly deals with active and reactive power control. Figure 2.13 shouws the block diagram of the control module that includes bothe the closed loop and open loops for reactive power control as well as the voltage regulation. It also includes closed loop control for the active power which is determined by the rotor generator speed, the initial value of which is determined by the MPPT curve that the type-4 wind turbine utilizes. In the shown figure 2.13, the reference value of power (P_{ref}) is calculated from the power flow. It is assumed that in this model, the wind speed is considered to be constant during the simulation and the generated wind power is assumed to match the power injected to the grid. The output of this control is sent to the converter module in terms of i_d and i_q reference values of the figure 2.12.

There have been different controlling strategies for the grid-feeding inverters but more or less they all work on the same principle of supplying the maximum extracted power from the RES to the grid. So far, there hasn't been that much of problems with the grid-feeding control. However, as the short-circuit ratio at the grid-connection point becomes less than 1.5 (which will be the case in future given the ambitious goals of governments around the world), the grid-following operation has been shown to be prone to instabilities [67] [48]. Additonally, the grid-feeding inverters lack inertia as they inject fixed-power setpoints, irrespective of the load levels, and hence cannot guarantee the frequency and voltage stability of the system [31], [79]. Moreover, as the penetration of RES increases in the power systems, the short-term voltage and rotor angle instability risks increase in the network. Furthermore, with the increasing PE-based generation, there are chances of high-frequency interactions with the current control loop, resulting in harmonic instability in the network [63] [68]. All these issues present to be a roadblock in the path of attaining 100% PE interfaced networks and thus calls the need of *grid-forming* control strategy.

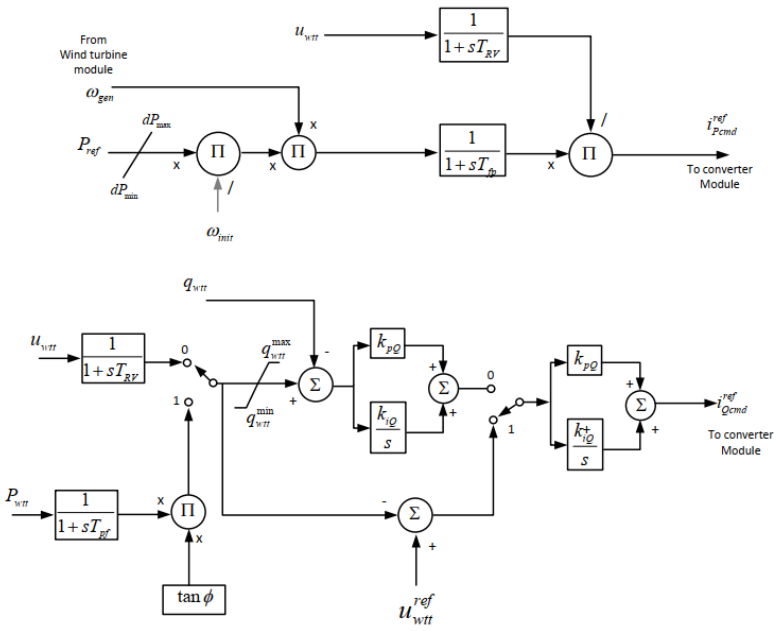

Figure 2.13: Outer Control loop for type4 wind turbine stability type model[68]

2.3.2. GRID FORMING INVERTER

In order to accommodate upto 100% of inverter-based generation in the power systems, new control schemes commonly referred to as the *grid-forming* control are foreseen as the leading capability necessary for power converters to operate stably in weak grids with low short-circuit ratio (SCR). The application of such control concepts could possibly expand in future towards MMC HVDC links as well as large batteries (storage devices) for grid-support services [1]. The *grid-forming* control scheme can ensure natural voltage source behaviour of the power converters during normal operation. Moreover, the dependency on the short-circuit power levels by the power converters can be eliminated. Additionally, together with a fast response of active power and fast voltage recovery, they can extend the boundaries of stability of the transmission network [70]. So far, most of the research on grid forming control is focused on microgrid application. Some works have come up recently in the transmission network models, however, they are mostly based on averaged models or RMS simulations [70], [33], which does not include many of the complexities involved in the operation of wind turbine converters as well as power systems. Although such works indicate that the application scope of the grid-forming control is evolving from standalone operation of batteries in microgrids to other renewable energy PE interfaces in transmission network [48].

The early developments in the grid forming control started with [28] in the development of Uninterruptible power supply Power Supply. Following such developments, the application of grid-forming control was extended in microgrids [58] [56]. For the microgrid application, the focus has mainly been on modifying the inner loop control [23]. To adapt to every situation, a common solution in microgrid is to switch from an islanded control mode to grid-connected control mode, and hence the inner control loop should be flexible enough to accommodate these changes. Most of the proposed solutions in literature in such a scenario is based on estimation of grid frequency using a PLL [92].

The work done in the area of microgrids has been extended in high power applications, where the proposed grid-forming VSCs provide support for controlling the voltage amplitude or frequency when the grid is considered weak or has low inertia. In terms of the transmission level operations, a lot of work has been focussed on eliminating the PLL as it has shown some destabilization properties in weak grids [50]. Different names have been given for operation without PLL such as "power-synchronization" [94], " Virtual Synchonous Machine" (VSM) [35], "Virtual Synchronous Generator" [95]. All these control schemes consist of adjusting the frequency reference according to the output power measurement. The power-frequency dependence recreates virtually the synchronization torque that stabilizes the voltage angle, and thus the frequency.

More recent works have been carried out in [51], [33], [42] in this domain. The works concluded in [51], [33],

[42] represents the current trends in the grid-forming technology and have more or less a similar current-limitation strategy to limit and control the output current of the converter. [33] investigates parallel-grid forming technologies without using PLL, and addresses the small-signal stability of the VSCs, however, the developed controls and adopted methodologies have a conservative industrial context. [42] covers almost all the major points relating to parallel grid-forming approach for symmetrical components, however, the scope of the work is mainly limited to the microgrids. An overall contribution of the wind turbines to the frequency and voltage stability has been extensively covered in [51], however most of the work has been on avereged models using RMS simulations. Moreover, the control strategy is limited to the symmetrical faults as the focus of the work was on minimizing the impact of positive sequence components during the fault. In the experiments conducted in [26], it was concluded that the key factor that contributes to the grid stability is the fact that the synchronous generators behave as a voltage source to support the grid, defying the earlier notions of inertia and active power being the key to stability of networks with high PE converter-interfaced generation. Moreover, the work in [26] focuses on establishing strategies that can work with symmetrical as well as unsymmetrical faults. [26] initially served as a reference for the development of this work, however, the limitations of RTDS component library, restricted the development of EMT models on RSCAD. The work developed in [51] covers almost all the factors of voltage stability by utilizing Direct Voltage Control concept which enhances the control of wind turbine PE converters allowing them to mimic the behaviour of synchronous generators, and hence was decided to be carried forward for extending in EMT simulations. Moreover, [51] also serves as a reference for the grid-forming approach in offshore wind-farms as suggested in [39] which allows HVDC converters to withstand faults and hence provides a whole range of operations for wind turbines in onshore as well as offshore grids.

2.4. OVERVIEW OF VSC-HVDC CONVERTERS

At the transmission level, the size and capacity of the converters has increased extensively with the advancements in technology of MMC based VSC-HVDC. The MMC topology allows for instant modulation in the output voltage which can further bolster the stability of the transmission network. The VSC-HVDC technology based on MMCis gaining more traction especially due to the developments in the offshore wind technology. Figure 2.14 represents a typical Offshore wind power plant with HVDC connection. The current topology involved in VSC-HVDC transmission is the point-to-point connection as represented in figure 2.14.

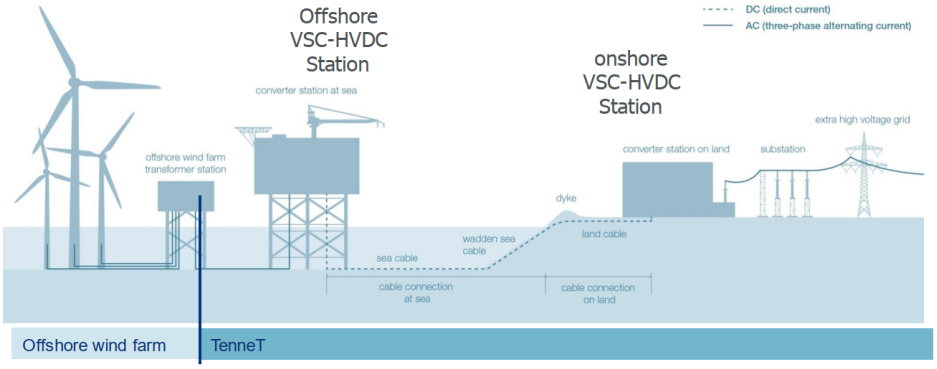

Figure 2.14: Offshore wind power plants with HVDC connection[68]

In the point-to-point connection, the Onshore converter station is connected to the main transmission grid and is mainly current controlled. The Offshore converter station which is located far in the sea, emulates the grid and provides voltage and frequency setpoints for the offshore wind parks to be connected which helps in synchronizing power in the HVDC system. The HVDC cables connecting the offshore and onshore grids are mostly XLPE cables (figure 2.15), several cable models are available for their modelling in power system studies [64] [29] [96]. The HVDC submarine cables have been utilized since 1950s and the highest installed HVDC submarine cable upto date is operating it +/- 500 kV and has a capacity of carrying 1400 MW per cable (Kii channel project crossing Japan). [60].
The VSC-HVDC technology does not require changing the polarity of DC voltage for current reversal, and neither does it needs reactive power compensation or large filters for harmonic distortion. Furthermore,

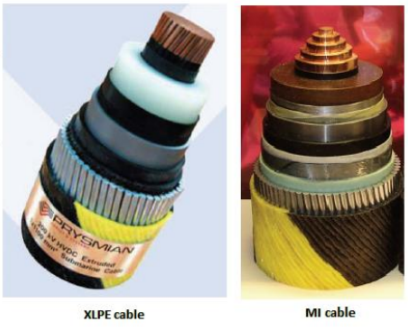

Figure 2.15: Marine cable technology[66]

with the utilization of suitable power synchronization control, it is possible to connect VSC-HVDC systems to the weak ac systems, where the short-circuit level is low or even zero [60]. Moreover, with new developed controls, discussed in [69], the FRT capability of the HVDC systems can be enhanced during balanced as well as unbalanced faults. For the grid-connection studies most of the modifications are proposed on the onshore converter as it is mainly responsible for integrating Offshore wind parks to the grid. However, the focus the developments in this work is mainly on the Offshore network (i.e., offshore VSC-HVDC converter and offshore wind farm). A typical control scheme of the offshore VSC station is presented in figure 2.16 whose main objective is to provide controlled AC voltage and frequency at the island offshore AC grid, allowing PLL of the wind turbines to synchronize to the island voltage. During the normal operating conditions at the offshore converter, the control module ensures that the rated power is respected [69]. As can be observed in the figure 2.16, the control approach uses an outer current control loop which sets the references of the inner control loop. There are several other benefits of using VSC HVDC converters apart from the economical incentives, the major ones being the superior control and quick power restoration during and after disturbances and hence forms an important part to be discussed in this thesis. The primarily aim of including the studies of offshore network includes less operational experience in bulk power transfer from offshore wind farms, as well as a possible extension of the work in the development of multi-terminal models on RTDS.

2.5. RESEARCH AND IMPLEMENTATION GAPS

Having gone through the various literature focussed in the *grid-forming* technology, the following research and implementation gaps are identified, that are addressed in the development of this work:

1. Based on the published works in [33] [26] and [51], it has been concluded that the wind turbines with their ineffective voltage control as well as non-existent frequency regulation, cannot stabilize the power systems in particular scenarios.

2. The controls developed in [51] addresses almost all the issues pertaining to dynamic operations of the wind farm, however it makes use of simplified Wind turbine models and does not tests the applicability of the developed control in real world scenarios.

3. The Direct Voltage Control developed in [51] and [39] has a fast dynamic response, however its dependence on the measurement filters is not addressed in the simplified RMS models. Moreover, the VDACC discussed in [82] to improve the transient response of the grid side converters has mainly been implemented for the type-3 wind turbine models.

4. No EMT models (RTDS) exist for the Direct Voltage Control approach for offshore and onshore studies which has shown extremely promising results in the RMS models. Moreover, the inertial response proposed in [51] based on washout-filter and lead-lag compensator has not been implemented and tested for its response and possible interactions with the system.

2.6. METHODOLOGY AND RESEARCH MILESTONES

In order to fulfill the thesis objectives and answer all the research questions, while covering all the research gaps, the milestones that are required to be accomplished for this work include:

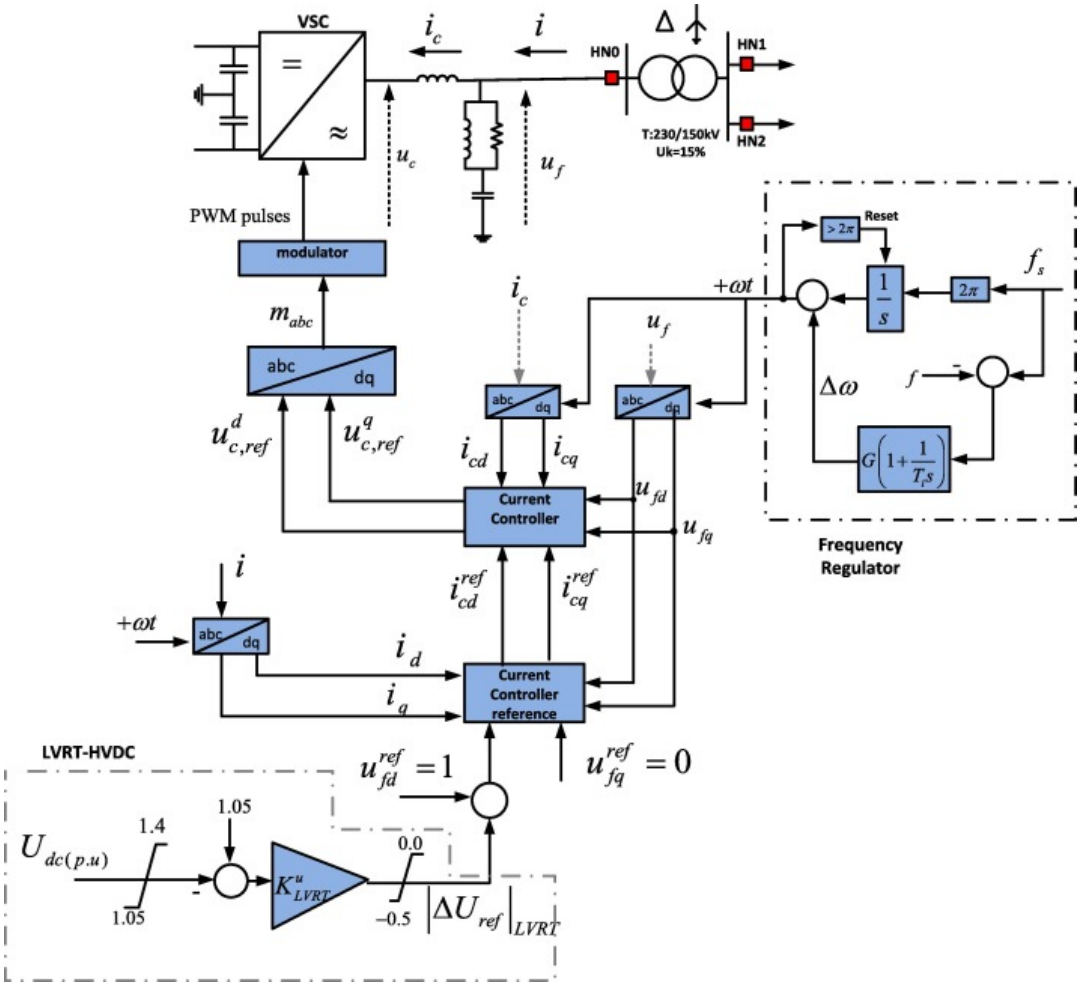

Figure 2.16: Offshore converter station model and its control loops. In the figure with dashed lines is the "LVRT-HVDC" control loop and the frequency regulator control loop.[69]

- Having identified the Direct voltage control approach for implementation in RSCAD, implement necessary modifications in the default type-4 wind turbine model of RSCAD library to make it work as a grid-forming wind turbine connected with an infinite grid (ideal AC source). Proper implementation of the current limitation strategy must be stressed upon to ensure accurate FRT capabilities of the wind turbine, as well as to preserve its synchronization during grid events.
- Following the execution of wind turbines with the infinite grid, identify and implement the upgrades required for enabling the standalone operation of wind-turbines. This upgrade is to be made without hampering the performance of the wind turbines in the grid-connected mode.
- Based on the execution with an infinite grid, extend the developed wind turbine control to larger networks to increase the share of wind energy generation. Further identify the improvements and modifications required to enhance the dynamic stability of the system.
- After establishing the dominance of the developed control strategy in large network operations, develop the offshore network model that enables bulk power transfer from offshore wind farms to onshore grids.
- Validate the implemented control strategy in the developed offshore network for reducing transient overvoltages in the HVDC converter and offshore wind farm transformer.
- Development of modified current control scheme and current limitation strategy to improve the dynamic and transient behaviour of wind turbine converters, and

3

ENHANCED GRID-FORMING CONTROL OF WIND TURBINES

This chapter focuses on the development of the detailed wind turbine model to be used in real-time simulations for the provision of voltage and frequency support to the grid with high penetration of PE converter-based generation. The identified control scheme is developed to operate the wind turbine with the equivalent grid in both grid-connected and islanded mode. The equivalent grid operation underlines the operation of the wind turbine in a stand-alone mode and includes modifications in the proposed control for operation in islanded mode.

This control mode uses an oscillator for generating 50 Hz reference because of which in case of standalone operation, the voltage and frequency of the wind turbine never goes out of bounds. The direct voltage Control developed in [51] is extended in this chapter for implementation in detailed models of wind turbine and its application is validated by testing it with an infinite grid (ideal ac source). Finally, the modifications proposed for its operation in standalone mode are implemented which also show the expected results.

3.1. DIRECT VOLTAGE CONTROL APPROACH

So far, with predominantly strong grids, the current injection control of the PE converters did not create any significant problems as the available synchronous generators were able to absorb any excess injected currents. However, in weaker grids dominated by PE converter interface, the situation is quite different. If a network is connected to the grid mostly through the PE interface and has little or no load of its own, as in the case of the offshore grid, the current injection cannot physically work. The current control scheme implemented has already been discussed in section 2.3.1. Another critical issue related to the PI-based current controller is the integration wind-up which might occur, causing the controller to go out of bounds. The PI controller might be useful in minimizing steady-state error, but it does not fit the requirements of the fast dynamic response required for enabling higher PE converter-based generation units. A novel control approach based on using high-pass washout filter has been developed in [37], which has a very promising application and has been followed for the development of this work.

Figure 3.1 represents the fundamental concept behind the proposed controller. As can be seen, the integral term is completely discarded; however, the proportional term is merely shifted towards the output terminal. Such action entails only a graphical implication without disturbing the controller performance. The absence of the integral controller makes the set-points of the PE converter shift from its original values. This shift in values has zero impact on the converter action as the set-points are decided only to limit the converter output current. Such a limitation is imposed based on the grid situation in the proposed control strategy. The use of high pass washout filter limits any disturbances in the dynamic behaviour of the PE converter control. Moreover, such a control design opens up the possibility for a frequency selective damping if the terms at the output of the current controller are supplemented with an appropriately designed band-pass filter.

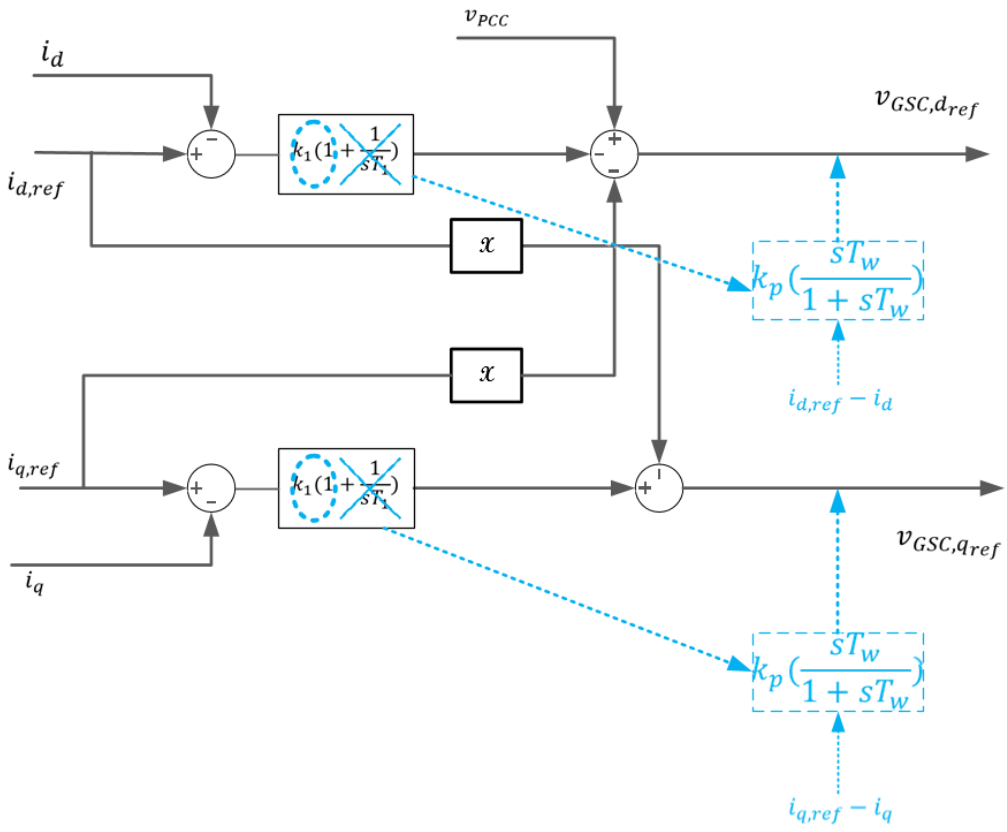

Figure 3.1: Modification of existing current controller for implementing direct voltage control [37]

For proper implementation of the direct voltage control method, the active and reactive power control loops are redesigned, as discussed further.

3.1.1. VAR-VOLTAGE CONTROL

The control scheme for providing fast reactive current injection during a fault scenario by the converter to prevent voltage collapse is further modified in [38]. As can be seen, reactive current injection requirement is no longer defined in this schema in favour of direct voltage control. The current adjusts itself optimally for the objective of voltage control according to the network conditions in response to a changing PE converter voltage arising due to changing power flows. Therefore, the scheme is more like the conventional voltage control in synchronous generators. The modified control scheme in [38] uses a hierarchical control approach in which an upper-level slow-acting controller is responsible for tracking set-point changes dictated by system-wide exigencies. The local fast-acting controller, on the other hand, responds to significant voltage dips close to the PCC and is governed mainly by the feed-forward term of voltage magnitude. The modified control scheme is represented by figure 3.2.

SLOW GLOBAL VAR CONTROL

The secondary controller can be implemented as a voltage, power factor or reactive power controller. The reference values are directly passed on to the PI controller downstream in case the controller works as reactive power or power factor control mode. The droop relation based on an adjustable voltage versus reactive power relationship is used for implementation as a voltage controller. For the V-q droop characteristics, a reference voltage value is determined (u = $U_{N_{ref}}$), which does not require any reactive power injection. The output from the droop characteristic passes through a PI controller with a small proportional gain and an integral time constant is chosen such that the reactive power injection by the converter precedes and forestalls possible transformer tap movements. Reasonable values for the time constant lie in the range $T_i = 5 - 30$ sec . A value towards the higher end of this range tends to stabilize, while lower values may excite oscillations and cause

interactions with other controllers. There are several reasons why a slow response if preferred in this scenario.

- A faster response may cause undesired interaction between other controllers or excite transient phenomena.
- The slow reactive power adjustment permits the deployment of reactive power injection by static compensators as per the deployment plan.

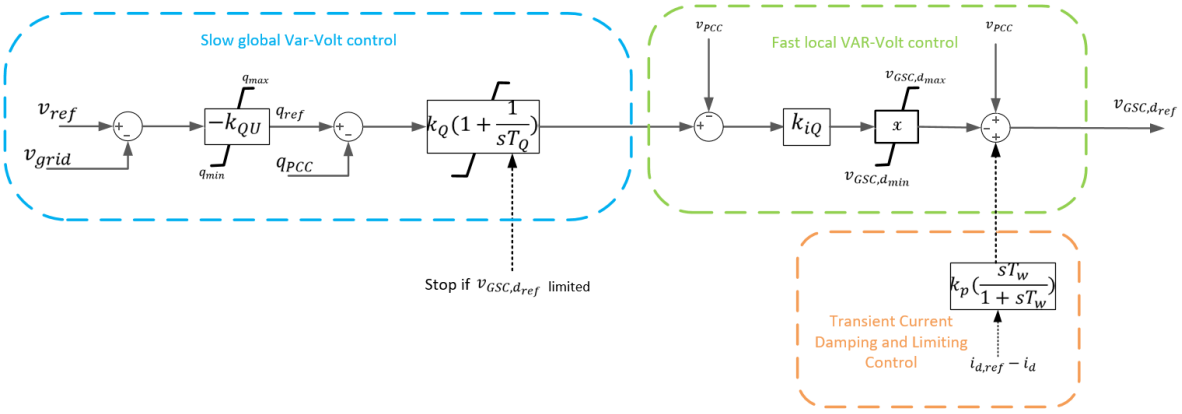

Figure 3.2: Modification of existing current controller for implementing direct-voltage control [38]

Automatic adjustment of reactive power with respect to voltage based on an adjustable functional relationship defined by using proportional gain k_{Q-U} makes operational sense. The proportional gain, i.e. the slope of the linear Q vs. U relationship, can be determined as:

$$k_{Q-U} = \frac{\Delta q_{vsc}}{\Delta u_N} \tag{3.1}$$

It seems theoretically possible to vary the proportional gain as per the variation in the network power flow. However, this is not very pragmatic, and the operational advantage of such an application does not justifiably outway its complex implementation. It is more practical to set the initial reactive power reference (q_{ref}), decided by the dispatcher based on actual load flow configuration in the network, and then regularly update this setting at fixed intervals.

It must be noted that the voltage $U_{N_{ref}}$ does not represent any desired target voltage value but is merely the voltage value at which no reactive current injection is required. In case of operation in large networks, the voltage $U_{N_{ref}}$ can also be the reference value of a different node in the network where the voltage drop is significant, or a node where a critical load is connected. The limits $q_{vsc_{max}}$ and $q_{vsc_{min}}$ represent the steady state continuous values which are determined using the P-Q diagram of the converter considering factors such as active power, voltage, frequency, and converter rating.

The slow acting PI controller, needs to be deactivated when the current limit of the converter is reached. This is likely to happen in case of short-circuit faults as voltage dips significantly and current demand increases consequentially. This deactivation is achieved by large integration time constant and a blocking signal as evident in figure 3.2.

FAST LOCAL VOLTAGE CONTROL

The output signal of the slow global VAR controller goes to a proportional controller which acts as a Fast local voltage controller. This block is primarily responsible for voltage support in case of fault events. The voltage boosting response of the controller is based on voltage sensed at the PCC and does not depend on remote quantities. 20-25 ms of rise time is considered ideal for this controller as this characteristic of boosting voltage significantly effects the operation of protection relays. The proportional gain of the

controller can be determined as follows:

$$k_{iQ} = \frac{\Delta i_{Q_{vsc}}}{\Delta u_N} \tag{3.2}$$

The value of k_{iQ} can range from 2-10 p.u. A value equal to 2, corresponds to 1 p.u. reactive current injection for a 50% drop in voltage. To simulate improved response similar to synchronous generators, a value equal to 4 is chosen for this work, based on the studies shown in [40].

It is also possible to use a lead lag compensator instead of a proportional controller. The transfer function in this case would be:

$$F(s) = k_{\mathrm{iQ}} \frac{1 + sT_{\mathrm{D}}}{1 + sT_{\mathrm{V}}} \tag{3.3}$$

The time constants T_D and T_V can be determined by controller design techniques or simply by trial and error. Irrespective of the tuning techniques, it is important to make sure that the controller should exhibit proportional characteristics in the steady-state operation. A method based on trial and error was used for the development of this work.

This controller is designed for only positively sequence voltages and current as the development of a controller that works with bot positive and negative sequence voltage and current is very complex and time consuming for development in RSCAD environment. Moreover, it is important to focus the action of fast primary control on removing any sustained positive sequence voltage dips, as it can lead to stalling of induction machines in the network eventually affecting the operation of other voltage sensitive devices.

3.1.2. ACTIVE POWER CONTROL

This part of the controller is responsible for providing improved frequency response by the wind turbines. The control scheme is represented in figure 3.3. The structure of DC controller is same as the one used in PI control scheme. For improved implementation in Real time simulation, an integration wind-up scheme is used to prevent the integral controller from becoming saturated and thereby in having an uncontrolled response. The output of the DC voltage controller is the active power injected into the network. This power output can be expressed as:

$$P = v_{pcc} i_d = -v_{pcc} \frac{u_{conv_q}}{x} \tag{3.4}$$

The above equation shows that the active power can be controlled based on the value of q-component of the voltage vector. The x in figure 3.3 and equation 3.4 is the reactance of the power electronic converter and presents the feed-forward action of the power electronic converter. The feed-forward term is responsible for the main controlling action of the direct voltage control, as the integral terms from inner control loop are eliminated. The output voltage that results from the product of currents (i_d and i_q) and x is the set voltage of the power electronic converter in the steady-state and this voltage corresponds to the supplied active and reactive power from the PE converter. The active power is controlled by the DC-link capacitor. Based on the modifications of direct-voltage control, the absence of the integral term induces a steady state error between reference currents and measured currents. However, as discussed earlier, this difference is not significant as the set-points are decided to limit the converter current output, which here, is taken care by the damping and transient current limitation scheme introduced in [37]. Moreover, since the control is done by the DC capacitor, the size and voltage of the capacitor has to be increased, in comparison to the PI based control method. For the control of frequency, three different methods have been proposed in [51] as shown in figure 3.3.

DIRECT FREQUENCY CONTROL

Direct frequency control works in a similar way as the over-frequency control, with a reduced deadband (20 mHz) which allows frequency support in steady-state operation. Moreover, since the deadband is reduced, direct frequency control works in both the directions to support any rise or decline in frequency based on active power injection or reduction.

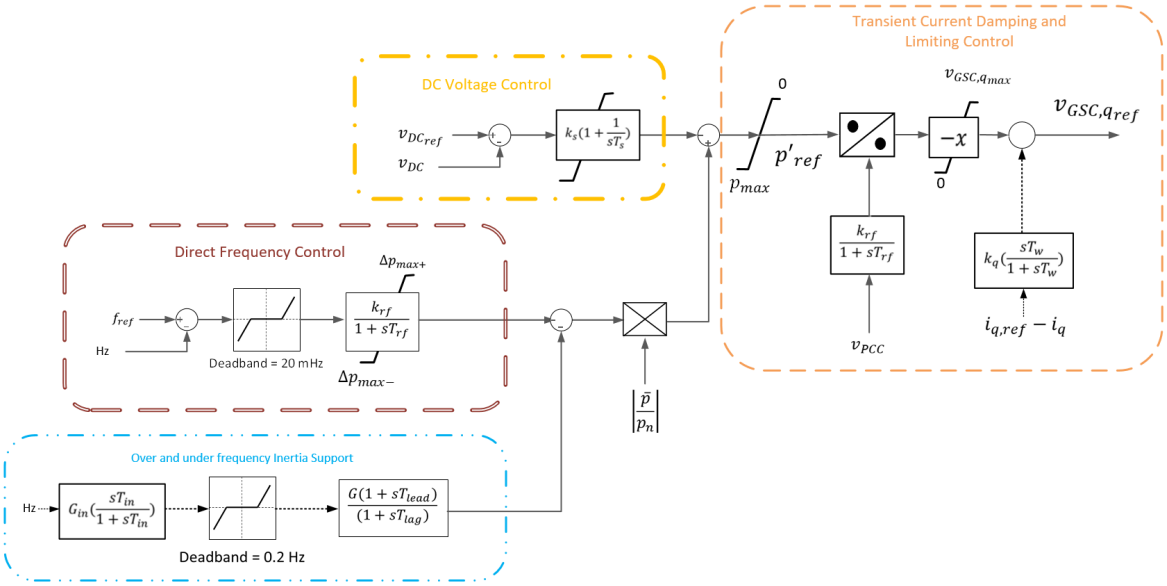

Figure 3.3: Active Power control channel for direct voltage controller [51]

UNDER AND OVER-FREQUENCY INERTIA CONTROL

This option allows for the implementation of well-known inertia control with extension in both frequency change directions. Several inertia emulation strategies have been discussed in [62][47]. As the name suggests, the inertial controller is activated in case of over or under frequency events and can quickly supply or absorb power temporarily. However, in order to implement the inertia controller, slight modifications are required to be made to the Machine Side Converter as well. This is done because the turbine mostly operates at MPPT and can not therefore, support large increase in power demand. However, the rotating mass of the wind turbine can be utilized for a short time frame to reduce the rate of change of frequency following connection of a load. Since the controlling of the PMSG is done by MSC, a signal for the change in frequency must be sent to the MSC as well because it is decoupled via the dc-link. The operational challenges that might arise in operation of inertial controller in high renewable scenarios are further explored in the section 4.2.

It is important to realise that it is possible to combine all three frequency control methods. However, Overfrequency emergy control becomes redundant if inertia control is designed to support over-frequency events as well. Moreover, a strategy developed in [82] based on reduction of active power in case of over-voltage can also be added to accompany these controllers. It is also possible to combine the above three frequency control methods. The inertia controller acts to provide quick response which can then be replaced by the slower normal frequency control. It is also possible to include voltage-dependent active power reduction scheme as described in [82].

3.1.3. CURRENT LIMITATION TECHNIQUE

The current limitation technique used in the direct voltage controller is represented by the figure 3.4. Figure 3.4 also includes an equation which describes the calculation of new reference current values if the PE converter current exceeds the maximum permissible current. The limits of the d and q components of the converter control voltages are then based on the impedance of the grid and new calculated maximum current values. The limitation of direct and quadrature axis converter voltages are also depicted in figure 3.4.

This current limitation scheme is different from the current vector saturation scheme implemented in [42] where the angle between d and q reference currents is taken into consideration. The current limiter block

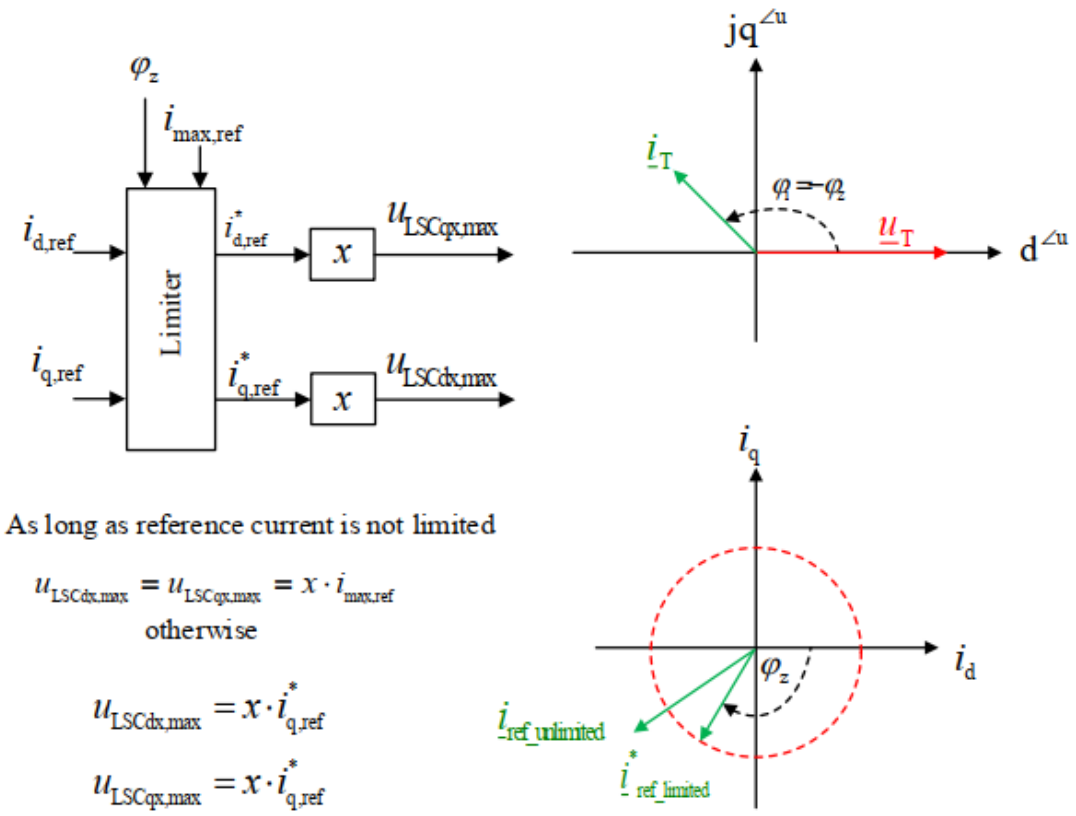

Figure 3.4: Current limitation algorithm for Direct Voltage Controller [51]

shown in figure 3.4 can also be described through the following equations:

$$\begin{aligned} i^*_{d,ref} &= \frac{i_{d,ref}}{\sqrt{(i_{d,ref})^2 + (i_{q,ref})^2}} i_{ref,max0} \\ i^*_{q,ref} &= \frac{i_{q,ref}}{\sqrt{(i_{d,ref})^2 + (i_{q,ref})^2}} i_{ref,max0} \end{aligned} \tag{3.5}$$

Based on the values of $i^*_{d,ref}$ and $i^*_{q,ref}$, obtained from equation 3.5, the figure 3.4 also contains equations for finding the values for the maximum reference voltages in d and q axis.

3.2. STANDALONE OPERATION

Having analysed the Direct Voltage Control for implementing Grid-Forming control, it was observed that the proposed controller has some problems with its functioning in standalone mode. This is because of the controller action relies heavily on a PLL. The PLL in real-time systems as well as practical systems has shown to effect the performance of wind turbines as the angle determined by the PLL is directly used for generating direct and quadrature axis voltages and currents. In lieu of this, during standalone measurements, the voltage at the point of common coupling is very high and hence the measured angle by the PLL generates abrupt values thereby undermining the entire control strategy. In order to cope with this scenario, the U-f mode control, mostly employed in Offshore HVDC stations, as well as in Microgrid master controllers was

added. This control is activated based on a central breaker information and is only operable when there is no grid support, i.e., no frequency reference being created for the Direct-Voltage control to operate. The U-f mode primarily uses an oscillator to generate 50 Hz frequency reference and for determining the angle for d-q transformation. It makes use of an anti-windup based PI control scheme which is sent as a reference to the converter to ensure that the voltage and frequency are maintained and do not go out of bonds. However, it must be realized that the stand alone operation of a wind turbine converter directly supplying a load (with no energy storage present) is highly unrealistic. This addition was made in the controller to investigate for the controller's operation where PLL might not be needed. The U-f control scheme based on microgrid application which is integrated with the Direct voltage control, for the standalone operation is depicted in the following figure 3.5.

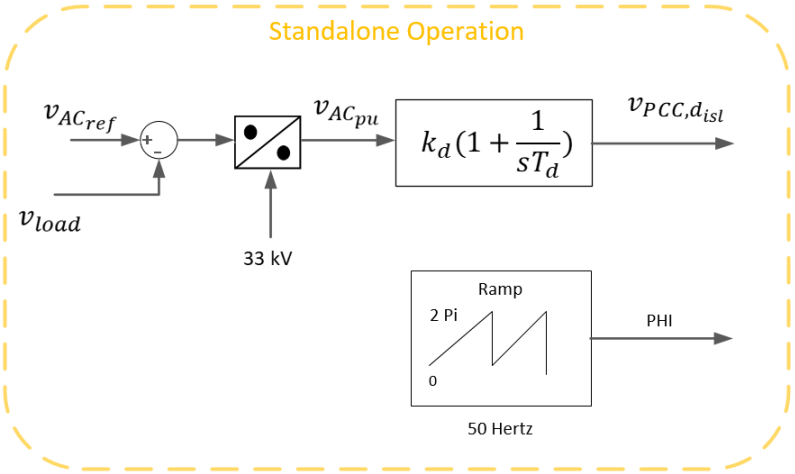

Figure 3.5: Standalone U-f mode based on microgrid operation of batteries

The Voltage reference generated from standalone mode is sent to the Direct Voltage Control's fast local controller in 3.2 (V_{PCC} of the fast local control is switched to $V_{PCC,d_{isl}}$), during the islanded mode based on central breaker information. Moreover, a signal for the operation of load voltage is also needed to which helps in satisfying the power requirements of the load. The V_{PCC} used in the Active power channel of Direct Voltage control is also switched to $V_{PCC,d_{isl}}$ for generating the value of $i_{d,ref}$ based on the equation 3.6.

$$I_{d,ref} = \frac{P'_{ref}}{V_{PCC,d_{isl}}} \tag{3.6}$$

3.3. VALIDATING THE CONTROL STRATEGY

In order to test the controllability of the aforementioned Direct Voltage Control and its modifications, a test system with the wind turbine connected to an infinite grid was used as shown in figure 3.6. Tests related to the three-phase line-to-ground fault as well as load connection or disconnection were made and evaluated as are described in the following subsections. Following its operation with the stiff grid, the capability of the wind turbine to fully supply the load by itself was analysed. However, it must be noted that the wind turbine supplying a load without any grid or storage connected is a highly unlikely scenario, and it would lead to overburdening the DC link capacitor if the power balance is not maintained (i.e. if the load is less than the power being supplied by the wind turbine).

$K_{p,d}$	2	$G_{w,p}$	0.15	$T_{w,p}$	10 s
$K_{p,q}$	15	$G_{w,q}$	0.15	$T_{w,q}$	10 s

Table 3.1: Determined parameters of Proportional control and washout filters used in Direct Voltage Control based on trial-and-error method

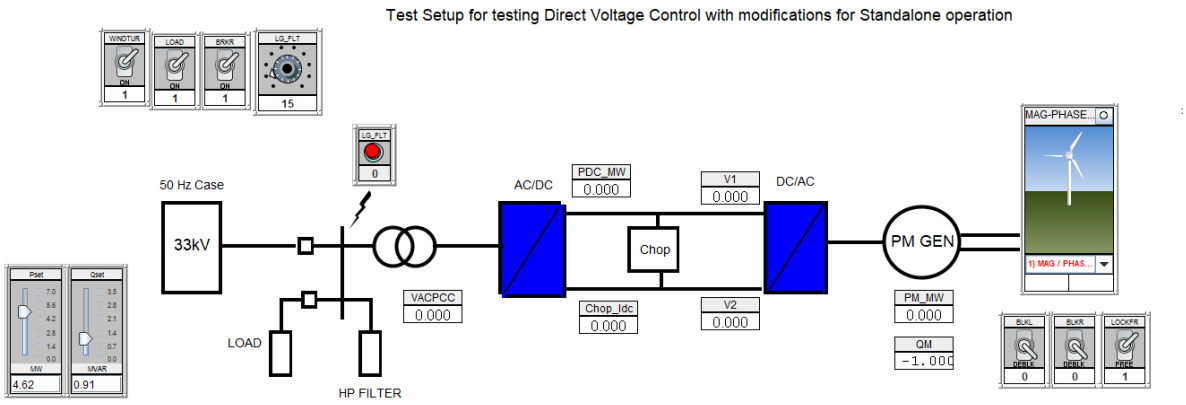

Figure 3.6: Test Setup for Validating Direct Voltage Control based *grid-forming* strategy

3.3.1. OPERATION IN GRID CONNECTED MODE

The first thing to be tested after finalizing the control strategy and implementing it on RSCAD was the performance of the wind turbine operating with Direct Voltage Control while being connected to an equivalent infinite grid. In order to analyze the performance and making sure the voltage and frequency stability was maintained a three-phase short circuit event as well as a load connection event was simulated. Based on trial and error, the proportional control and washout filters used in the inner loop control were tuned, whose parameters are listed in table 3.1. These parameters were used throughout the development in this thesis. Although, no small signal stability assessment was carried out for the determination of these parameters, yet these values were consistent, as the trial-and-error was based on real-time modifications during the simulation.

PERFORMANCE UPON LOAD CONNECTION

The response of the system under test (figure 3.6) when a load of 4.62 MW and 0.9 MVAR is connected at 2 seconds is recorded in figure 3.7. Until 2 seconds, the system is balanced and the wind turbine is providing 5.6 MW of power to the infinite grid. Upon connection of load (4.62 MW and 0.9 MVar) at 2 seconds the frequency and voltage slightly drop at the PCC which is the expected response of the system. The drop in voltage is observed because of the reactive power requirement of the load. However, as can be observed the system restores its stable operation within two seconds and the voltage settles at a new value (0.98 p.u.) within a second of load connection.

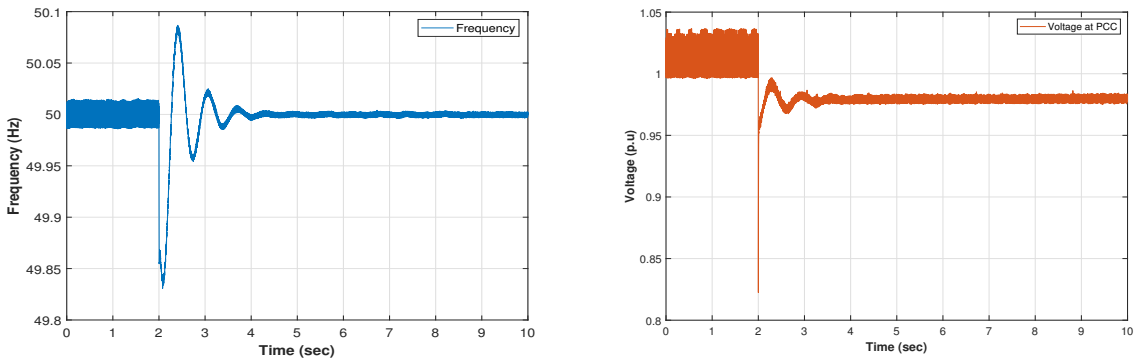

(a) Frequency at the measured bus upon load connection of 4.62 MW and 0.9 MVAR

(b) Voltage at the measured bus upon load connection of 4.62 MW and 0.9 MVAR

Figure 3.7: Voltage and frequency at the PCC following load connection

THREE PHASE LINE-TO-GROUND FAULT

A three phase line to ground fault with a clearing time of 140 ms was created at the PCC. In this scenario, no load was connected to the system. The frequency and the voltage during and following the fault are recorded in figure 3.8a and 3.8b respectively. When the fault occurs at the PCC the wind turbine generator's power is lost for 140 ms as the generation in the system is lost. The presence of the infinite grid means that the load is still connected to the system leading the drop in frequency following the fault. However, as soon as the fault is cleared, the system restores to its pre-fault operation case. The voltage oscillates slightly following the fault recovery because of the fast dynamics of the controller and reactive power requirement of the system.

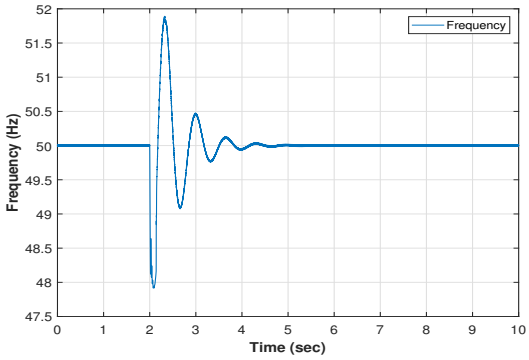

(a) Frequency at the measured bus following the fault

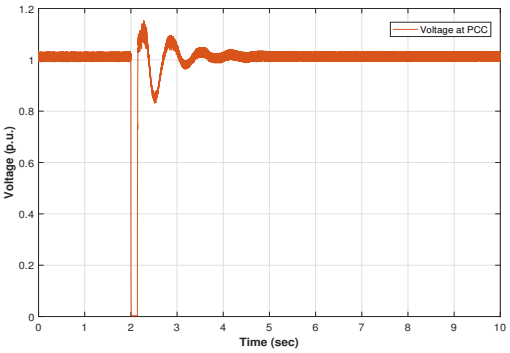

(b) Voltage at the measured bus following the fault

Figure 3.8: Voltage and frequency recovery by wind turbine following a fault in grid-connected operation

3.3.2. STANDALONE OPERATION IN ISLANDED MODE

After establishing the wind turbine control that fulfills all the grid requirements in load and short-circuit events when operating in the presence of an infinite grid, the performance of the modification suggested for standalone operation is analyzed in this section. The scenarios analyzed mainly relate to the disconnection of the grid, as well as connection of load while operating in standalone mode.

GRID DISCONNECTION

The voltage and frequency response of the system following the grid disconnection is shown in figure 3.9. Prior to the grid disconnection at 1 sec, a load of 2.3 MW and 0.91 Mvar remains connected to the sytem. This is because if there is no load, the wind turbine in standalone mode will operate as an open circuit as there will be no power transfer taking place. Thus prior to grid-disconnection the load (2.3 MW, 0.91 MVar) remains connected.

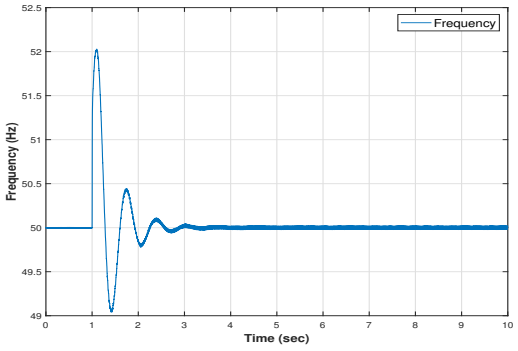

(a) Frequency at the measured bus following the grid disconnection

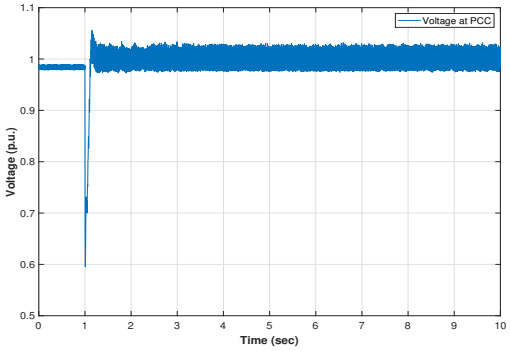

(b) Voltage at the measured bus following the grid disconnection

Figure 3.9: Voltage and frequency recovery by wind turbine following grid disconnection

As can be observed from the figure 3.9a, the frequency at the instant of grid disconnection increases. This happens because, the wind turbine is producing more power than that required by the load and hence at the instant of fault there is more power being generator than that required by the system. However, the frequency recovers within 2 seconds after disconnection of the grid thereby stabilizing the load. Moreover, the voltage as observed in figure 3.9b increases as the power being generated is more than that required, although it remains within the permissible limits of 1.05 p.u. One thing to notice here is that the voltage has some fluctuations when operating without any grid. The main reason for that is the measurement filters being used. The measurement filters are tuned for the washout filters used with Direct Voltage Control and hence during the standalone mode (disconnection of grid), the control switches to using the Standalone operation as explained in section 3.2 which induced fluctuations in voltage measurement. These high frequency components are primarily because of the measurement filters and do not impact the performance of the control as the voltage waveforms are more or less sinusoidal (figure 3.10). However, there are slight fluctuations in power as well owing to these fluctuations in voltage, but without any grid or storage present in the system, such fluctuations can be expected

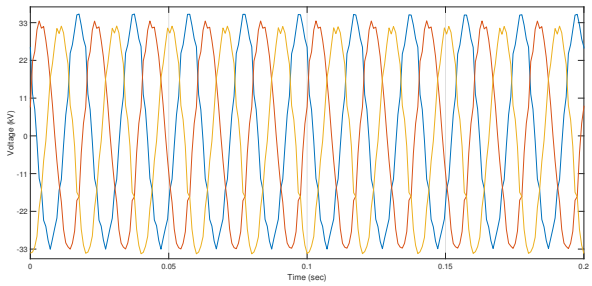

Figure 3.10: Voltage waveform during standalone operation with no grid connection

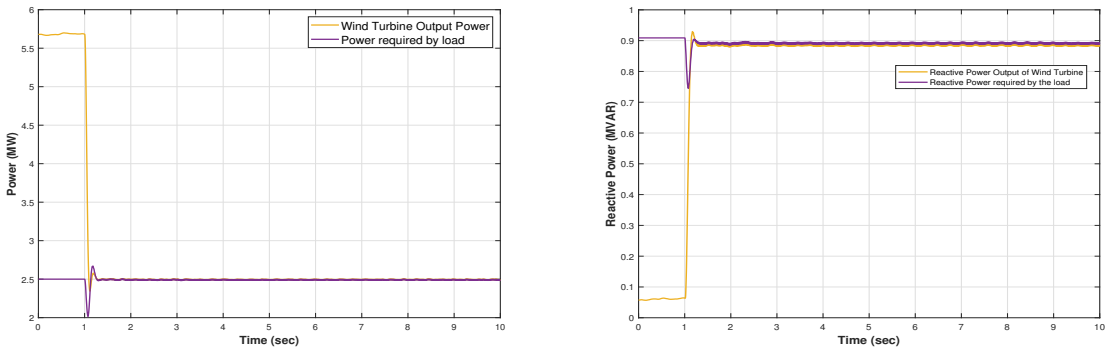

(a) Active power of the wind turbine and the load

(b) Reactive power of the wind turbine and the load

Figure 3.11: Active and reactive power output of the wind turbines

Moreover, following the disconnection of the grid, the power output of the Wind turbine, tries to match the power output of the load. As the load is only 2.5 MW, the wind turbine matches the load requirement, however this increases the DC link power and thus its voltage. This will lead to the mechanical chopper acting more frequently which is undesirable[1]. The Active and reactive power response of the wind turbine following the grid disconnection can be observed in figure 3.13.

[1] The inertial support from the wind turbine can not work for an extended time period, and therefore in order to protect the DC link, the Yaw control of the wind turbine should act which will change its direction from the wind making it produce less power. Although, yaw control is a slow response as it involves rotating the wind turbine along its vertical axis and hence the DC link should be capable of withstanding such frequent chopper actions. However, such operational scenarios are not considered here

LOAD CONNECTION IN STANDALONE OPERATION

In this scenario, the wind turbine was made to operate without any grid or load connected initially. The voltage reference for the Standalone Operation in section 3.2, was set to be equal to 33 kV instead of the load voltage to ensure that the voltage value never goes out of bounds. A load of 4.62 MW and 0.9 MVar was connected at 1 sec. Figure 3.12 shows the voltage and frequency response of the system under such a scenario. The frequency slightly drops when more active power is demanded at the PCC upon the load connection. In case of voltage, since before load connection the wind turbine is basically open circuited, the voltages of 1.1 p.u is open circuit voltage. Upon connection of load requiring 0.9 MVar of the reactive power, the voltage drops back to 1 p.u (with slight fluctuations as has been explained previously).

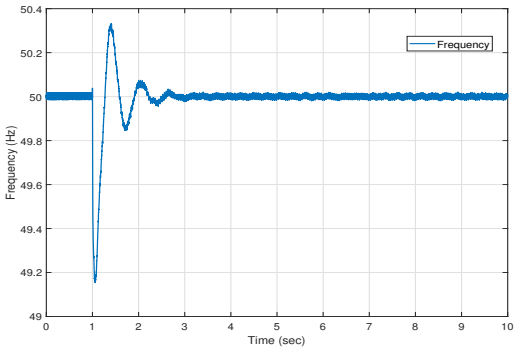

(a) Frequency at the measured bus upon load connection of 4.62 MW and 0.9 MVAR

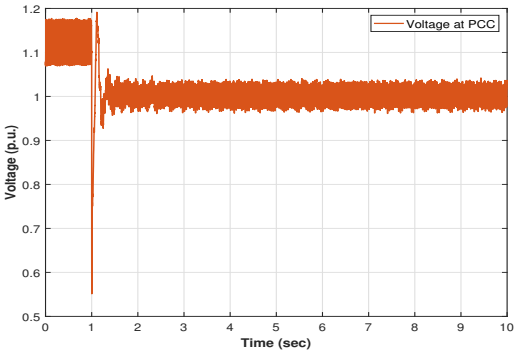

(b) Voltage at the measured bus upon load connection of 4.62 MW and 0.9 MVAR

Figure 3.12: Voltage and frequency at the PCC following load connection in standalone operation

For the active and reactive power, since the wind turbine is initially open circuited, no current and hence no power is being delivered as an output by the wind turbine. Upon connection of the load, the wind turbine provides enough power to meet the load requirements [2]. Therefore, the Direct Voltage Control when complimented with the U-f mode control strategy based on microgrid applications, can enable the operation of wind turbine even in a standalone mode.

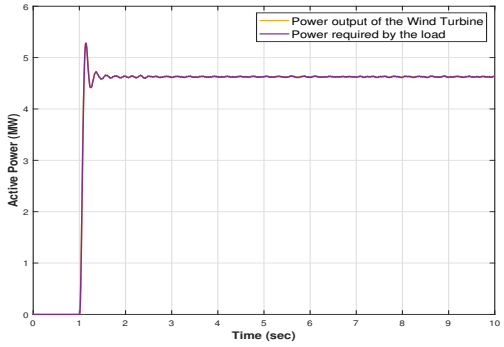

(a) Active power of the wind turbine and the load in standalone

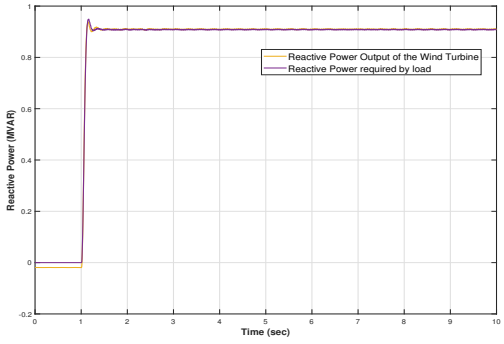

(b) Reactive power of the wind turbine and the load in standalone operation

Figure 3.13: Active and reactive power output of the wind turbines

The developed *grid-forming* control based on the Direct Voltage Control complimented with the Standalone operation mode based on the microgrid application works well in both grid connected and standalone mode and is able to meet the grid requirements during short-circuit or load events. However, it is highly

[2] It is assumed that the maximum load that can be connected in this case can not exceed the output power of the wind turbine as it cannot provide any excess power

unlikely that the wind turbine will be operating in a standalone mode, as even in microgrids there will be a diesel generator or a battery connected. Therefore, it is more important to validate the control strategy in a larger network where its operation makes more practical sense. With the *grid-forming* control strategy it is possible to increase the penetration of the PE interfaced generation extensively more than what could be accomplished by the *grid-following* control. The next chapter puts that notion to test and analyzes the performance of the Direct Voltage control in network integrated with high PE converter based generation.

4

CONTROL CHALLENGES IN GRID-CONNECTED MODE

After successfully establishing the *grid-forming* control in standalone operation, it makes sense to look into the performance of the developed wind energy systems in bigger networks. The *grid-forming* should be able to operate in islanded and grid-connected mode, and the performance should be better or as good as other developed control strategies working in grid-following mode. This chapter discuss and analyzes the performance of the developed control in 9-bus system for 52% PE-converter based generation (Wind Energy) in RSCAD. Later on, the chapter also explores the transient performance of the controller in higher PE converter based scenarios reaching up to 75%. For both the test systems, the controller capability is tested for both voltage and frequency support. Moreover, for frequency support during normal operation, the inertia emulation is used for extracting power from wind turbine's kinetic energy [55], as will be further explored. In order to achieve these functions of properly balancing voltage and frequency regulation, slight modifications and additions are done to the Direct Voltage Control discussed in Chapter 3. The IEEE 9-bus system on RSCAD was modified to include wind energy systems and the developed network model is represented in figure 4.1. In the test setup of 4.1, a wind turbine delivering 5.6 MW of active power with the developed control strategy is scaled up to 15 times to create two equivalent wind farms delivering 84 MW each.

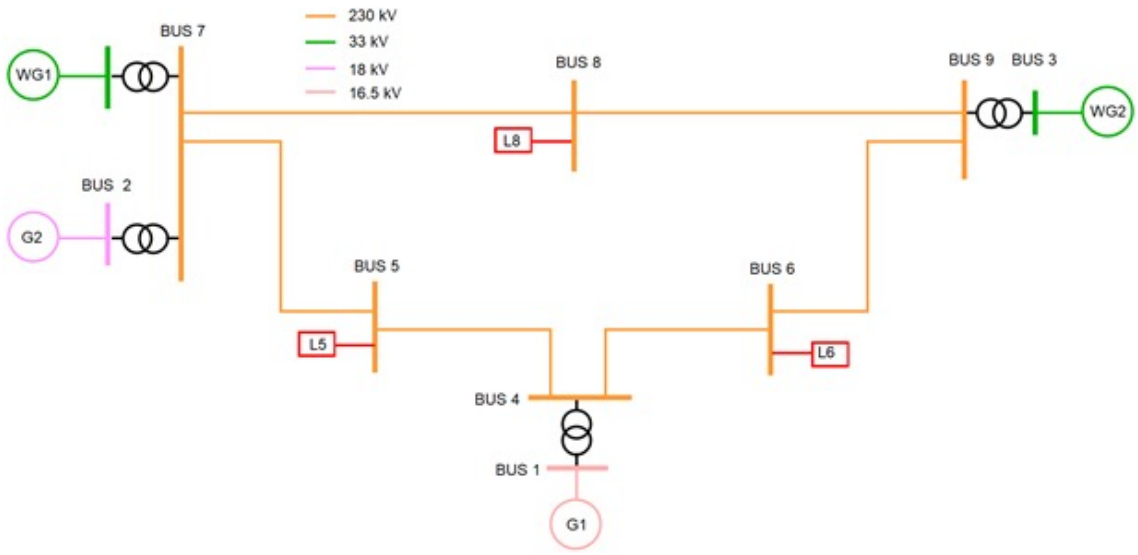

Figure 4.1: Modified IEEE-9 bus system for including 52% generation from Wind Turbines

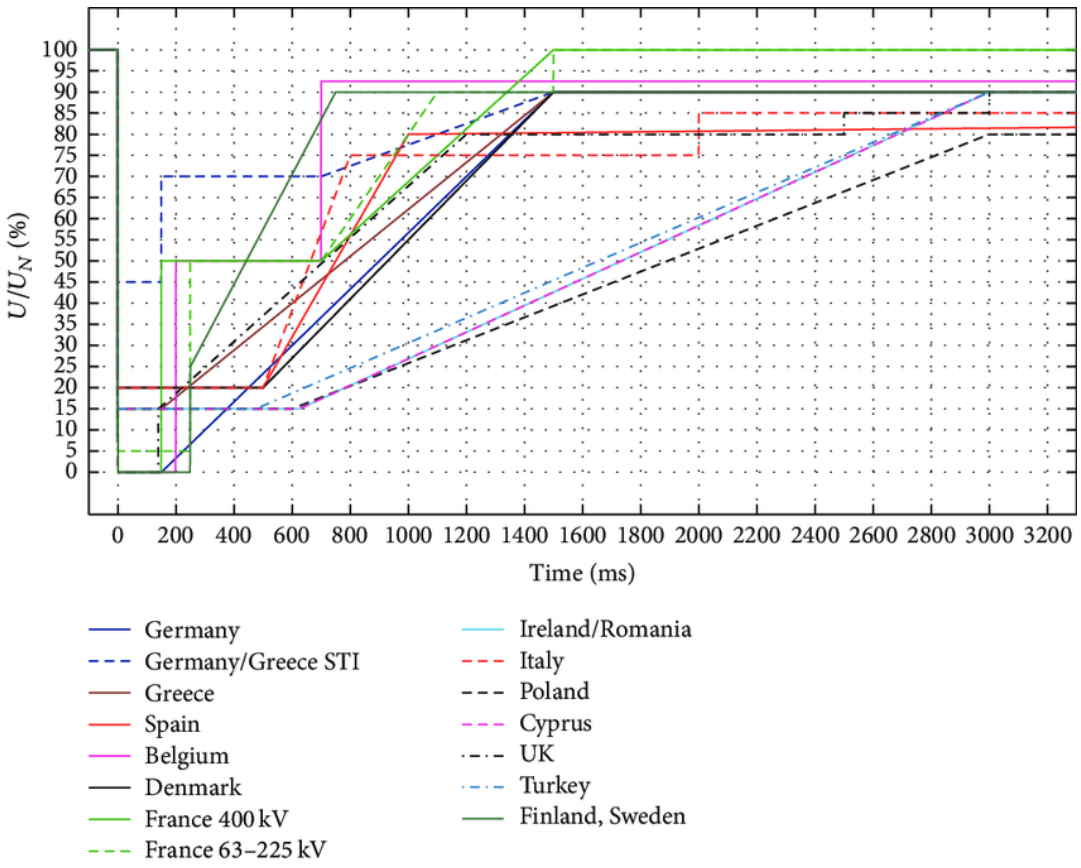

Figure 4.2: LVRT requirements for wind farms in various grid codes [83]

4.1. FAULT-RIDE THROUGH CAPABILITY OF THE CONVERTER

The low voltage ride through is the most important requirement regarding wind farm operation that has been recently introduced in the grid codes. It is vital for a stable and reliable operation of power supply networks, especially in regions with high penetration of wind power generation [83]. In the past, the wind farms were allowed to be disconnected following a fault, however, such a disconnection is not possible in case of high PE converter-interfaced renewable generation. A very recent example of consequences of such a disconnection of the wind farm came into light in UK [19], [24] when the Offshore wind farm got disconnected following a fault in the onshore grid. Figure 4.2 shows the requirements of different grid codes for the wind farms to remain connected to the grid.

In order to investigate the controllers performance in case of short-circuits and ensuring that the equivalent wind farms remain connected to the grid, the wind turbines should follow the grid-codes based on the network they're connected to. This can be a bit tricky because every grid code has a different requirement as can be concluded from figure 4.2. For instance the grid code requirements by Tennet TSO GmbH, Germany, requires the wind farms to be connected even when the voltage at PCC (point of common coupling) drops to zero, and requires injection of active power by the wind farms as soon as the fault is released, which should increase linearly. On the other hand, Sweden has two different LVRT requirements based on the total power capacity of the wind farms (less than or greater than 100 MW). Therefore, the design of the controller should be such that it can work with more or less all the grid-code requirements. The Direct Voltage control allows for such a capability. Moreover, the use of washout filter allows it to have a faster response to any short circuit events making the controlling action similar to that of synchronous generators.

However, such fast controlling action can sometimes lead to an overshoot in the voltage following the fault recovery. In order to avoid the injection of active power during this overvoltage scenario, the control scheme based on Voltage Dependent Active Current Control (VDACC) [82] is added to the Active power control

channel. It must be stated that the Direct voltage control does not rely on the injection of reactive current for voltage control but rather uses the feed-forward term of the voltage at PCC, for controlling voltage, because of which the voltage control is not severed with by the action of VDACC.

4.1.1. ADDITION OF VDACC FOR IMPROVEMENT IN FRT CAPABILITY

In the case of faults, the current output of the wind turbines needs to be limited. This limitation of current is mainly due to the current capability of power electronics converters, as they cannot provide excess current. Below 0.9 p.u. of voltage, reactive current priority applies which leads to a reduction in injection of active current. This allows for improved FRT capability to the Direct Voltage Control, allowing it to meet the grid-code requirements. In Direct Voltage control, this limitation is ensured by the Current limitation algorithm discussed in Section 3.1.3. However, to ensure the stable operation of wind farm, a further reduction in current might be required which is governed by the equation 4.1 [36]. In equation 4.1, Z is the grid impedance as seen by the equivalent wind farm and U_{grid} is the grid voltage.

$$I_{conv_{max}} = \frac{-U_{grid}}{Z} \tag{4.1}$$

It is not at all counter-intuitive that increasing the reactive current during the fault, will lead to reduction of active power. This certainly has a positive impact on the transient stability. However, some control schemes implemented by different manufacturers focus on fulfilling only the minimum grid code requirements because of which they limit the reactive current injection to 1 p.u. [67]. However, this limit on the reactive power can leave room for active current injection, which can negatively impact transient stability[36].

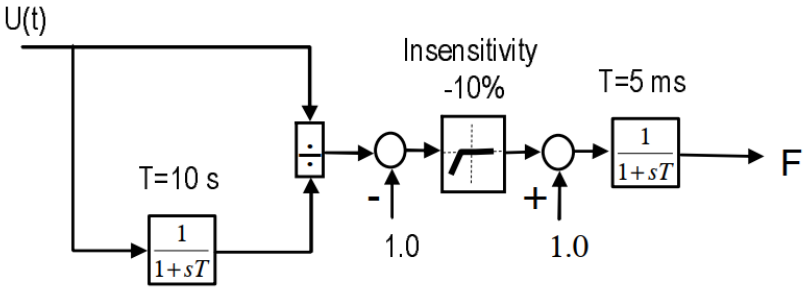

Figure 4.3: Voltage-Dependent Active Current Control

Although Direct voltage control, automatically adjusts its reference according to the grid voltage and voltage at PCC, it might require a further controlling in the active current to make sure that injection of active current component is limited. In order to accomplish that, the control strategy used in [82] [36] is added to Direct Voltage control to have the active power output based on the experienced voltage dip. The implementation of the VDACC is based on the block diagram represented in figure4.3. The output of this control is implemented along with the active current control loop based on the following equation 4.2 [82]. In this governing equation, P'_{ref} is the power reference generated by the DC voltage control and frequency support control discussed previously in Section 3.1.2 (figure 3.3).

$$I_{d,ref} = F^2 \frac{P'_{ref}}{V_{PCC}} \tag{4.2}$$

The effect of this is fast voltage recovery accompanied with reduced (or no) overshoot in the voltages as is discussed in Section 4.3. Moreover, the VDACC allows for an improved frequency recovery because of being able to control active power instantly after the fault is released.

4.2. MODIFICATION IN MSC FOR INERTIA EMULATION

The control modification for emulation of inertial response was introduced in Chapter 3 in subsection 3.1.2. The modifications proposed were only for the Grid-side converter. The signal generated for the inertial response based on frequency change in the network, is also required to be sent to the machine side

converter for extracting rotor kinetic energy. The modifications required to be made in the Machine side controller are shown in figure 4.4. The signal generated based on the frequency change is added to the machine power which is responsible for calculation of the *optimal rotor speed*. Any changes in the power measurement are reflected in the value of rotor speed which helps in extracting inertia from the rotor. As the rotor speed and the torque A sudden decrease in the rotor speed, for instance increase the power output of the turbine, thereby allowing the wind turbine to provide inertial support.

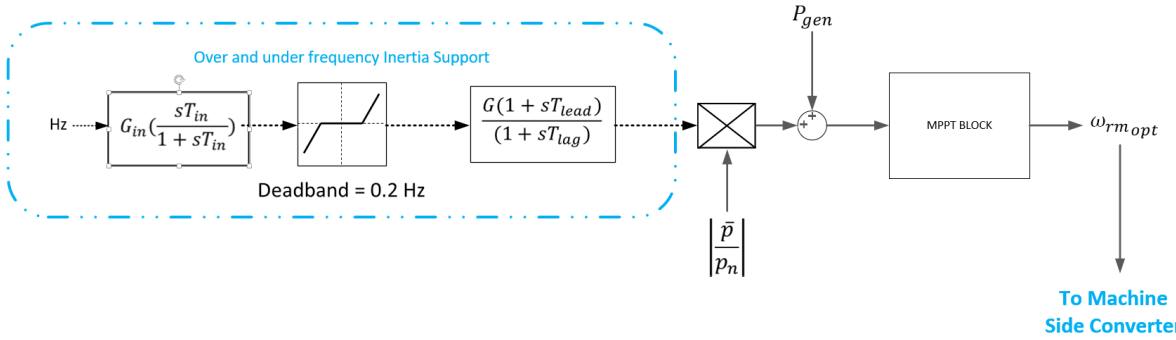

Figure 4.4: Addition of Inertia Controller to MSC

Various strategies exist in literature regarding provision of inertial support from wind turbines. Most of them are based on providing a supplementary signal to the pitch controller of the wind turbine. GE's WindINERTIA^{TM} feature provides an inertial response capability for WTs by introducing a washout filter to temporarily increase the output power of the wind turbine [59]. A washout filter based strategy is also proposed in [62] to make wind turbines act in a transient way using the stored kinetic energy. However, the control response based on the derivative of the frequency ($\frac{df}{dt}$ like the one used in [59], [62] have an inevitable response delay as they are based on measurement of frequency (frequency measurement delays can cause response delay)[81]. In order to cope with it, a lead-lag compensator is used to minimize the delay in operation. Other methods based on providing Virtual Synchronous Control and optimizing the PLL have also been considered in several works [81], but all the methods essentially accomplish the same task of extracting the kinetic energy of the wind turbine to support any power changes in the grid, and each has their own pros and cons. The method based on using a washout filter cascaded with a deadband and lead-lag compensator was chosen for this work as it can be easily integrated with the Direct Voltage Control scheme, without requiring any major modifications in the controlling action. However, the inertial response by the wind turbine using the method of figure 4.4 can sometimes cause slight issues during the FRT mode operation of the wind turbines as the frequency of the system also changes temporarily during the fault. Since the method used here detects any changes in the frequency, it might cause some oscillations in the wind turbine operation during fault recovery. This issue was identified prior to making the test on the performance and hence the control was designed such that the inertial response is disabled during the time period of the fault. As both the direct voltage control and the inertial response makes use of the washout-filter their response is very quick and thus it becomes necessary to disable the inertial response from the wind turbine to avoid any controller interactions. Moreover, the VDACC scheme discussed in the previous section 4.1.1 makes sure that any active power requirements of the system are met.

The inertial control when cascaded with the Direct Voltage control performs as expected during any power changes in the network. The next section describes in detail about the tests performed for validating the controller's performance.

4.3. SIMULATION SCENARIOS FOR 52% WIND ENERGY GENERATION

The modifications made in the Direct Voltage Control of Chapter 3 have been discussed in this Chapter so far. In this section, several tests are performed with the Direct Voltage control with and without the modifications proposed in this chapter. Tests are made on the modified 9-bus system (figure 4.1) to anlayze

the LVRT requirements of the equivalent wind farms. After analyzing the controller for short-circuit events [1], load change events are simulated to test the performance of the inertial controller discussed in the previous section 4.2.The controllers performance is tested for load change events, to analyse whether the proposed inertia controller in section 4.2 was working as intended and if further modifications might be needed to further enhance the performance of the controller. The parameters for the generation and loads of the modified 9 bus system are recorded in table 4.1

WG1	84 MW	L8	100 MW	G2	76 MW
WG2	84 MW	L6	90 MW	G1	Slack Generator (~ 75 MW)
		L5	125 MW		

Table 4.1: Load and generation parameters for the developed test system working at 52 % PE interfaced generation

4.3.1. TRANSIENT STABILITY OF DIRECT VOLTAGE CONTROL WITH VDACC

The test setup developed in figure 4.1 was used to test the performance of the controller in the grid connected mode. The developed control's performance is tested for the transient stability following a three-phase line to ground fault.

FRT COMPARISON WITH DIFFERENT CONTROL SCHEMES

In order to investigate the performance of the developed controller for fault-ride through capability, several test were made and compared with the existing control strategies in grid-following wind turbines as well as the performance of the synchronous generator. The controller proposed in section 4.1.1 outperformed the other control strategies and gave results which were very close to the performance of the Synchronous generator. It must be noted, that the time constant of the first delay block in figure 4.3 was changed from 10 sec to 0.3 sec to reduce the delay in the control of active power.

Figure 4.5 and figure 4.6 compares the performance of different control schemes for a three-phase line to ground fault. The Direct Voltage Control developed in this work was cascaded with two other controllers to identify the performance of each modification. Moreover, it is compared with the performance of the synchronous generator, and a grid following wind turbine with Synchronous Damping Control activated. Based on the figures 4.5 and 4.6, the following observations can be made

- It is interesting to note that the *grid-following* wind turbine control with Synchronous Damping (SDC) provides improved performance as well, in the given test network, and was thus also used as a basis for comparision with the Direct Voltage Control. Moreover, SDC might further improve the *grid-forming* Direct Voltage control if they can be successfully integrated.

- One modification made in the DVC was the inclusion of FRT control mentioned in [67], which directly sets the reactive current reference to 1 p.u., and bypasses the Direct Voltage control altogether. As mentioned in [82] and [36], it was observed that the control scheme based on directly setting the reactive current reference to 1 p.u. does create some oscillations in operation following the fault-recovery. Moreover, the inclusion of such a control rather hinders the performance of the Direct Voltage Control, as can be observed in figures 4.5 and 4.6.

- The second modification in the Direct Voltage Control (3.1.1) is discussed in this chapter based on VDACC (section 4.1.1). As previously stated, the modifications made by the VDACC does not affect the voltage control, which can also be observed based on figure 4.5. The voltage recovery of the Direct Voltage control with and without VDACC is more or less the same. However, a major improvement is observed in the frequency response following the fault, when Direct Voltage control is supplemented with VDACC. The improvement in the frequency is very close to that of a synchronous generator, as shown in figure 4.6, and hence the direct Voltage control supplemented with VDACC can be considered to outperform all the existing control strategies.

[1] The faults analyzed in this work are three-phase line to ground faults (symmetrical) as this controller does not provide controllability of negative sequence components

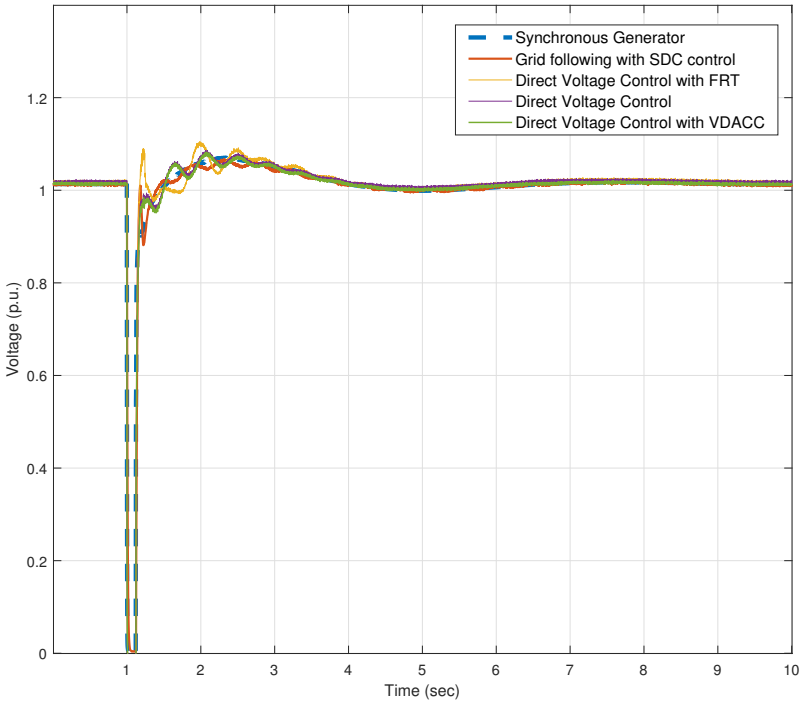

Figure 4.5: Frequency recovery following the fault

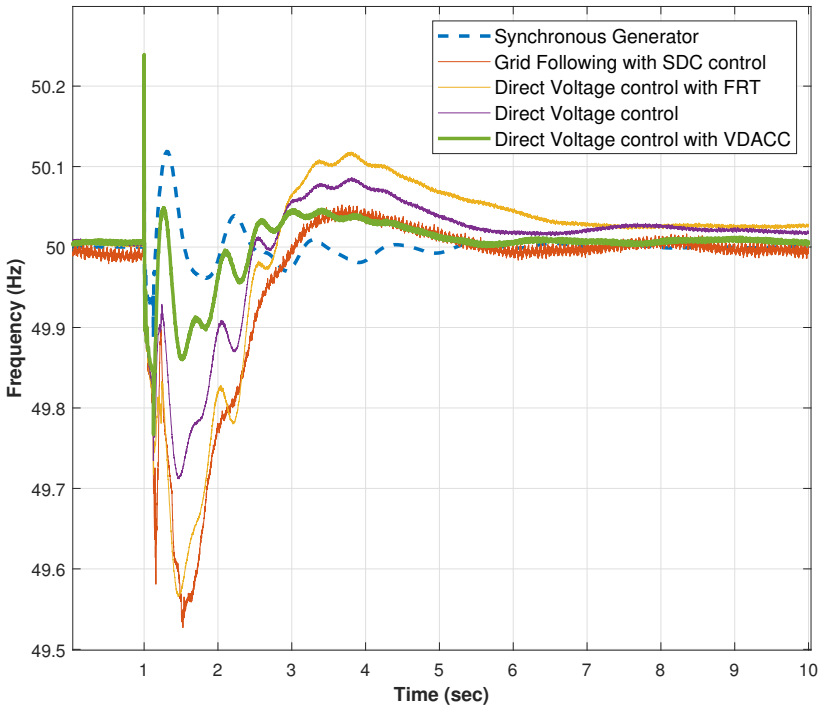

Figure 4.6: Frequency recovery following the fault

It must however, be noted that in figure 4.6, the initial transient at 1 sec is due to the delay in measurement, as it occurs exactly at the same instant when the fault happens. This measurement delay does not affect the performance of the control in any aspects, and exists because of the PI controllers of the PLL used for measuring frequency.

ADVANTAGES OVER THE EXISTING SDC CONTROL

One might argue that the voltage performance of the *grid-following* converter is equally good as of the developed control of Direct Voltage Control with VDACC. Even the frequency response of SDC control if not as good as that of the developed control, still satisfies the grid-code requirements. Therefore, it becomes necessary to state the importance of the developed control strategy. This can be done simply based on a comparison between the converter current output of both the control strategies 4.7. The converter current output of the SDC control is based on minimizing the rotor angle instabililty following a fault, which might become a critical factor in operation of onshore wind-farms in weak grid. Hence, the converter current output of the *grid-following* wind turbine with synchronous damping control (SDC) fluctuates more during the fault. The Direct Voltage Control with VDACC accomplishes the same results of minimizing rotor angle deviation, with no increase in converter current output. Moreover, the converter current limits are never exceeded using the Direct Voltage control with VDACC, and hence there is no operational risk the power electronic components of the converter. Although in case of SDC control, the converter currents go as high as 1.45 p.u. which might cause stress on the power electronic components of the converter and might even trip the internal breakers of the wind turbine converters, stalling their operation [2]. The spikes in the current measurement of the SDC are due to the use of washout filters for measuring the rotor angles. Such an approach corresponds to the shown converter currents as during the fault the rotor angle of the syncrhonous generators changes were quickly which leads to such spikes in the converter current measurement. On the other hand, the use of VDACC also helps in improving the rotor angle stability of the system during fault conditions. This happens because VDACC tries to reduce the active power injection of the wind turbines during the fault, thereby allowing the synchronous generator in the system to inject some power thereby improving rotor angle stability. All these factors highlight the clear benefits of the *grid-forming* control scheme using Direct Voltage Control with VDACC over any other existing control schemes.

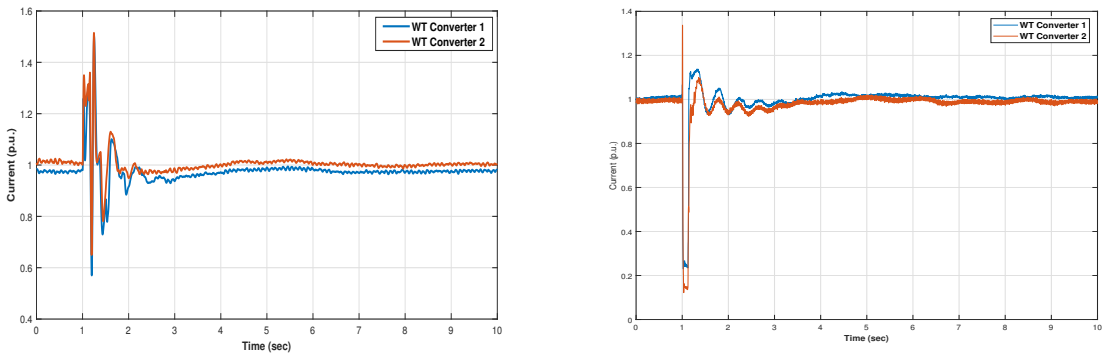

(a) Converter current output for *grid following* wind turbines with SDC control

(b) Converter current output for *grid forming* Direct Voltage control supplemented with VDACC

Figure 4.7: Comparison of converter output currents based on different control strategy

ROBUSTNESS OF THE DEVELOPED CONTROL

In order to test the developed control strategy to its limits, another test was made by creating a fault at all the buses in the network to identify the controller's performance in critical scenarios. Instead of plotting all the aspects of the system, the emphasis was made on measuring the frequency as it is a global parameter and

[2] It must be noted that the first transient in both the cases in current measurement is due to the measurement delay as it occurs at the instant of the fault (1 sec). However, for other spikes in the converter current of SDC, it is due to the control and not the used measurement filters.

indicative of the system's stability. The results obtained for the faults created at various buses are recorded in figure 4.8. As can be observed, the faults occurring close to the load buses, did not affect the system frequency to that extent as the support from the three generators was present. Although, the faults close to the generation buses were more severe. In case of fault at bus 4, which is the closest to the slack bus, the frequency tends to increase. This happens because of the quick power injection by the synchronus generator at bus 1 because of which the frequency and voltage recovery is governed more by the synchronous generator rather than the equivalent windfarms.

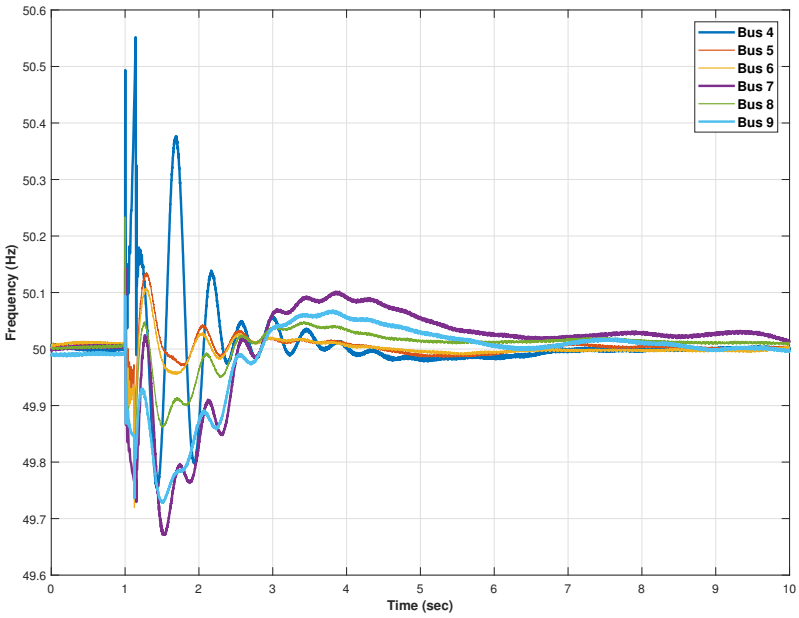

Figure 4.8: Frequency at the measured bus for faults at different buses in the 9 bus system

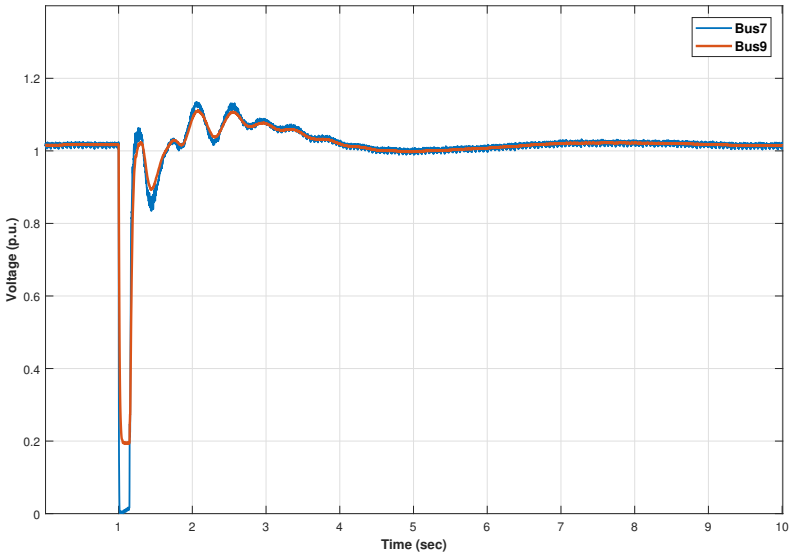

Figure 4.9: Low voltage ride through of the connected wind farms during fault at bus 7

Moreover, as can be expected, the most severe fault was at bus 7 which has a total generation of 160 MW connected to it, because of which frequency takes the longest to recover back to 50 Hz. However, even during such an instance the system remains stable, as frequency eventually stabilizes and the connected windfarms operate under the LVRT requirements of the grid code. The voltage at the buses at which the wind farms are connected is plotted in figure 4.9. As can be observed the voltages recover quickly following the fault clearing. However, the voltage might be a bit higher than 1.05 p.u. for a few seconds, but based on the grid codes mentioned in [57], such a behaviour can be tolerated by the system [3].

4.3.2. OVER-FREQUENCY AND UNDER-FREQUENCY PERFORMANCE OF THE INERTIA CONTROLLER

In this subsection, two load change scenarios are simulated to analyze the performance of the inertial controller in both over and under frequency scenarios.

UNDER-FREQUENCY INERTIAL SUPPORT

The Direct Voltage Control with VDACC is a robust control strategy for enabling the power systems with high PE converter-based generation, as has been established in the previous subsection. However, the previous subsection is focused on the performance in case of short-circuit events and the Direct Voltage Control with VDACC does not improve the system's performance in case of load events. The modifications proposed in the section 4.2 must be included with the Direct Voltage control to provide for the improved performance in case of load changes. In this subsection, a scenario for 5% load change was simulated and the performance of the wind turbine with Direct Voltage Control was compared with the case without Direct voltage Control and when the Direct Voltage Control had Inertial support. The frequency response of the system with 50% generation from PE converters is recorded in figure 4.10. The inertial response demands more power from the wind turbine rotor to be extracted, in case of frequency change. The controller mentioned in section 4.2 helps in achieving that extraction of power. However, this power is available for a limited time, as the kinetic energy can only be extracted for short span of time to avoid any swings in the wind turbine rotor. It must be realized that in figure 4.10 the response of the Direct Voltage Control is still superior than the base case where a grid-following wind turbine was used as a basis of comparison. The Direct Voltage control performs better mainly because of the increased capacitor size required by it (mainly upto 15%) when compared to a PI control based strategy, which allows it to have maintain the output power as can be observed in figure 4.11b. The wind turbine remains almost static to the power disturbance in the network. The Direct frequency control which accompanies the DC voltage control in the active power channel in figure 3.3 allows for maintaining constant power output at the point of common coupling so that the synchronous generators present in the system can act for providing excess required power. Figure 4.11 compares the system performance when Direct voltage Control is supplemented with the inertial controller and when it operates without it[4]. Clearly the inertial controller shows improvement in the frequency response as it allows extra power to be extracted from the kinetic energy to support the sudden increase in load. Since the operation of wind turbine is at high speeds, the mechanical and electrical power follow each other almost at the same instant of their increase or decrease, as is expected [65].

OVER-FREQUENCY INERTIAL SUPPORT

Over-frequency is a rare event in electrical power system. However, there is a possibility that it happens and the grid-connected wind turbine must be able to cooperate on frequency support during that kind of disturbances. The Direct Voltage control having inertial support provides for such a capability. As mentioned in [65], the wind turbine's electrical power can be reduced to provide frequency support as long as the rotor of the wind turbine does not reach its maximum value. The time required by the rotor to reach its maximum value is also dependent on the wind turbine speed. For our case used throughout the development of this work, the wind speed is 16 m/s which is equal to 1.33 p.u. (12 m/s being the rated wind speed). Under such an operation only inertial support can be relied upon for frequency regulation as the instant of drop (or increase) of the mechanical and electrical power of the wind turbine is the same. The control strategy discussed in

[3] The grid-code requirements might vary from one network to another. However, the requirements mentioned in [57] are mainly for steady-state operation (which are more stringent) as following a fault some overvoltage around 1.15 p.u. can be expected in high renewable scenarios.

[4] Figure 4.11 shows Power output of the wind turbine, which is scaled up to 15 times to create equivalent wind farms connected to the modified 9 bus system.

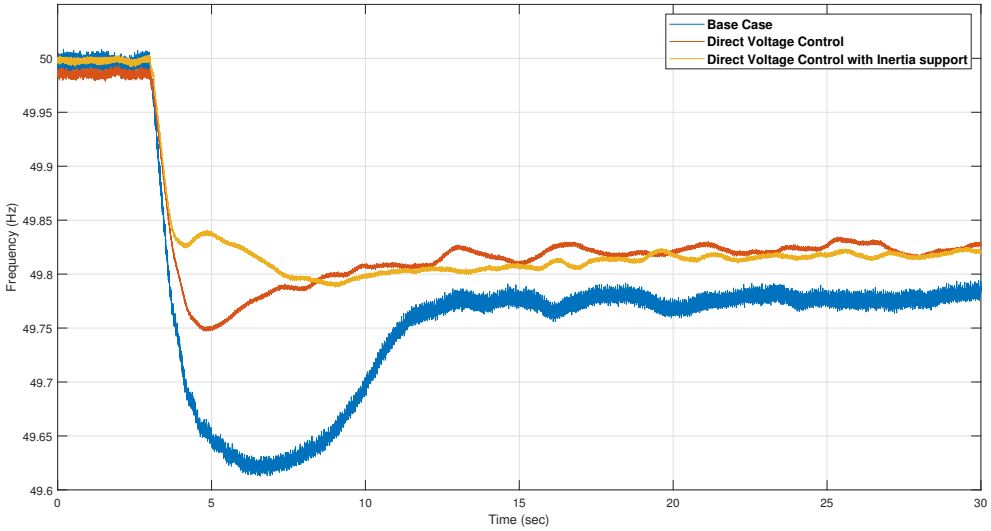

Figure 4.10: Frequency response of the system with 5% load increase

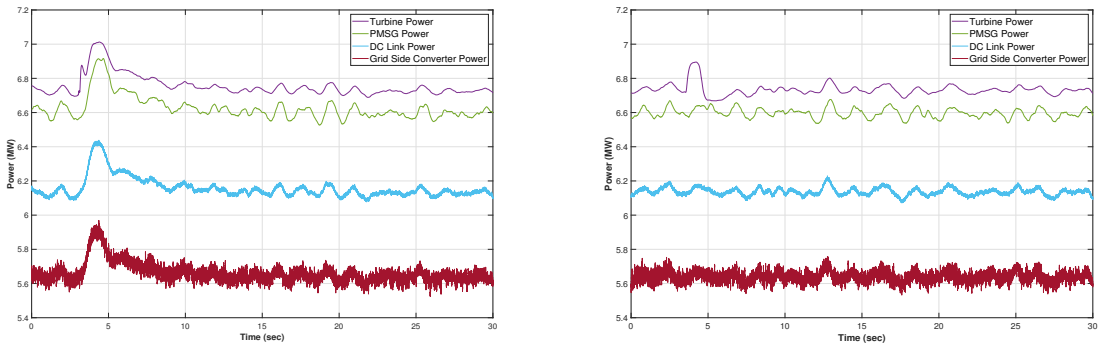

(a) Power Output of the wind turbine with DVC supplemented with inertial support

(b) Power Output for Wind Turbine with DVC without inertial support

Figure 4.11: Comparison between output powers of Direct Voltage control with and without inertial support

section 4.2 allows for such a provision for frequency support to the system. As can be distinguished from the figure 4.12, the Direct Voltage Control with inertial support significantly enhances the frequency of the system following a load event (load decrease of 20 MW). The corresponding increase in the wind turbine power and the output of the grid side converter are documented in figure 4.13. Since the operation of the inertial support has already been established in the previous subsection, no comparisons are made here, and the results recorded are more representative of the performance of the Inertial support based on the Section 4.2.

So far, the modifications and additions made to the Direct Voltage Control have improved the performance of the Direct Voltage control in both the load increase and decrease as well and three-phase line to ground faults. However, in the inertia controller, the impact on the wind turbine rotor is not analyzed. This can be an important issue while increasing the penetration of PE converter interfaced generation. The dynamics of the wind turbine rotor under inertial control can initiate some unforeseen interactions amongst other rotating mass in the network. Moreover, the implemented scheme for emulating inertia by wind turbines can have issues with its tuning primarily because of the presence of lead-lag compensator and washout filter. With increasing renewable generation, this again might initiate some controller interactions which can be difficult to predict because of the fast dynamics of the control scheme. One control scheme that might be provide

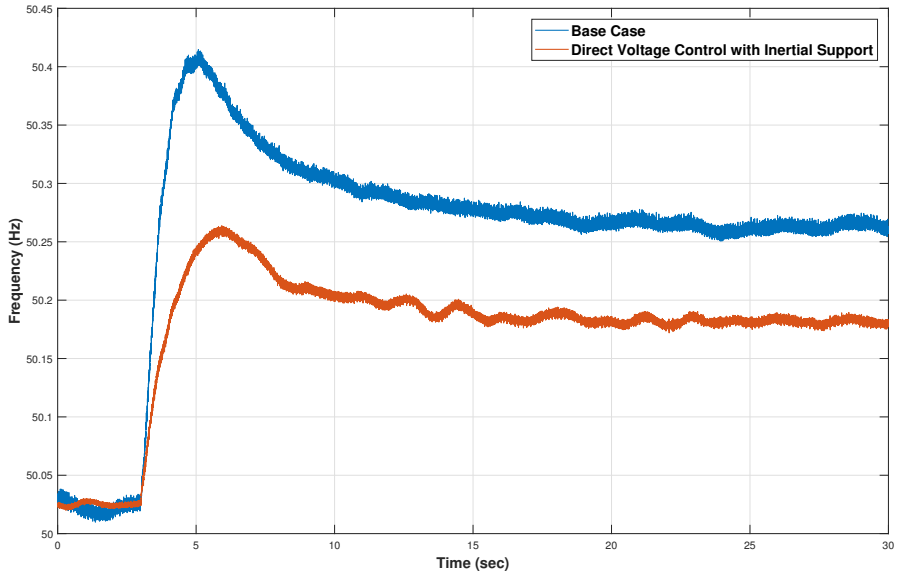

Figure 4.12: Frequency response of the system with loss of 20 MW of load (5% load change)

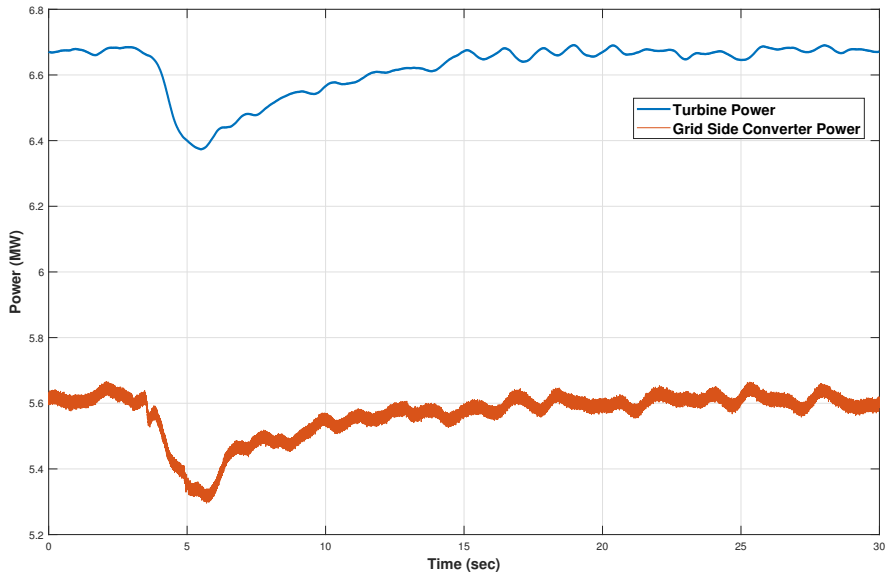

Figure 4.13: Mechanical and Electrical power outputs of the wind turbine for frequency support

a solution to avoid these interactions is based on Optimizing the PLL [47], [81], and might be interesting to look for future developments. It can possibly also improve the performance of the Direct Voltage control based *grid-forming* capability of the wind turbines as this control itself relies heavily on the performance of the PLL. Although, even without optimization of the PLL parameters[5], the Direct Voltage control scheme in itself is quite robust as has been established by its performance in high PE converter-interfaced generation scenarios (upto 52%). Having established the controller's performance in over 50% generation by wind energy systems, it makes sense to extend its application to higher PE converter based generation scenarios. The next

[5]In RSCAD different base models for PLL are available and the one giving the best response for the control application was chosen without any modification in its parameters.

section discusses more about testing Direct voltage Control with even higher penetration of wind energy (PE interfaced generation).

4.4. SIMULATION SCENARIOS FOR 88 % WIND ENERGY GENERATION

Based on the Control strategy discussed so far in this work, it was made possible to stabilize the 9 bus system even when the generation from Wind energy systems was as high as 88%. This section elaborates more about the tests performed and the areas where this control might lag behind. The test setup used for this section is represented in figure 4.14. The parameters of different generation and loads used in the system are mentioned in table 4.2.

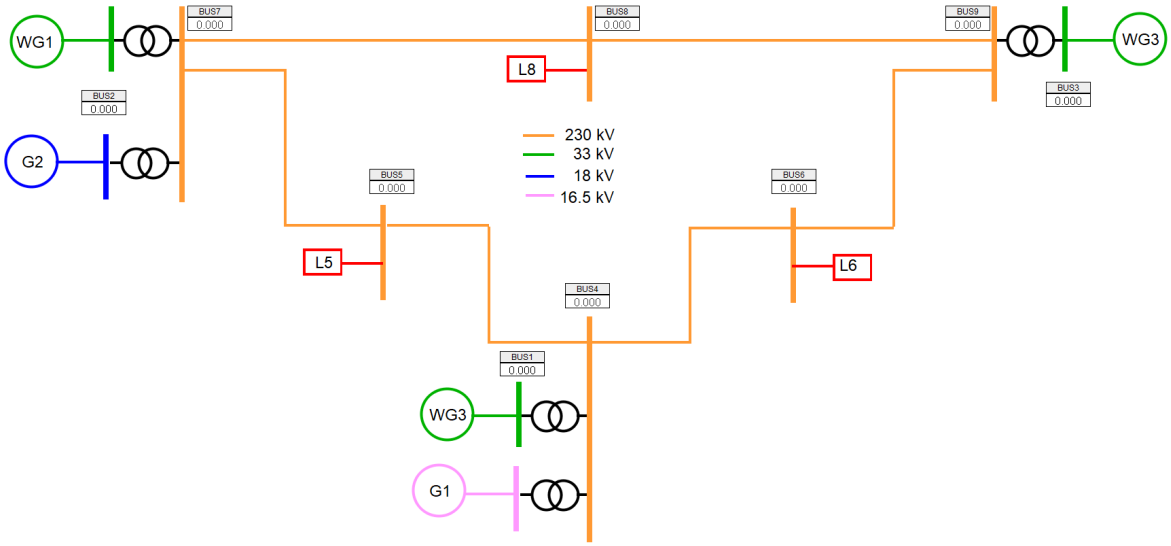

Figure 4.14: Modified IEEE 9 bus system for Transient stability assessment of the Direct Voltage Control in high renewable energy scenarios

WG1	168 MW	L8	120 MW	G2	17 MW
WG2	84 MW	L6	90 MW	G1	Slack Generator (~25 MW)
WG3	44.8 MW	L5	125 MW		

Table 4.2: Load and generation parameters for the developed test system working at 88 % PE interfaced generation

For the development of this test system operating with such high PE converter interfaced generation, two major challenges were encountered. When power electronic components are connected to the System, RSCAD software does not allow to run loadflow studies. This creates some initialization problems in the system because of which the synchronous generator G2 in bus 2 is still needed along with the generator G1. As the initial power flow can not be solved by RSCAD, in order to increase the PE converter interfaced generation, the load L8 was hence increased by 20 MW in comparison to the system used with 52% wind energy systems. Such a load increase was essential for stabilization of system frequency at 50 Hz. This scenario mainly deals with the testing of the system for transient voltage stability, as it was not possible the simulate for load change events in such high penetration of wind energy without any storage device or other inertial source present. The challenges for implementation of the frequency control are discussed later in this section.

4.4.1. FAULT RIDE THROUGH CAPABILITY

As described previously, the short circuit test was made similar to the section 4.3. The wind turbine control used for simulations in this section is the Direct Voltage Control with VDACC. As the advantages of VDACC

with Direct Voltage Control have already been established, no further comparisons were made without it being present. A three-phase short circuit event, with a fault clearing time of 120ms was simulated and the frequency response of the system following the fault is recorded in figure 4.10. As can be observed, the frequency recovers back to 50 Hz within 4 seconds. It might have some variation in the order of 10 mHz, but such deviations are expected in such high PE converter scenarios. The voltage at all the three buses where different wind farms are connected in the system also recovered within the grid codes and can be observed in figure 4.16.

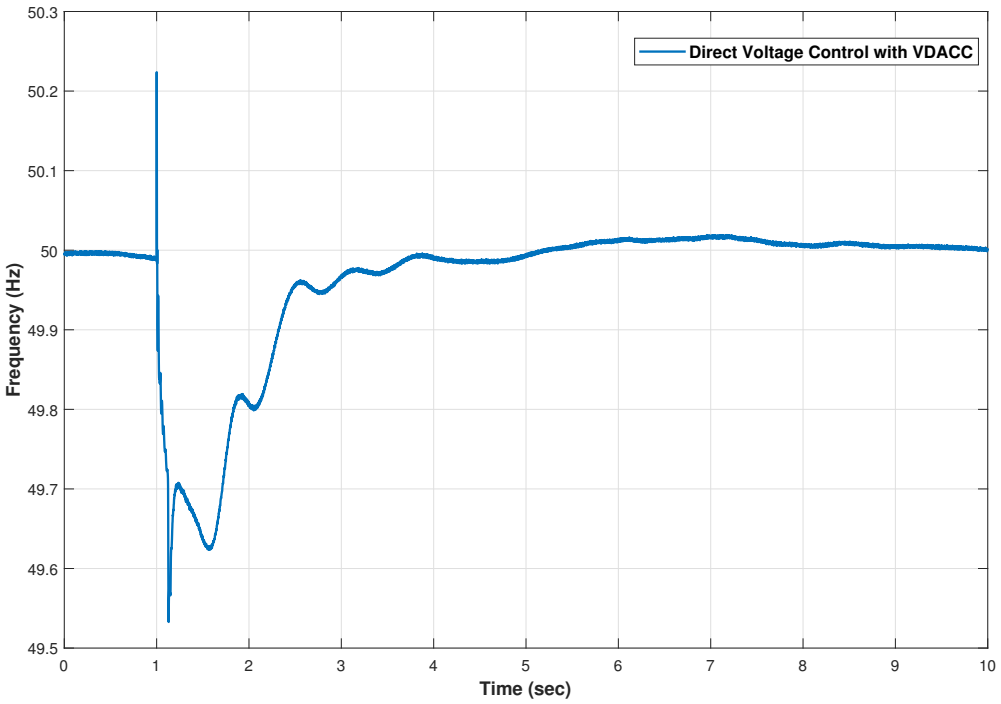

Figure 4.15: Frequency response of the system with 88% wind energy generation following fault at bus 8

As can be observed from the figure 4.16, the voltage drop is least for the windfarm 3. This is because it is connected along with the slack generator which has a very high inertia constant and it also acts quickly following the fault. The voltage drops to 0.1 p.u during the fault for the windfarm 2, as it has not synchronous generator connected to the adjoining bus. However, it will still satisfy most of the gridcode requirements of the figure 4.2 and will remain connected as this voltage drop exists for a time less than 200ms. The oscillations in the voltage (figure 4.16) following the fault recovery is because of the reactive power requirements of the network for maintaining the voltage. In this scenario, more reactive power is demanded from wind turbines as the percentage of synchronous generator in the system is very low. The advantage of the VDACC can be explicitly be appreciated from the figure 4.17. The power output of all the windfarms reaches to their pre-fault value as soon as the fault is released. Moreover, at no instant during the fault or post fault phase, are the converter current output of the wind turbines exceeded, implying that the grid code requirements and the network stability is fulfilled without any additional stress on wind turbine converters. Thus the Direct Voltage Control supplemented with VDACC can provide transient voltage stability even in renewable penetration scenarios as high as 88%.

4.4.2. FREQUENCY SUPPORT FROM THE WIND TURBINES

Even though the under and over frequency performed significantly well in the 9 bus system with 52% wind energy generation, it did not perform as expected in the test system for 88% wind energy generation. The primary reason which lead to its performance in an unexpected way include:

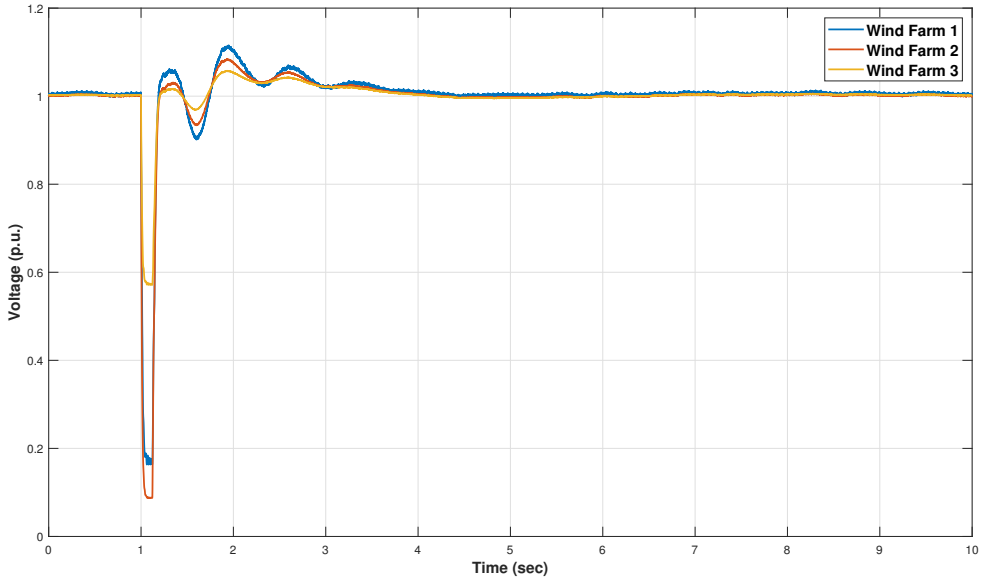

Figure 4.16: Voltage recovery by the windfarms measured at their respective connection bus (PCC)

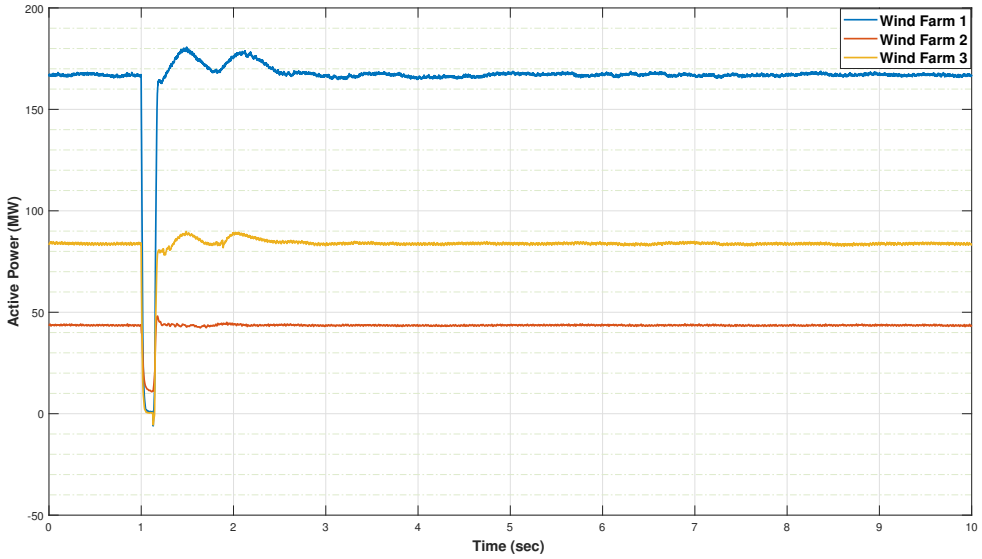

Figure 4.17: Active Power Injection by windfarms following the fault

1. The inertial support provision based on using washout filter and lead-lag compensator is very difficult to tune in the test network for 87% wind energy generation. This is to be expected as the number of wind turbines (equivalent wind farms) increase from 2 to 3. Moreover, due to the fast action of the Direct Voltage Control with inertial support, determining the parameters of the washout filters and lead-lag compensators become more challenging in the 87% PE interfaced generation network.

2. The fast dynamics of the Direct Voltage Control are complemented with the reduced system inertia. In this specific system the total generation from the synchronous generator is 13% which means other than the short-termed inertial support from the windfarms, very less inertia is available in the system to cope with major load changes.

3. Furthermore, the washout filter based inertial support of wind turbines coupled with the low inertial response available from the synchronous generator threatens the rotor angle stabililty of the system. Any errors in the parameters of lead-lag compensator or the washout filter can destabilize the system as the windturbines will provide inertial support before or after the time instant when needed. Even a slightest of the delay in the active power injection from the wind turbines can effect the rotor angle stability of the system making the system go completely unstable.

To deal with the aforementioned challenges, following solutions are proposed:

1. It will be a huge advantage if heuristic optimization techniques can be integrated with the RSCAD for determining optimal parameters of the washout filter and lead-lag compensators used in the work so far. The values of time constants and gains if tuned in some other software might still not give expected results on RSCAD. Hence an optimization algorithm that can extract values from RSCAD during real-time operation must definitely be considered. Such an implementation can be accomplished by using the *Aurora* link available in RSCAD which makes it communicate with other softwares.

2. Even after having optimal parameters of the lead-lag compensator and washout filter, the inertia in the system is still low as the wind turbines can only provide 10% more of their rated power for inertial support that too for a very short time. Under such scenarios the use of storage devices becomes inevitable as they can support load changes which are beyond the capacity of the wind turbines. Moreover, the fast injection of active power using additional batteries have proven to provide improved frequency stability in the system [78], [77].

3. In order for extracting more power from the DC link for supporting load changes, the strategy proposed in [72] can also be leveraged as it makes us of the DC voltage controller which is inherently faster than the pitch controller used in Machine side converter. However, such a strategy is based on switching between two control strategies which might also cause some unforeseen transients. The well established strategy for minimizing power oscillations presented in [93] and [41] can also be a viable option if they can somehow be integrated with the Direct Voltage Control.

5

MMC-HVDC BASED OFFSHORE WIND FARMS

The large-scale development of wind farms along the European coasts is progressing at a fast paced rate and is set to continue in the coming years. The offshore wind capacity grew by 18.5% to a total of 18.5 GW in 2018, as depicted in figure 5.1. The first half of 2019 has already seen an increase of 1.92 GW of offshore wind with UK's Hornsea 1 contributing a staggering 931 MW so far [16]. An overview of planned OWF in the North Sea can be found in [4]. The increasing scale and distance from shore of these OWF has led to a transition in transmission technology from HVAC to HVDC. The high losses associated with HVAC transmission requires reactive power compensation at the receiving end, which forces a breakeven distance between HVAC and HVDC offshore technology at approximately 50-60 km [13]. Modular Multilevel Converter (MMC) based voltage source controlled High Voltage DC (VSC-HVDC) technology has economically and technically evolved to become a singular option for linking these OWF to the onshore grid [43], [61], [12]. However, the operational experience for VSC-HVDC technology for bulk power transfer over long distances is still limited as so far there are only seven HVDC offshore wind connection systems [12].

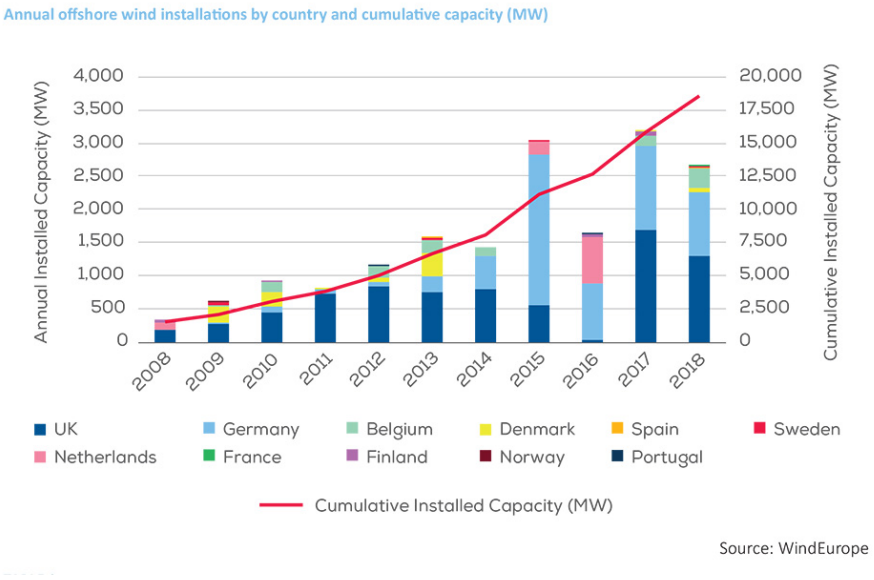

Figure 5.1: Installed capacity of Offshore wind in Europe [17]

This chapter focuses on identifying the challenges associated with the operation of OWF delivering high power over long distances. A specific transient phenomenon encountered during the islanded operation of

OWF is observed following the blocking of MMC-HVDC converter. The resonance encountered in the operation while delivering bulk power are also identified and the effect of these resonance on the transient phenomenon is also analysed. The emphasis is laid upon the influence of developed wind turbine control on the overall transient phenomena and how it addresses the accompanying voltage surge that might cause excessive stress on the converter.

5.1. MODELLING FOR TRANSIENT PHENOMENA IN OWP

There is very little operational experience concerning VSC-HVDC technology for capacity over 800 MW and beyond. It is therefore highly likely that some phenomena are observed during test and commissioning phases that were not anticipated at the design stage. One such example is the excitation of resonances due to the HVDC transformer, AC submarine cables and offshore main transformer by the HVDC controller [51]. Moreover, the resonances induced by the HVDC controller are not damped out by the passive filter components available in the offshore network and require modification in HVDC control scheme [52]. In order to analyse the resonance and further the transient phenomena, a test-case is developed on RSCAD with an MMC based VSC-HVDC connected to an equivalent type-4 wind turbine based OWF as shown in figure 5.2.

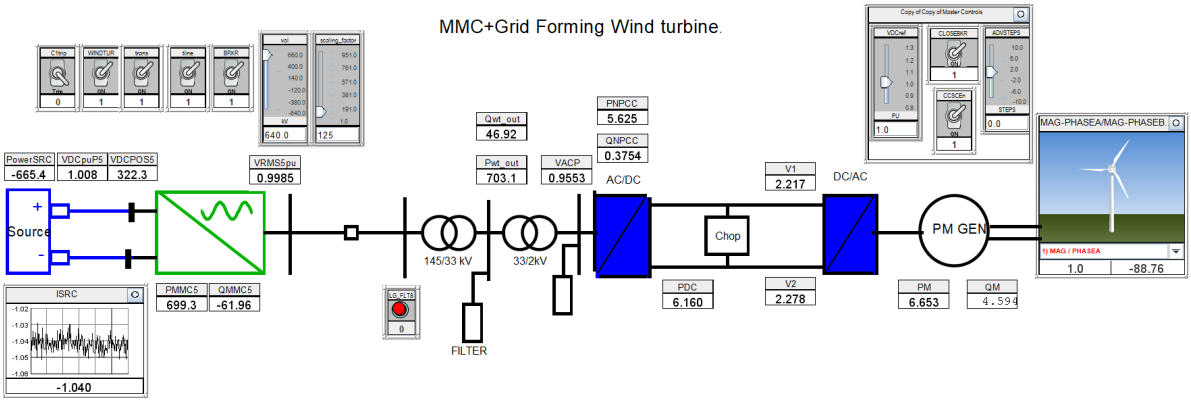

Figure 5.2: Test setup for analysis of Transient phenomenon in OWF

5.1.1. IDENTIFICATION OF RESONANCE IN THE OFFSHORE NETWORK

The Offshore grid is mainly composed of the PE-converters and thus has a limited short-circuit ratio. As the short circuit ratio is based on the impedance of the network, it is important to have a lower impedance for a higher short circuit capacity [22]. As there are no synchronous generators or loads connected directly to the offshore network, the impedance of the AC cables connecting the OWF to the HVDC station plays a crucial role in determining the short circuit ratio. The offshore network as a whole can be categorized as a weak grid, as it has a limited capacity for maintaining the voltage if excess reactive power is required [20]. Moreover, for the offshore network, the grid impedance is primarily based on the transmission line or the cable connecting the offshore wind park to the VSC-HVDC station as shown in the figure 5.3. As the offshore network is mainly comprised of PE-converters connected to one another, any harmonics present in might initiate an interaction with the controller, creating a cascading effect. As RTDS environment is very close to the real world, it can detect those anomalies are instantly detected by the software which can lead to the failure of entire modelled system. Thereby every component needs to be modelled very carefully. Importantly, the cable parameters play a crucial role in the development of this model. Because there might be harmonics due to the AC cable, a cable with improper parameters will lead to resonance in the voltages. This can be quite misleading as is later discussed, because there are several sources of harmonics in an offshore network and hence it because very important to identify their origin. Moreover, there is a requirement for a properly designed filter, which can actively filter out harmonics due to the cable. In the developed model for validating the Wind turbine *grid-forming* control, this filter was missing which can make tracking the source of these harmonics more difficult.

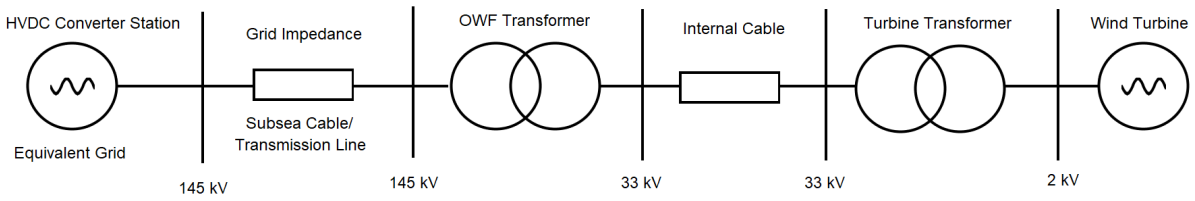

Figure 5.3: Equivalent model of the Offshore network [44]

The resonance due to cables in the absence of a filter is misleading mainly because of the other source of harmonic injection being present (which is the VSC-HVDC). Since, the VSC-HVDC comprises of hundreds of submodules with very high capacitances, there is some DC injection in the voltage. This DC component can overtime make the transformer saturated which then injects harmonics in the network. The active filters present in the network, can damp out the harmonics from AC cables but not from the MMC based VSC-HVDC [39] [51]. Therefore, the absence of these filters makes it difficult to trace the harmonic injection. More importantly, the equivalent OWF model which is created by scaling up the Wind turbine current injection can also be a source of harmonics. This is because, even the smallest harmonic component in the current waveform of the wind turbine can amplify when scaled up to 140 times for delivering 800 MW. Hence, it becomes important to use a properly designed cable for modelling in RTDS. Evidently, the effect of cable parameters on the offshore network is explored further in this section.

5.1.2. SELECTION OF CORRECT CABLE PARAMETERS FOR THE DEVELOPMENT OF MODEL

This section deals with determination of parameters for the cable used in transmitting power from OWP to the MMC based VSC-HVDC converter station. Figure 5.9 shows the power at both the ends of the cable. For a length of 60 km there is power loss of 40 MW. A cable length of 60 km used for delivering power at 145 kV is expected to exhibit losses in transmission. It must also be noted that the length of the transmission cable does not impact the harmonics component in the network by a very large extent [27]. It must however be considered that this section does not deal with optimum cable parameters, but more importantly focuses on the impact of selecting cable parameters carefully.

CABLE 1

The parameters in this case for Cable 1, the selected RLC parameters are shown in the following figure 5.4:

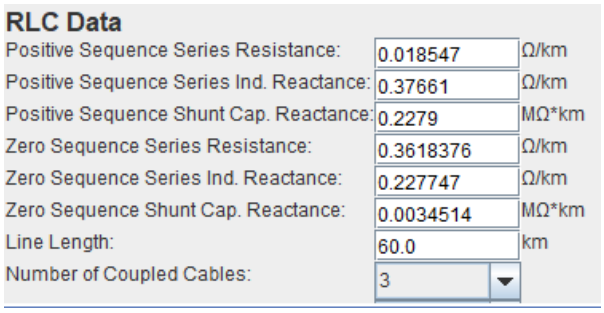

Figure 5.4: Parameters of Cable 1

There are different available models for Cables in RSCAD based on the parameters required to be entered. The detailed cable model based on the frequency and phase, is used for determination of propagation vector |H| and admittance matrix $|Y_c|$ [64]. The RSCAD simulation software for cables allows for determination of all the parameters for different models. Moreover, it is possible to calculate the different electrical parameters based on the insulation and conductor parameters of the cable [96]. However, these parameters do not give a stable response for high frequency oscillations because of which there are harmonics induced in the voltage waveforms of Wind turbines and MMC converter, which can have a fatal impact on the operation of OWP. The voltages in the network are distorted as can be observed from the figures 5.5a and 5.5b. The magnitude

of the harmonic components are represented in the frequency response of the system obtained using FFT in the figure5.6.

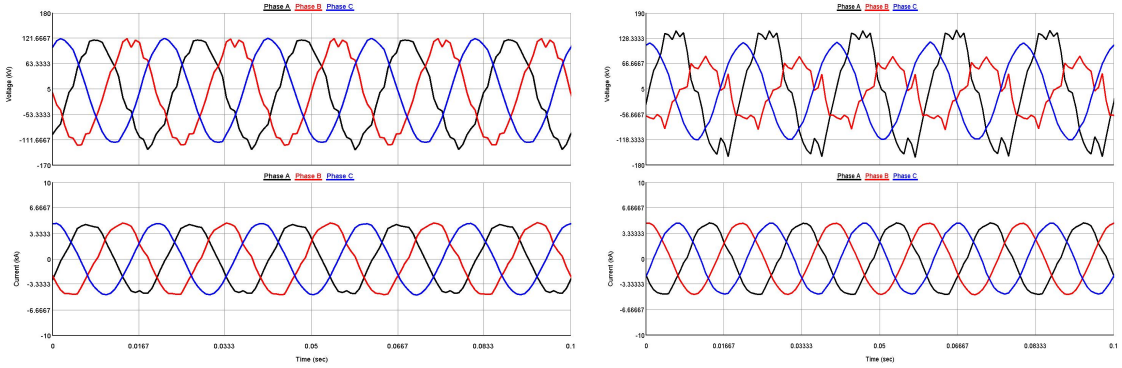

(a) Voltage and Current measured at the transformer in MMC converter

(b) Voltage and Current output of the Offshore Wind Farm transformer

Figure 5.5: Harmonics observed in voltages due to parameters of Cable 1

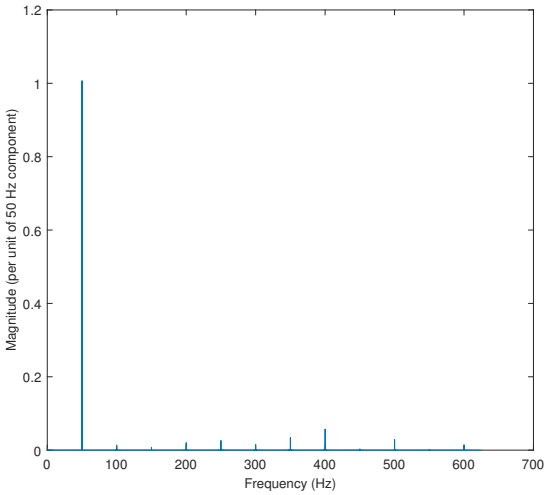

Figure 5.6: FFT for Phase A of OWF Voltage in previous figure 5.5b

CABLE 2

In order to deal with the issues stated in previous section, the cable parameters were modified, and the modified cable parameters are recorded in figure 5.7. Consequently because of the selection of correct cable parameters, the voltages across both the ends of the cable is a pure sinusoidal waveform as can be clearly noticed in figures 5.8a and 5.8b [71].

As can be easily observed from the parameters of both the cables, in figures 5.4 and 5.7, the main difference is in the values of Zero sequence impedance. These values in 5.4 help in reducing the overall impedance of the cable and allow for reduced power losses. However, based on the parameters for 5.7, there is loss of power as high as 100 MW (figure 5.9). The power loss is too high, but also is the length of the cable. Offshore wind Parks are mostly located at a distance of 30-40 km from the MMC based VSC-HVDC station [1]. Therefore, a decision was made to go forward with these cable parameters as the harmonic attenuation was much better. Moreover, the objective of this work is more focused in identifying the possible harmonics in the offshore network, and analyze their impact on the operation of Offshore networks.

Irrespective of the source of harmonics, it is important to realize that harmonics in any network hinders their

[1] In this chapter, HVDC, VSC-HVDC and MMC-HVDC are used synonymously and all these terms refer to the MMC based VSC-HVDC

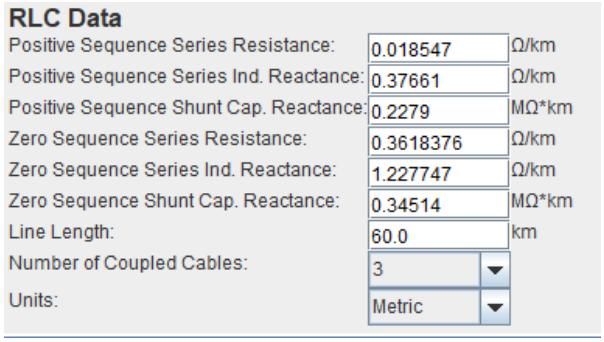

Figure 5.7: Modified Parameters for Cable 2

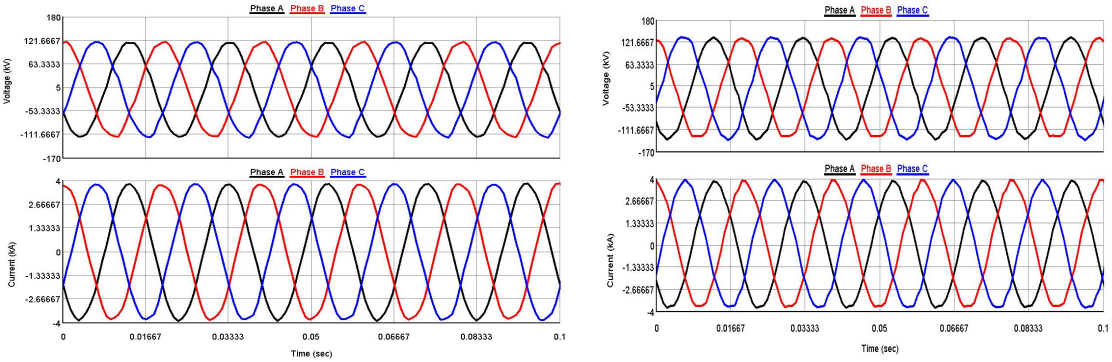

(a) Voltage and Current measured at the transformer in MMC converter

(b) Voltage and Current output of the Offshore Wind Farm transformer

Figure 5.8: Harmonics observed in voltages due to parameters of Cable 2

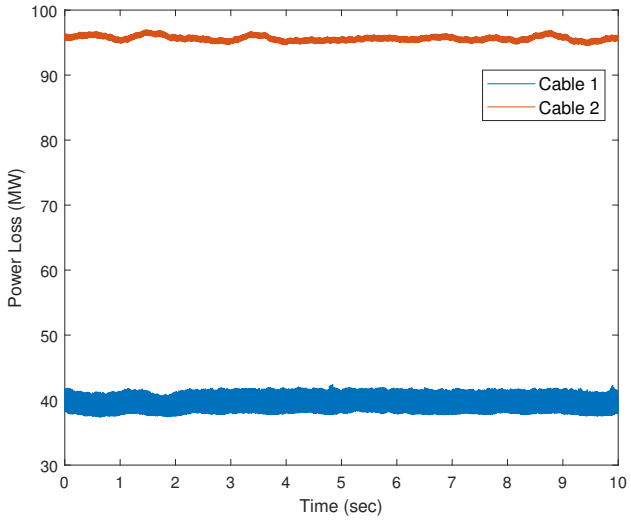

Figure 5.9: Power losses in Cable 1 and Cable 2

performance. However, as Offshore Network is mainly comprised of PE-converters, these harmonics can have an even higher impact on the fast acting controllers of wind-turbines and MMC and also can lead to huge financial losses, if overlooked. As previously discussed, the harmonic injection by the MMC based VSC-HVDC converter is not considered here as that can not be removed by active filters, and requires modification in the control of MMC converter for elimination [51] [37]. Having determined the correct parameters for the

cables, the overvoltage problem in the Offshore network needs to be addressed. The parameters for cable 2 are used for the development of remaining of this work.

5.2. OVERVOLTAGE PROBLEMS FOLLOWING VSC HVDC BLOCKING

This section deals with the specific transient phenomena of overvoltages during the practical operation of the OWP occurring due to the blocking of the HVDC converter, possibly due to the action of the control system. Regardless of the origin of the blocking signal, the challenge is to ascertain that the ensuing transient process and the accompanying voltage surge do not cause excessive stress on the power electronic converter [51] [39]. The overvoltage phenomena in the offshore voltages has also been identified in [51] [39] [71]. Figure 5.10 represents the overvoltages observed at the 145 kV bus of the offshore wind farm the MMC converter is blocked (this blocking scenario is mainly recorded for the fault at Onshore network [51] [39]). The blocking of MMC converter is a complex scenario in itself, and requires in depth investigation. The frequency is calculated based on these voltages. This section investigates further into the blocking of HVDC converter and its implication on the performance of the offshore network. Moreover, the impact of the developed control (Direct Voltage Control) on the MMC converter, following its blocking is also analysed.

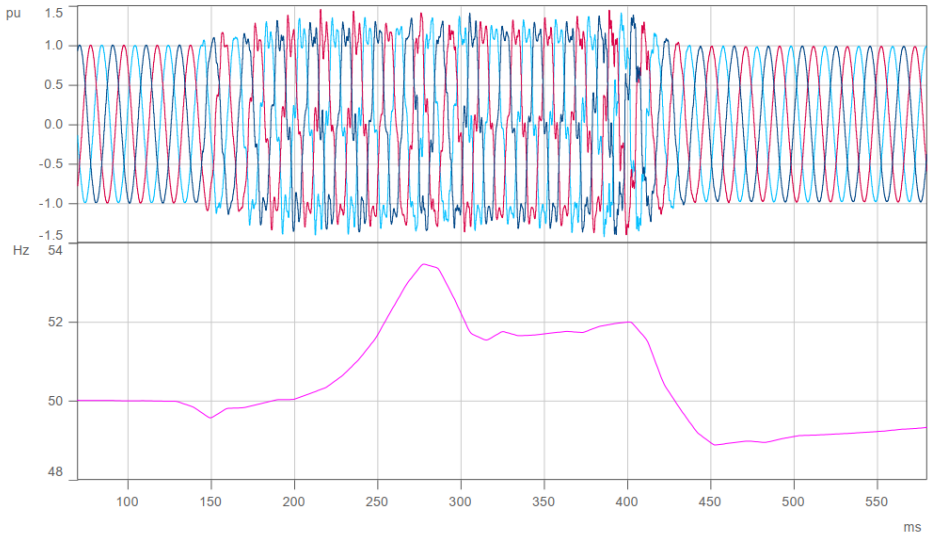

Figure 5.10: Voltage and Frequency measured at 145 kV bus after blocking of HVDC converter [51] [39]

5.2.1. FAULT AT OWF TRANSFORMER

In order to observe the overvoltage phenomenon in the offshore network, fault was created at the bus of OWP transformer which lead to blocking of the converter. In the available model, the blocking of the converter is triggered based on the current through the HVDC link. This is a special case scenario for blocking the HVDC converter as this might not happen in practical life. This is because, following the fault in the Offshore end the direction of the current in the HVDC link is reversed and all the current tries to flow through to the fault location. In practical scenarios, instead of an ideal DC source connected to the HVDC link in our case, an Onshore converter is installed which will try to block the reversal of current. For such cases, a different control can be used for triggering the blocking. Since in our case, the important thing to look into is the transient phenomena following the converter blocking and unblocking, and not the source of blocking signal, such a scenario was used.

BLOCKING OF MMC BASED VDC-HVDC CONVERTER

In case of fault scenarios, in order to protect itself, the VSC-HVDC converter goes into the blocking state, and it operates under the free-wheeling diodes as shown in figure 5.11 [88]. This happens so that the other terminal of the DC network is not affected by the AC fault. From the figure5.11, the MMC in blocked state is an equivalent circuit with diodes and capacitor as irrespective of the direction of flow of current [88] [89]. Each of the submodule of the MMC has a capacitor which acts in during the blocking state and the

short-circuit is blocked as long as the capacitor voltage is greater than the grid voltage [89]. Moreover, during the blocking state, the capacitor voltages of the submodules do not discharge owing to which they can be blocked as long as needed. Sometimes a fault can lead to a permanent blocking one which can stall the operation of the HVDC network and it needs to be reconfigured eliminating the blocked MMC [87]. However, the reconfiguration of the HVDC network so far is not possible as Multiterminal DC networks are still in research and development phase, and hence a permanent fault in case of the Offshore network can stall its operation completely. Blocking the MMC HVDc network in our case is not practical and hence is not considered in this work, therefore, the MMC is blocked for a limited time frame. Moreover, in case of

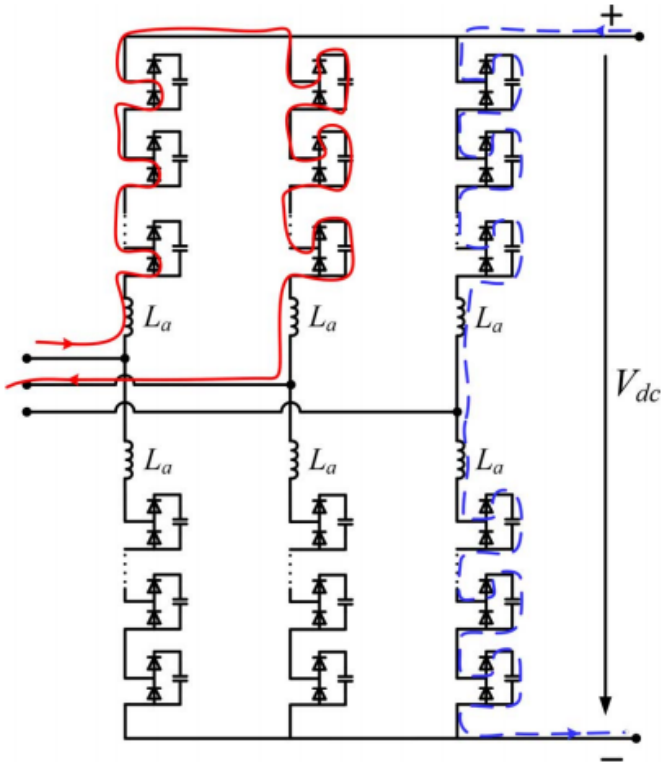

Figure 5.11: MMC based VSC-HVDC in Blocked state [88]

blocking, the OWP can cause overvoltages on the AC side of the HVDC converter (because of its islanded operation) which can cause stress to the power electronic components (diodes and IGBTs) of the HVDC station. In this section a few tests were performed to address the overvoltage problem that can hinder the operation of MMC. When the equivalent wind farms based on the classical PI control was used for aggregated wind farm models, there were observed overvoltages at the 145 kV bus of the MMC transformer, which were over 1.3 p.u., as stated in [39] [51]. The results for overvoltages at the MMC and OWF transformer is represented in figure 5.12. In the recorded results, the fault is cleared after 200ms and the VSC-HVDC is blocked for another 500ms. During this time, the overvoltages recorded at the terminal of the transformer of MMC converter, is reflected directly to the MMC.

The primary reason for the overvoltages is that the wind turbines have to follow LVRT requirements of the grid [83] owing to which, the Wind Turbines start delivering power as soon as the fault is released. However, when the VSC-HVDC is blocked, there is no power going to the offshore converter station and the OWF operates in islanded mode. As there is no power going through the HVDC station, the voltages at the OWF end as well as the HVDC end rises. These overvoltages in turn can cause stress to the power electronic components of the HVDC converter. Moreover, if these overvoltages persist for a longer period of time, the HVDC cable will be burdened by these overvoltages in case the Onshore Converter is also blocked. This will happen, because the MMC will try to protect itself from these overvoltages and the diodes used in the submodules will help facilitate that, which might also expose the HVDC link to these overvoltages.

Such scenarios can be prevented by modification of the control scheme based on Chapters 3 and 4. As discussed in section 4.1 the Direct Voltage control coupled with VDAPR, automatically tries to balance the

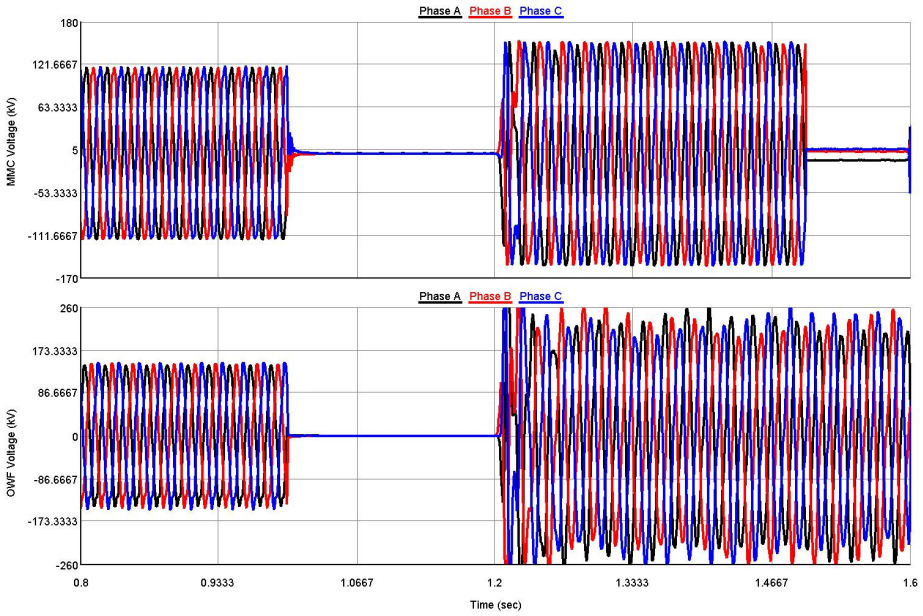

Figure 5.12: Overvoltages at the VSC-HVDC (top) and the Offshore Wind Farm end (bottom)

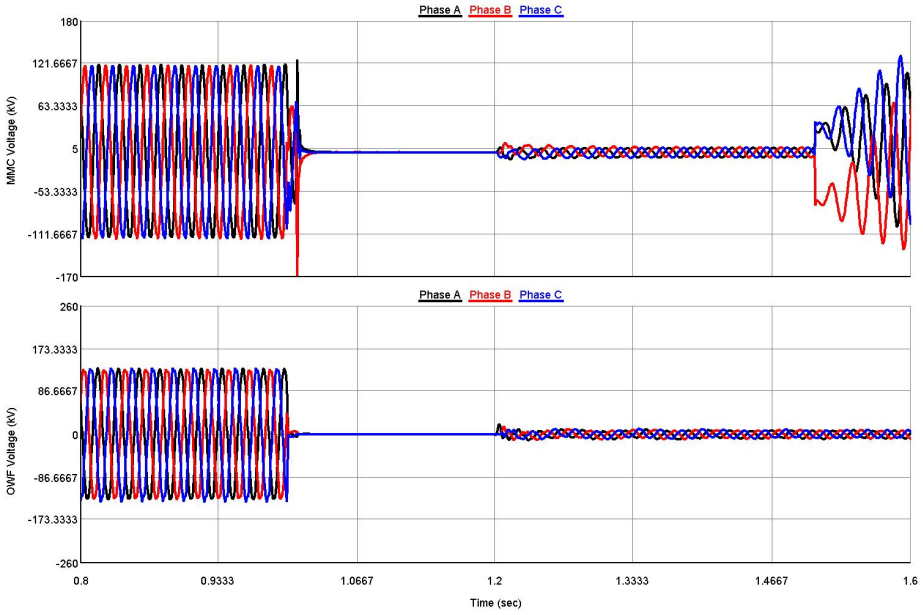

Figure 5.13: Elimination of overvoltages at VSC-HVDC (top) and the Offshore Wind Farm end (bottom)

voltages based on the requirements of the network. The performance of Direct Voltage Control is far better than the classical PI based controllers because, the currently used controllers perform indirect voltage control by injecting reactive power. Such an indirect control will cease its operation if there is no load connected or if the link to the onshore grid is severed. The results for the voltages at the at the Offshore wind park and MMC transformer nodes, when the Wind turbine control is changed from PI based controller to the DVC the obtained results are recorded in figure 5.13. The simulation scenario is the same as the previous one with a fault clearing time of 200ms and MMC being blocked for additional 500ms.

5.2.2. EFFECT ON WIND TURBINES BECAUSE OF OVERVOLTAGE REDUCTION

As previously discussed, the Direct Voltage Control can successfully overcome any overvoltages problem associated with faults close to offshore wind farm. However, during this period, there is no power transfer from offshore wind farms to the HVDC converter station, as the VSC-HVDC is blocked. This means that there is no current going to the HVDC station from the OWF. The current and voltage waveform for the offshore wind farm output are shown in figure 5.14. As the current is zero, this means that there is no power being provided by the wind turbines. The active and reactive power curves of a single wind turbine of the aggregated OWF during the HVDC blocking mode is shown in figure 5.15.

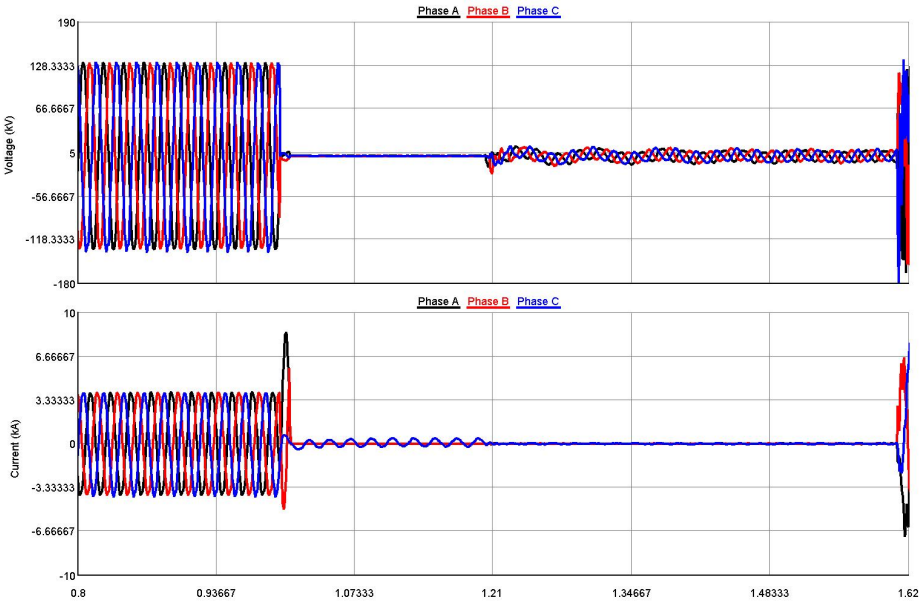

Figure 5.14: Voltage and current of the OWF during blocking of VSC-HVDC converter

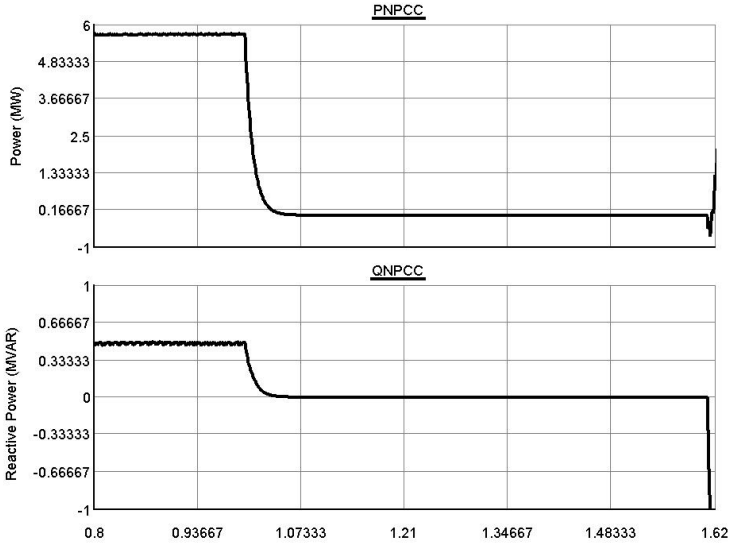

Figure 5.15: Active and Reactive power output of the wind turbine during blocking of VSC-HVDC

However, as there is no power injection in the network by the offshore wind turbines, this leads to a build up of power in the DC-link capacitor of the wind turbines, as voltage across it increases. Usually all the wind turbines operational today use a chopper circuit, which prevents the DC-link capacitor from exploding. The

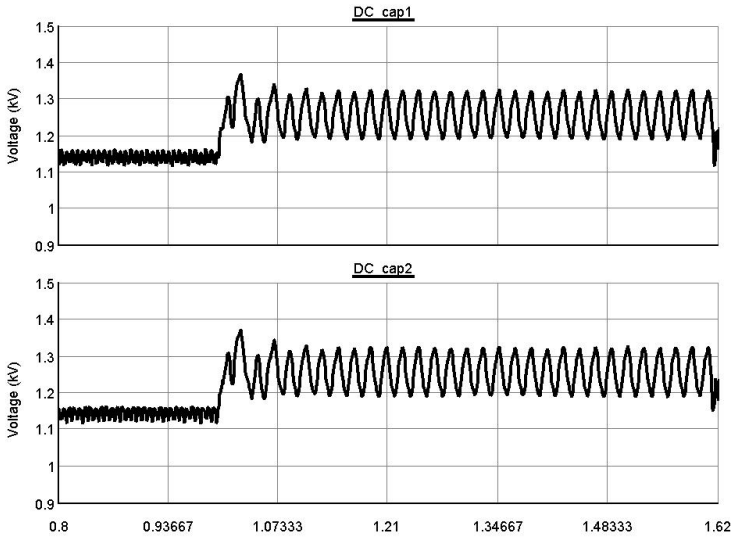

Figure 5.16: Voltages across the capacitors used in DC-link of the wind turbines

voltage across the 2 DC-link capacitors in the inverter is represented as V1PU and V2PU in the figure 5.16. As it can be observed because of the chopper, the dc link voltages never exceed a certain threshold. However, if the VSC-HVDC converter is blocked for a longer duration of time, this can impact the Chopper action as the chopper is not designed to act continuously for longer duration of time. This can consequentially affect the DC-link of the wind turbine converters which can get damaged making the wind turbine non-operational. Although, increasing the size of capacitance used in DC-link is also dependent on various other factors along with the cost and is a topic based on techno-economical analysis. Although, it is difficult to make a proper decision on the sizing of the capacitors, because the blocking period of the HVDC converter might not be known. In such a scenario, the pitch controller in the Machine Side converter should be activated to reduce the Power input to the DC-link from PMSG.

5.2.3. DEBLOCKING OF THE MMC

There are different submodule topologies for the blocking of the MMC. The nominal voltage across each of the submodule's capacitance is usually equal (V_{HVDC}/N) where V_{HVDC} is the voltage of the HVDC link and N is the number of submodules in each valve of the MMC. During the blocking state, only the free-wheeling diodes conduct. During this period, the voltage across each submodule drops from its nominal value and becomes close to ($V_{HVDC}/2N$) (figure 5.17).

Having addressed the problem of transients following the blocking of the converter, it becomes important to understand the behaviour of the offshore network, following the deblocking of the VSC-HVDC. After the converter is deblocked it can again be regarded as a controllable AC source as depicted in the figure [88]. During the deblocking mode, the submodule voltages try to reach their nominal value as fast as possible from their steady state value of ($V_{HVDC}/2N$) during the blocking mode (figure :5.17). Because of this change being very fast, significant voltage strikes and current surges are generated at the instant of deblocking of the MMC. This leads to a current surge at the windpark end due to the submodule voltage difference at the deblocking instant.However, in RTDS, the MMC is modelled such that following the deblocking the internal distribution of capacitor voltage within each submodule of the valve is not jeopardized by the transients in circulating current, although they do impact the total change in voltage.

VOLTAGE AND CURRENT WAVEFORMS

As previously discussed, the submodule voltage difference at the deblocking instant can lead to high current spikes. The Voltage and Current waveforms for the MMC following the deblocking is shown in figure 5.18. The Voltage and current waveform for the offshore wind farm is recorded in figure 5.19. As can be observed, there is a high current spike due to which the currents in the offshore network take a longer time to be synchronized

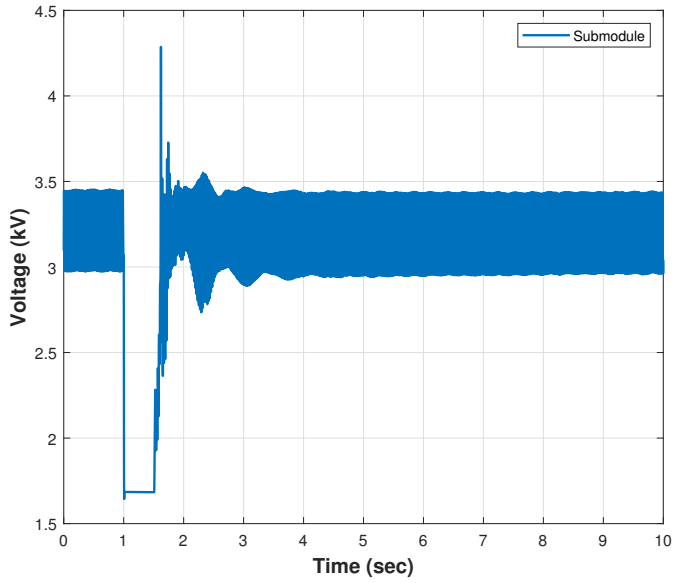

Figure 5.17: Submodule Voltage during blocking and deblocking

with the one another[2]. There is also a voltage transient which can go as high as 1.3 p.u at the terminal of MMC transformer. Since such transients are influenced by the VSC-HVDC converter itself and not the wind turbines (equivalent windfarm), the optimal way of controlling such transients is by controlling the increase of submodule voltage from $V_{HVDC}/2N$ to V_{HVDC}/N by using half DC voltage control scheme [88].

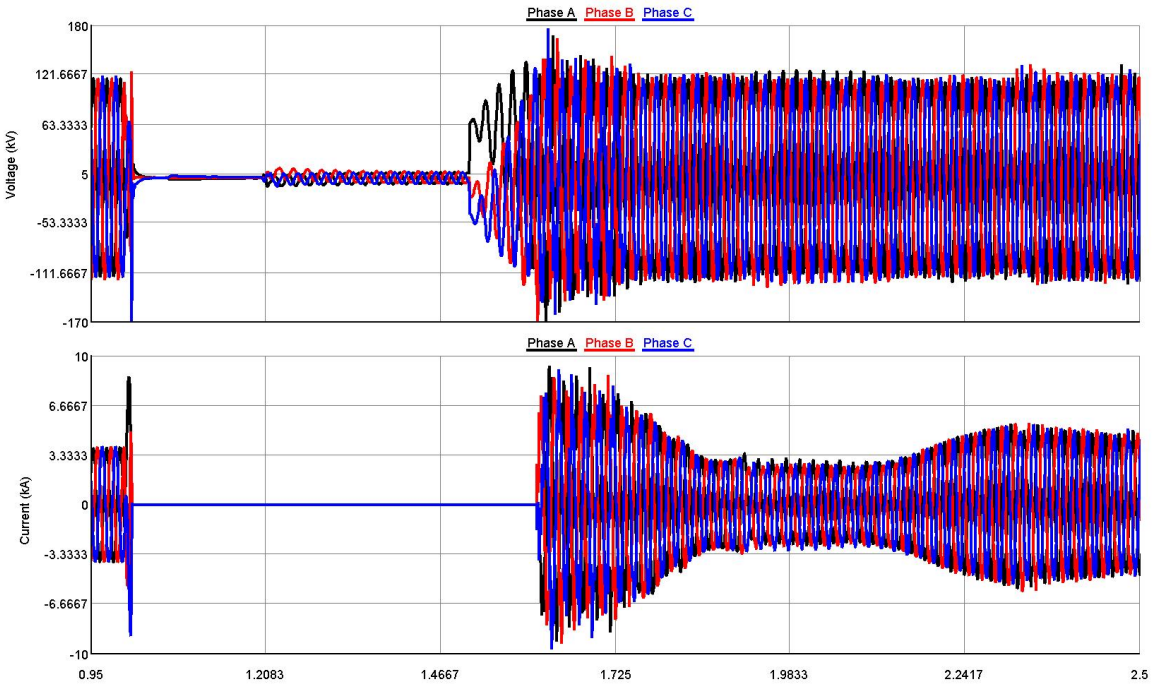

Figure 5.18: MMC transformer voltage (top) and current (bottom) following the deblocking

[2] The currents synchronize around 3.8 sec as can be observed from the stabilization of wind turbine parameters in figure 5.20 and 5.21

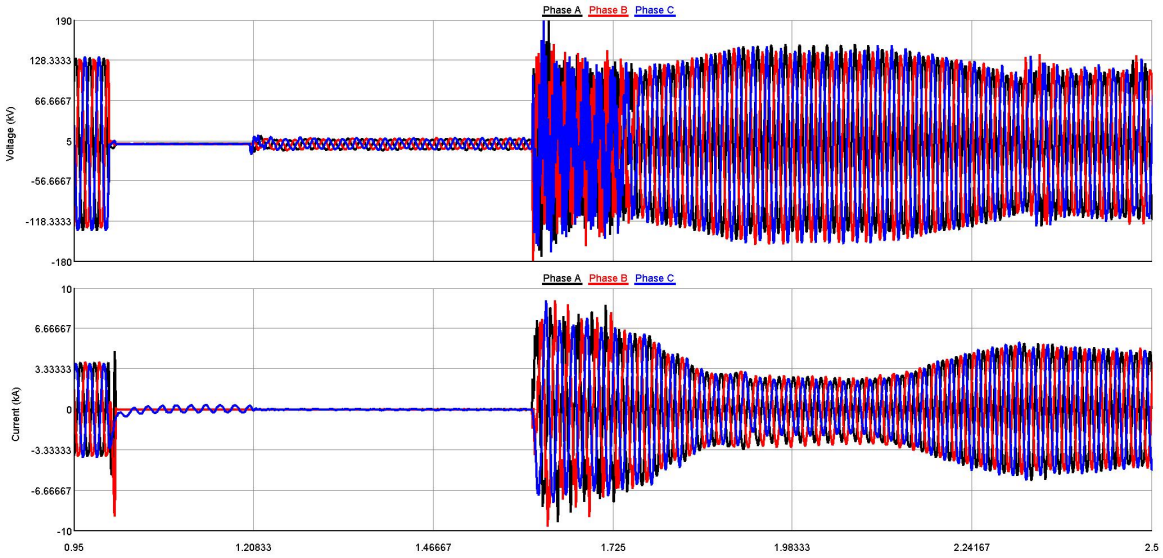

Figure 5.19: OWP transformer voltage (top) and current (bottom) following the deblocking

EFFECT ON WIND TURBINES

The current surge and voltage spikes observed in figures 5.18 and 5.19 can cause oscillations in the active and reactive power output of the wind turbines as observed in figures 5.20a and 5.20a. Moreover, such spikes are directly reflected on the wind turbine converters, as the current during that instant can reach as high as 2.0 p.u as shown in figure 5.21a. Since the time frame of such a current spike is very small, it might not impact the power electronic components of the wind turbine converter, however it still depends on the rating of the components and may or may not severely impact them. Moreover, the DC link voltage also oscillates as shown in figure 5.21b. Although the chopper in the DC link protects it from overvoltages, such oscillations in the DC link voltage are undesirable.

It must be noted for figures 5.20 and figure 5.21, the time scale is from 0-10 sec which includes the fault occurrence at 1 sec, followed by fault clearing at 1.2 sec and MMC deblocking at 1.7 sec. The same order of events is followed in all the results produced in this chapter and some figures are zoomed in to correctly represent the transient phenomena.

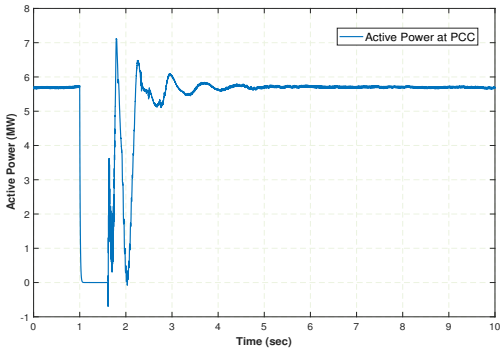

(a) Active power of the wind turbine following the deblocking

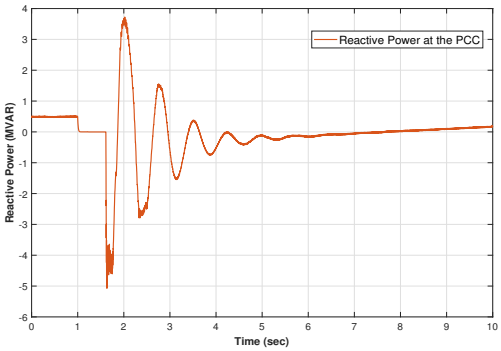

(b) Reactive power of the wind turbine following the deblocking

Figure 5.20: Active and reactive power of Wind Turbine

As previously discussed, the transient phenomena following the deblocking has more to do with the behaviour of the HVDC converter than with the controlling of wind turbines in the offshore wind park. However, the current surge and voltage spike due to the deblocking of individual submodules can directly

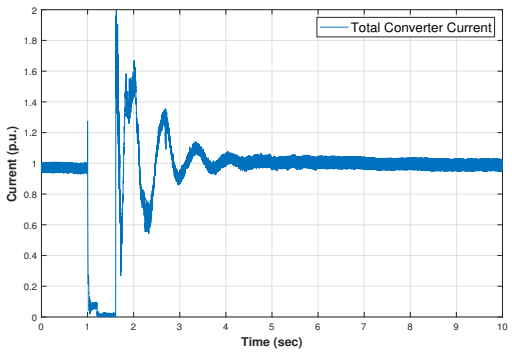

(a) Converter Current output of the Wind turbine

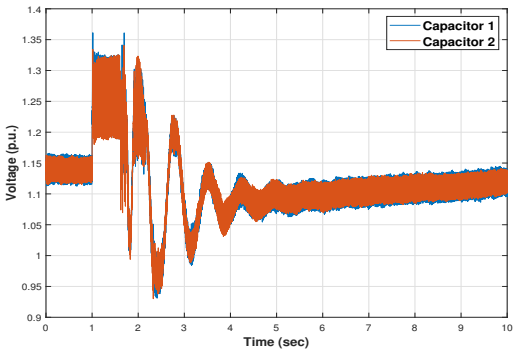

(b) DC link voltage of the wind turbine

Figure 5.21: Converter current output and DC link voltage of the wind turbines

affect the converter output currents and dc link voltages of the wind turbine. Hence, the submodule voltages must be properly controlled using the scheme proposed in [88] or similar schemes, so that the current surge can be reduced for a more reliable operation of the offshore network following the converter blocking.
Moreover, in-case of a permanent fault, which can lead to blocking of the converter for an extended amount of time, the offshore wind farm operating with direct voltage control is able to reduce the Overvoltages in the offshore network, however, the wind farm operation is stalled in such a scenario. Since during the blocking mode, the submodule capacitors of the MMC do not discharge, it can be put on a hot start after the removal of permanent fault. However, for the wind turbines since no power is flowing to the network, this leads to overburdening of the dc link of the wind turbines, making the chopper act more frequently than it is designed for. Hence the offshore wind turbines need to be regulated such that the dc link of the wind turbines can be saved.

6

Conclusions and Future Work

The results of the EMT simulations performed in RTDS confirm that the wind turbines can have grid forming capabilities if their control systems are modified properly. An investigation on the effect of wind turbines on the power system stability is made in this thesis. The identified control strategies from the literature are implemented on detailed working models of wind turbines for simulation in Real-Time (RTDS). Moreover, modifications and upgrades are imposed on the identified control scheme to make it work in islanded mode, as well as improve its performance for mitigating voltage and frequency instabilities. A major question lurking around the current research going in grid-forming control strategy is whether a 100 % converter based grids are possible? Before answering this question the voltage and frequency control by the wind turbines should be properly addressed which has been the primary focus of this thesis. Based on the implemented control strategy and the modifications, a grid that operated stably with 88% wind energy generation has been simulated and has shown excellent FRT capabilities even closely mimicing the response of the synchonous generators for the voltage recovery following the fault.
The main highlights of the work can be concluded as follows:

1. The Direct Voltage control for enabling grid-forming capability in the wind turbines have been successfully implemented in RSCAD. The default RSCAD type-4 model has been completely modified which allows its operation in connection with the infinite grid as well as in standalone mode. Although the standalone mode requires an islanding detection based on the central breaker information, as the Direct Voltage Control does not provide such standalone operation capabilities.

2. The necessary upgrades for improving the dynamic behaviour of the wind turbines during fault and load events have been implemented along with the Direct Voltage Control approach. The modifications implemented include Voltage Dependent Active Current control for improving the transient response of the wind turbines following the fault. Another modification based on extracting inertia from the wind turbine rotors has been implemented which operates in both under- and over- frequency events. The implemented modifications improve the stability of the system that operates with PE converter penetration levels as high as 88%

3. The Offshore VSC-HVDC model has been developed which allows for bulk power transfer ranging as high as 1.2 GW. Although the tests have been made for the HVDC converter station receiving 700 MW of power. The transients occurring in the offshore network during the blocking mode of the VSC-HVDC following a fault have been identified, as well as the implemented Direct Voltage Control has successfully mitigated those harmonics thereby providing stability to the offshore network.

6.1. Answers to the Research Questions

Once the results of the simulations have been obtained and analysed, it is granted the authority to answer the research questions that were stipulated at the beginning of this very MSc thesis report.

- **What are the required modifications in the default RSCAD type-4 wind turbine model to make it work as a grid-forming wind turbine?**

The required modifications required to enable grid forming control of the default type-4 model are discussed in Chapter 3. The major modification is made in the inner control loop where the PI controllers are replaced with a washout filter. The classical controllers based on PI control strategy have initially shown high frequency oscillations which are eliminated by using the Washout filter. Moreover, the washout filter enables quick dynamic response.

- **What modifications and additions are required to be done in the identified *grid-forming* control strategy to enable its operation in standalone mode, as well as improve its dynamic performance in the grid-connected mode?**
  A major modification is made in the outer control loop of the i_q reference which is based on global and local voltage control. Additionally, the frequency control capability is cascaded with the DC voltage controller for generating i_d reference values. Eventually to make the wind turbine operate in standalone mode, a control scheme based on Microgrid is adapted and implemented. For improving the dynamic performance in high PE scenarios VDACC and inertial response is added to the Direct Voltage control which has successfully shown significant improvements.

- **Can the implemented control strategy help in mitigating voltage and frequency instabilities in power networks having more than 50% share of wind energy (power electronic interfaced) generation?**

  Based on the modifications proposed in Chapter 4, the dynamic performance of the wind turbines is significantly improved. As a matter of fact, the performance in the 52% grid is significantly better than other controllers tested. The simulation scenarios for the 88% RES have been successfully simulated for the FRT capability of the wind turbine. The inertial response however in such high PE generation scnerios by itself is not capable of providing frequency support and can further introduce interactions with the rotor angle stability of the system

- **Can the implemented control scheme operate in islanded mode of Offshore Wind Farms while the HVDC converter station is blocked and simultaneously prevent overvoltages during the islanded operation?**

  The offshore network model has been successfully developed in RSCAD with a reflection on the possible resonance effects due to the cable impedance in chapter 5. This is an important discovery for further improving models on RSCAD as this resonance can be quite misleading given there are several sources of harmonics in the network, mainly the VSC-HVDC transformer. Moreover, the overvoltages experienced during the blocking of VSC HVDC transformers have been successfully mitigated by utilizing the implemented Direct Voltage Control approach in the equivalen windfarms.

6.2. CONTRIBUTIONS TO THE IEPG

- A full scale model for type-4 wind turbine has been developed which works in grid-forming mode,providing stability to the network. Necessary modifications that enable its operation in the standalone mode have been executed.

- The test network in which the wind turbines can stably operate at 88% PE converter penetration in steady-state has been modelled. The voltage stability and the FRT response of the wind turbines have been executed, along with the development of inertial response for frequency stabilization based on Washout-filter and lead-lag compensator. This can in the future be extended for developing a test network which can operate at even higher penetration of PE converter generation, possibly reaching up to 98 - 100 %

- An Offshore network model for bulk power transfer has been developed. The network model can work stably with power levels of 1.2 GW. This opens up the possibility of development of MTDC offshore network models.

6.3. CHALLENGES ENCOUNTERED

For the development of this work in RTDS several challenges were encountered. These were mainly relating to the software implementation, the way RSCAD compiles the code and unavailability of all the components in the library. The few major challenges which have been tackled include:

- The RSCAD software does not directly allow integration with optimization tools such as MATLAB and python. This limited the scope of optimization of the parameters of washout filters as well as other measurement filters used. In order to tackle this, the trial-and-error method was employed which can become painstakingly time consuming if the network complexity increases (i.e., when the penetration level of wind turbines in the network increase). In order to mitigate such scenarios, integration of python scripts that work in synchronism with the RTDS simulations must be created and integrated with RSCAD using the Aurora link. This can significantly reduce the time in determining the parameters of different control logics employed.
- A major challenge was identified while implementing the inertial control in 88% wind energy model. The first problem was mainly because of the 3 washout filters and 3 lead-lag compensator that needed to be tuned to operate the system stably. Moreover, the inertial response of the wind turbines made the system more unstable as the inertial response is based on the derivative control of power which has inherent delay. The lead-lag compensator can minimize that delay in operation, however, a system working with high penetration of RES like the one with 88% is highly sensitive to even the slightest delays in power injection as this can significant impact the rotor angle stability of the system. In order to mitigate this, the inertial response of the wind turbines must be integrated with some sort of storage device that can inject Active power in the system without any delay.
- For developing the offshore network model, not much help is available in regards to determination of cable parameters. If these values are not known initially, some problems might be encountered in making the system work. This can become increasingly complex when integrating individual system in a single model such as the Offshore test network developed. Such a development required the MMC working with U-f mode as well as the type-4 wind turbine working with Direct Voltage control to be put together. Since these systems and controls itself are complicated, having errors in the model due to cable can be misleading during the development process. Hence, utmost attention must be paid to the cable parameters when integrating different PE converters in RSCAD.

6.4. FUTURE WORK AND RECOMMENDATIONS

The future work and recommendations following the simulations performed in this work, directly extend to addressing the challenges faced, as well as the tasks that could be accomplished if such challenges are mitigated.

- If optimal tuning methods are integrated with RSCAD, the lead lag filters as well as the washout filters that initiated the delayed power injection as well as the rotor angle instbability in the 88% win energy generation model, could be tuned properly. This can enable a fully functional test bench that operates at 88% wind energy systems on RSCAD. Furthermore the proper tuning of these parameters can make the system stable enough for the wind energy generation to be extended further to over 95% in the 9 bus system.
- Even after optimally tuning all the control parameters, it might not be possible to achieve 100 % PE interfaced generation scenario using wind energy systems. In order to accomplish such a penetration level, the modifications in the Machine side controller must be done. This mainly involves implementing a DC link voltage controller as opposed to the Pitch controller used for MPPT in wind turbines. Such an approach can enable starting up the system without any synchronous generators required [72], given that enough power is available in the DC link of the wind turbine converter.
- The developed model for the offshore network, is fully operational. It can be extended in two further directions. One can be removing the DC source and replacing it with another MMC HVDC to create a point-to-point model that can be integrated with the AC grid. Moreover, the Offshore model can be integrated with the Multi-terminal HVDC (three-terminal model for Cobra Cable) to enable system studies for offshore windparks win multi-terminal HVDC systems.

BIBLIOGRAPHY

[1] E publishes the implementation guidance document (igd) on high penetration of power electronic interfaced power sources (hpopeips) as result of a consultation process from 5th april to 5th may. URL https://docs.entsoe.eu/cnc-al/2017/08/10/igd-update/.

[2] Wind energy frequently asked questions (faq): Ewea. URL http://www.ewea.org/wind-energy-basics/faq/.

[3] The massive integration of power electronic devices. URL https://www.h2020-migrate.eu/.

[4] Onshore projects germany. URL http://www.tennet.eu/our-grid/onshore-projects-germany/.

[5] In R. Krishnan M. P. Kazmierkowski and F. Blaabjerg, editors, *Control in Power Electronics: Selected Problems*. Academic Press, 2002.

[6] In B. K. Bose, editor, *Power Electronics and Motor Drives: Advances and Trends*. Academic Press, 2006.

[7] Wind generators and modeling. In N. Zargari B. Wu, Y. Lang and S. Kouro, editors, *Power Conversion and control of Wind Energy Systems*, chapter 3, pages 73–76. John Wiley and Sons, 2011.

[8] Wind energy system configurations. In N. Zargari B. Wu, Y. Lang and S. Kouro, editors, *Power Conversion and control of Wind Energy Systems*, chapter 5, pages 190–195. John Wiley and Sons, 2011.

[9] Variable-speed wind energy systems with synchronous generators. In N. Zargari B. Wu, Y. Lang and S. Kouro, editors, *Power Conversion and control of Wind Energy Systems*, chapter 9, pages 274–316. John Wiley and Sons, 2011.

[10] Grid code - high and extra high voltage - tennet tso gmbh bernecker straße 70, bayreuth, Dec 2012. URL https://docplayer.net/17055474-Grid-code-high-and-extra-high-voltage-tennet-tso-gmbh-bernecker-st
html.

[11] 01 - 72 abb review special report: 60 years of hvdc, Aug 2014. URL https://search-ext.abb.com/library/Download.aspx?DocumentID=9AKK106103A8195&LanguageCode=en&DocumentPartId=&Action=Launch.

[12] Hvdc technology for offshore wind is maturing, Oct 2018. URL https://new.abb.com/news/detail/8270/hvdc-technology-for-offshore-wind-is-maturing.

[13] Turning the tide, Apr 2018. URL https://www.elp.com/articles/powergrid_international/print/volume-23/issue-4/features/turning-the-tide.html.

[14] Stakeholder workshop, brussels, 2017, Mar 2018. URL https://www.h2020-migrate.eu/_Resources/Persistent/74052ce0f8d46313f0e08390066c07580ea0f020/MIGRATE_Stakeholder_Workshop.pdf.

[15] Ge's 12 megawatt haliade-x offshore wind turbine destined for testing in the uk, Jul 2019. URL https://cleantechnica.com/2019/06/26/ges-12-megawatt-haliade-x-offshore-wind-turbine-destined-for-testing-in-the-uk/.

[16] Europe installs 4.9 gw of new wind energy capacity in first half of 2019, Jul 2019. URL https://windeurope.org/newsroom/press-releases/europe-installs-4-9-gw-of-new-wind-energy-capacity-in-first-half-of-2019/.

[17] Offshore wind in europe – key trends and statistics 2018, Mar 2019. URL https://windeurope.org/about-wind/statistics/offshore/european-offshore-wind-industry-key-trends-statistics-2018/#findings.

[18] Research on cost reduction of a hybrid dc cb in wp6, Jul 2019. URL https://www.promotion-offshore.net/.

[19] Uk power cut: National grid promises to learn lessons from blackout, Aug 2019. URL https://www.bbc.com/news/uk-49302996.

[20] Mehriar Aghazadeh Tabrizi. Integration of renewable energy sources: Strong challenge for a weak grid, May 2015. URL https://blogs.dnvgl.com/energy/integration-of-renewable-energy-sources-strong-challenge-for-a-weak-grid.

[21] Anonymous. Accord de paris, Feb 2017. URL https://ec.europa.eu/clima/policies/international/negotiations/paris_fr.

[22] Davood Babazadeh. Short circuit capacity estimation for hvdc control application, May 2017. URL https://www.opal-rt.com/wp-content/uploads/2017/05/07_SCC_OFFIS.pdf.

[23] E. Barklund, N. Pogaku, M. Prodanovic, C. Hernandez-Aramburo, and T. C. Green. Energy management in autonomous microgrid using stability-constrained droop control of inverters. *IEEE Transactions on Power Electronics*, 23(5):2346–2352, Sep. 2008. ISSN 0885-8993. doi: 10.1109/TPEL.2008.2001910.

[24] Guy Birchall. Uk power cut fury as ofgem demands urgent investigation into 'fiasco' of mystery blackout - as cyber attack ruled out, Aug 2019. URL https://www.thesun.co.uk/news/9694119/uk-power-cut-national-grid-blamed-generator-failures/.

[25] E.j. Bueno, S. Cobreces, F.j. Rodriguez, A. Hernandez, and F. Espinosa. Design of a back-to-back npc converter interface for wind turbines with squirrel-cage induction generator. *IEEE Transactions on Energy Conversion*, 23(3):932–945, 2008. doi: 10.1109/tec.2008.918651.

[26] Luis Reguera Castillo and Andrew Roscoe. *Analysis and Practical Assessment of Converter-Dominated Power Systems : Stability Constraints, Dynamic Performance and Power Quality*. PhD thesis, Glasgow, September 2018. URL https://strathprints.strath.ac.uk/65944/.

[27] Chan. Harmonic analysis of collection grid in offshore wind installation, Oct 2017. URL http://resolver.tudelft.nl/uuid:37ddf689-adb3-4834-ac99-efbf22a98a0b.

[28] Mukul C. Chandorkar. Distributed uninterruptible power supply systems, 1995.

[29] Sanjay Chaudhary, Cristian Lascu, Bakhtyar Hoseinzadeh, Remus Teodorescu, Łukasz Kocewiak, and Troels Sørensen. Challenges with harmonic compensation at a remote bus in offshore wind power plant. 2017. doi: 10.20944/preprints201703.0110.v1.

[30] M. Chinchilla, S. Arnaltes, and J.c. Burgos. Control of permanent-magnet generators applied to variable-speed wind-energy systems connected to the grid. *IEEE Transactions on Energy Conversion*, 21(1): 130–135, 2006. doi: 10.1109/tec.2005.853735.

[31] Karel De Brabandere. Voltage and frequency droop control in low voltage grids by distributed generators with inverter front-end (spannings- en frequentieregeling in laagspanningsnetten door gedistribueerde opwekkers met vermogenelektronische netkoppeling), 2006. URL $$Uhttps://lirias.kuleuven.be/retrieve/411251$$DThesis_Karel_De_Brabandere_KULeuven_2006.pdf[freelyavailable].

[32] G. Denis, T. Prevost, M. Debry, F. Xavier, X. Guillaud, and A. Menze. The migrate project: the challenges of operating a transmission grid with only inverter-based generation. a grid-forming control improvement with transient current-limiting control. *IET Renewable Power Generation*, 12(5):523–529, 2018. ISSN 1752-1416. doi: 10.1049/iet-rpg.2017.0369.

[33] Guillaume Denis. *From grid-following to grid-forming : The new strategy to build 100% power-electronics interfaced transmission system with enhanced transient behavior*. Theses, Ecole Centrale de Lille, November 2017. URL https://tel.archives-ouvertes.fr/tel-01905827.

[34] W. C. Duesterhoeft, Max W. Schulz, and Edith Clarke. Determination of instantaneous currents and voltages by means of alpha, beta, and zero components. *Transactions of the American Institute of Electrical Engineers*, 70(2):1248–1255, 1951. doi: 10.1109/t-aiee.1951.5060554.

[35] Salvatore D'Arco, Jon Suul, and Olav Fosso. A virtual synchronous machine implementation for distributed control of power converters in smartgrids. *Electric Power Systems Research*, 122, 05 2015. doi: 10.1016/j.epsr.2015.01.001.

[36] I. Erlich, F. Shewarega, S. Engelhardt, J. Kretschmann, J. Fortmann, and F. Koch. Effect of wind turbine output current during faults on grid voltage and the transient stability of wind parks. *2009 IEEE Power & Energy Society General Meeting*, 2009. doi: 10.1109/pes.2009.5275626.

[37] I. Erlich, B. Paz, M. K. Zadeh, S. Vogt, C. Buchhagen, C. Rauscher, A. Menze, and J. Jung. Overvoltage phenomena in offshore wind farms following blocking of the hvdc converter. pages 1–5, July 2016. ISSN 1944-9933. doi: 10.1109/PESGM.2016.7741697.

[38] I. Erlich, F. Shewarega, and W. Winter. A method for incorporating vsc-hvdc into the overall grid voltage-reactive power control task. In *2016 Power Systems Computation Conference (PSCC)*, pages 1–7, June 2016. doi: 10.1109/PSCC.2016.7540895.

[39] I. Erlich, A. Korai, T. Neumann, M. Koochack Zadeh, S. Vogt, C. Buchhagen, C. Rauscher, A. Menze, and J. Jung. New control of wind turbines ensuring stable and secure operation following islanding of wind farms. *IEEE Transactions on Energy Conversion*, 32(3):1263–1271, Sep. 2017. ISSN 0885-8969. doi: 10.1109/TEC.2017.2728703.

[40] Jens Fortmann. *Reactive Power Control of Wind Plants*, pages 113–158. Springer Fachmedien Wiesbaden, Wiesbaden, 2015. ISBN 978-3-658-06882-0. doi: 10.1007/978-3-658-06882-0_6. URL https://doi.org/10.1007/978-3-658-06882-0_6.

[41] Durga Gautam, Vijay Vittal, Raja Ayyanar, and Terry Harbour. Supplementary control for damping power oscillations due to increased penetration of doubly fed induction generators in large power systems. *2011 IEEE/PES Power Systems Conference and Exposition*, 2011. doi: 10.1109/psce.2011.5772501.

[42] Aris Gkountaras. *Modeling techniques and control strategies for inverter dominated microgrids*. PhD thesis, Mar 2016. URL http://dx.doi.org/10.14279/depositonce-5520.

[43] J. Glasdam, J. Hjerrild, Ł. H. Kocewiak, and C. L. Bak. Review on multi-level voltage source converter based hvdc technologies for grid connection of large offshore wind farms. In *2012 IEEE International Conference on Power System Technology (POWERCON)*, pages 1–6, Oct 2012. doi: 10.1109/PowerCon.2012.6401377.

[44] Anna Golieva. Low short circuit ratio connection of wind power plants, Oct 2015. URL http://resolver.tudelft.nl/uuid:ebae4f63-7dee-4091-876e-5ff46f15c6d0.

[45] F. M. González-Longatt, P. Wall, and V. Terzija. A simplified model for dynamic behavior of permanent magnet synchronous generator for direct drive wind turbines. In *2011 IEEE Trondheim PowerTech*, pages 1–7, June 2011. doi: 10.1109/PTC.2011.6019425.

[46] Christian Hachmann, Maria Valov, Gustav Lammert, Wolfram Heckmann, and Martin Braun. Unterstützung des netzwiederaufbaus durch ausregelung der dezentralen erzeugung im verteilnetz. 01 2018.

[47] Jiabing Hu, WenMing Tang, Shuo Wang, and XueJun Xiong. Full-capacity wind turbine with inertial support by optimizing phase-locked loop. *IET Renewable Power Generation*, 11, 09 2016. doi: 10.1049/iet-rpg.2016.0155.

[48] Alex Huang. Dphotovoltaic syncrhonous generator: From grid following to grid forming, August 2017.

[49] Jean-Claude JUNCKER. Commission regulation (eu) 2016/631 of 14 april 2016, Apr 2016. URL https://eur-lex.europa.eu/legal-content/EN/TXT/PDF/?uri=CELEX:32016R0631&from=EN.

[50] G. C. Konstantopoulos, Q. Zhong, and W. Ming. Pll-less nonlinear current-limiting controller for single-phase grid-tied inverters: Design, stability analysis, and operation under grid faults. *IEEE Transactions on Industrial Electronics*, 63(9):5582–5591, Sep. 2016. ISSN 0278-0046. doi: 10.1109/TIE.2016.2564340.

[51] Abdul Korai. *Dynamic Performance of Electrical Power Systems with High Penetration of Power Electronic Converters: Analysis and New Control Methods for Mitigation of Instability Threats and Restoration.* PhD thesis, Dept. of Electrical Engg., Universität Duisburg-Essen, Germany, 2018.

[52] Abdulwahab Korai and István Erlich. Damping control of hvdc links to mitigate controller interaction with resonances of the offshore wind farm. *IFAC-PapersOnLine*, 50(1):85 – 89, 2017. ISSN 2405-8963. doi: https://doi.org/10.1016/j.ifacol.2017.08.015. URL http://www.sciencedirect.com/science/article/pii/S2405896317300277. 20th IFAC World Congress.

[53] Samir Kouro, Mariusz Malinowski, K. Gopakumar, Josep Pou, Leopoldo G. Franquelo, Bin Wu, Jose Rodriguez, Marcelo A. Perez, and Jose I. Leon. Recent advances and industrial applications of multilevel converters. *IEEE Transactions on Industrial Electronics*, 57(8):2553–2580, 8 2010. ISSN 0278-0046. doi: 10.1109/TIE.2010.2049719.

[54] Hubert Kowalski. Dnvgl energy transistion outlook 2017 executive summary, Apr 2018. URL https://issuu.com/hubertkowalski3/docs/dnv_gl_energy_transistion_outlook_2.

[55] M. Krpan and I. Kuzle. Inertial and primary frequency response model of variable-speed wind turbines. *The Journal of Engineering*, 2017(13):844–848, 2017. ISSN 2051-3305. doi: 10.1049/joe.2017.0449.

[56] Robert H. Lasseter and Paolo Piagi. Control and design of microgrid components. Technical report, University of Wisconsin, Madison, 01/2006 2006.

[57] Ruiqi LI, Hua GENG, and Geng YANG. Fault ride-through of renewable energy conversion systems during voltage recovery. *Journal of Modern Power Systems and Clean Energy*, 4(1):28–39, Jan 2016. ISSN 2196-5420. doi: 10.1007/s40565-015-0177-0. URL https://doi.org/10.1007/s40565-015-0177-0.

[58] J Pedro Lopes, C. L. Moreira, and A. G. Madureira. Defining control strategies for microgrids islanded operation. *IEEE Transactions on Power Systems*, 21:916–924, 2006.

[59] Jason M. Macdowell, Kara Clark, Nicholas W. Miller, and Juan J. Sanchez-Gasca. Validation of ge wind plant models for system planning simulations. *2011 IEEE Power and Energy Society General Meeting*, 2011. doi: 10.1109/pes.2011.6039485.

[60] Ndreko Mario. Offshore wind plants with vsc-hvdc connection and their impact on the power system stability: Modeling and grid code compliance, delft university of technology, 2016.

[61] Jorun I. Marvik and Harald G. Svendsen. Analysis of grid faults in offshore wind farm with hvdc connection. *Energy Procedia*, 35:81 – 90, 2013. ISSN 1876-6102. doi: https://doi.org/10.1016/j.egypro.2013.07.161. URL http://www.sciencedirect.com/science/article/pii/S1876610213012472. DeepWind'2013 – Selected papers from 10th Deep Sea Offshore Wind R&D Conference, Trondheim, Norway, 24 – 25 January 2013.

[62] J.m. Mauricio, A. Marano, A. Gomez-Exposito, and J.l. Martinez Ramos. Frequency regulation contribution through variable-speed wind energy conversion systems. *IEEE Transactions on Power Systems*, 24(1):173–180, 2009. doi: 10.1109/tpwrs.2008.2009398.

[63] H2020 Migrate Project. Deliverable 1.1: Report on systemic issues, 2016. URL https://www.h2020-migrate.eu/downloads.html.

[64] A. Morched, B. Gustavsen, and M. Tartibi. A universal model for accurate calculation of electromagnetic transients on overhead lines and underground cables. *IEEE Transactions on Power Delivery*, 14(3):1032–1038, July 1999. ISSN 0885-8977. doi: 10.1109/61.772350.

[65] Bardia Motamed. The effect of high penetration of wind power on primary frequency control of power systems, Oct 2013. URL https://pdfs.semanticscholar.org/600d/8812b363016ab891abf2c41fe112f74a49c6.pdf.

[66] M. Ndreko, A. A. van der Meer, M. Gibescu, and M. A. M. M. van der Meijden. Impact of dc voltage control parameters on ac/dc system dynamics under faulted conditions. In *2014 IEEE PES General Meeting | Conference Exposition*, pages 1–5, July 2014. doi: 10.1109/PESGM.2014.6939233.

[67] Mario Ndreko. Migrate – massive integration o f power electronic devices.

[68] Mario Ndreko. Dynamic stability at high variable renewable energy system penetration, June 2018.

[69] Mario Ndreko, Marjan Popov, and Mart A.M.M. van der Meijden. Study on frt compliance of vsc-hvdc connected offshore wind plants during ac faults including requirements for the negative sequence current control. *International Journal of Electrical Power & Energy Systems*, 85:97 – 116, 2017. ISSN 0142-0615. doi: https://doi.org/10.1016/j.ijepes.2016.08.009. URL http://www.sciencedirect.com/science/article/pii/S014206151630758X.

[70] Mario Ndreko, Sven Rüberg, and Wilhelm Winter. Grid forming control for stable power systems with up to 100 % inverter based generation: A paradigm scenario using the ieee 118-bus system. 10 2018.

[71] T. Neumann, I. Erlich, B. Paz, A. Korai, M. Koochack Zadeh, S. Vogt, C. Buchhagen, C. Rauscher, A. Menze, J. Jung, and et al. Novel direct voltage control by wind turbines. *2016 IEEE Power and Energy Society General Meeting (PESGM)*, 2016. doi: 10.1109/pesgm.2016.7741744.

[72] Leonel Noris, J L Rueda, Elyas Rakhshani, and A W Korai. Power system black-start and restoration with high share of power-electronic converters. 01 2019.

[73] Leonel Noris Martinez. Modelling and assessment of restoration in electrical power systems with high penetration of power electronic converters, Oct 2018. URL http://resolver.tudelft.nl/uuid:2e6cc09f-3288-4522-8b94-86c82f251eb9.

[74] Józef Paska, Mariusz Kłos, Łukasz Rosłaniec, and Karol Pawlak. Hvdc converter stations to enable offshore wind farm integration with power system. *Acta Energetica*, 2/27:127–132, 08 2016. doi: 10.12736/issn.2300-3022.2016211.

[75] H. Polinder. Delftx: Energyx sustainable energy: Design a renewable future. URL https://courses.edx.org/courses/course-v1:DelftXEnergyX3T2017/course/#block-v1:DelftXEnergyX3T2017type@sequentialblock@bc9d6f14c0904ffe9554c74f847911fe.

[76] M. Pucci and M. Cirrincione. Neural mppt control of wind generators with induction machines without speed sensors. *IEEE Transactions on Industrial Electronics*, 58(1):37–47, Jan 2011. ISSN 0278-0046. doi: 10.1109/TIE.2010.2043043.

[77] Elyas Rakhshani and Pedro Rodriguez. Inertia emulation in ac/dc interconnected power systems using derivative technique considering frequency measurement effects. *IEEE Transactions on Power Systems*, 32(5):3338–3351, 2017. doi: 10.1109/tpwrs.2016.2644698.

[78] Elyas Rakhshani, Daniel Remon, Antoni Mir Cantarellas, Jorge Martinez Garcia, and Pedro Rodriguez. Virtual synchronous power strategy for multiple hvdc interconnections of multi-area agc power systems. *IEEE Transactions on Power Systems*, 32(3):1665–1677, 2017. doi: 10.1109/tpwrs.2016.2592971.

[79] J. Rocabert, A. Luna, F. Blaabjerg, and P. Rodríguez. Control of power converters in ac microgrids. *IEEE Transactions on Power Electronics*, 27(11):4734–4749, Nov 2012. ISSN 0885-8993. doi: 10.1109/TPEL.2012.2199334.

[80] T. Sebastian and G.r. Slemon. Transient modeling and performance of variable-speed permanent-magnet motors. *IEEE Transactions on Industry Applications*, 25(1):101–106, 1989. doi: 10.1109/28.18878.

[81] Lei Shang, Jiabing Hu, Xiaoming Yuan, and Yongning Chi. Understanding inertial response of variable-speed wind turbines by defined internal potential vector. *Energies*, 10(1):22, 2016. doi: 10.3390/en10010022.

[82] F. Shewarega, I. Erlich, and J. L. Rueda. Impact of large offshore wind farms on power system transient stability. In *2009 IEEE/PES Power Systems Conference and Exposition*, pages 1–8, March 2009. doi: 10.1109/PSCE.2009.4840006.

[83] Constantinos Sourkounis and Pavlos Tourou. Grid code requirements for wind power integration in europe. *Conference Papers in Medicine*, 2013:1–9, 06 2013. doi: 10.1155/2013/437674.

[84] N. P. W. Strachan and D. Jovcic. Stability of a variable-speed permanent magnet wind generator with weak ac grids. *IEEE Transactions on Power Delivery*, 25(4):2779–2788, Oct 2010. ISSN 0885-8977. doi: 10.1109/TPWRD.2010.2053723.

[85] E Telaretti, G Graditi, Mariano Ippolito, and Gaetano Zizzo. Economic feasibility of stationary electrochemical storages for electric bill management applications: The italian scenario. *Energy Policy*, 94:126–137, 07 2016. doi: 10.1016/j.enpol.2016.04.002.

[86] Jogendra Singh Thongam and Mohand Ouhrouche, Jun 2011. URL http://cdn.intechopen.com/pdfs/16255/intech-mppt_control_methods_in_wind_energy_conversion_systems.pdf.

[87] Puyu WANG, Xiao-Ping ZHANG, Paul F. COVENTRY, and Zhou LI. Control and protection strategy for mmc mtdc system under converter-side ac fault during converter blocking failure. *Journal of Modern Power Systems and Clean Energy*, 2(3):272–281, Sep 2014. ISSN 2196-5420. doi: 10.1007/s40565-014-0064-0. URL https://doi.org/10.1007/s40565-014-0064-0.

[88] Puyu Wang, Xiao-Ping Zhang, Paul F. Coventry, and Ray Zhang. Start-up control of an offshore integrated mmc multi-terminal hvdc system with reduced dc voltage. *IEEE Transactions on Power Systems*, 31(4):2740–2751, 2016. doi: 10.1109/tpwrs.2015.2466600.

[89] Yingjie Wang, Bo Yang, Huifang Zuo, Haiyuan Liu, and Haohao Yan. A dc short-circuit fault ride through strategy of mmc-hvdc based on the cascaded star converter. *Energies*, 11(8):2079, Oct 2018. doi: 10.3390/en11082079.

[90] Will. Wind vs solar – which green energy is winning?, Aug 2017. URL https://compareyourfootprint.com/wind-vs-solar-green-energy-winning/.

[91] Venkata Yaramasu, Bin Wu, Paresh C Sen, Samir Kouro, and Mehdi Narimani. High-power wind energy conversion systems: State-of-the-art and emerging technologies. *Proceedings of the IEEE*, 103:740 – 788, 05 2015. doi: 10.1109/JPROC.2014.2378692.

[92] M. A. Zamani, A. Yazdani, and T. S. Sidhu. A control strategy for enhanced operation of inverter-based microgrids under transient disturbances and network faults. *IEEE Transactions on Power Delivery*, 27(4):1737–1747, Oct 2012. ISSN 0885-8977. doi: 10.1109/TPWRD.2012.2205713.

[93] Lorenzo Zeni. Power oscillation damping from vsc-hvdc-connected offshore wind power plants. *Modeling and Modern Control of Wind Power*, page 233–256, 2017. doi: 10.1002/9781119236382.ch12.

[94] Lidong Zhang. *Modeling and control of VSC-HVDC links connected to weak AC systems*. PhD thesis, Royal Institute of Technology, Stockholm, Sweden, 2010.

[95] Q. Zhong and G. Weiss. Synchronverters: Inverters that mimic synchronous generators. *IEEE Transactions on Industrial Electronics*, 58(4):1259–1267, April 2011. ISSN 0278-0046. doi: 10.1109/TIE.2010.2048839.

[96] Markel Zubiaga, Gonzalo Abad, Jon Andoni, Sergio Aurtenetxea, and Ainhoa Crcar. Evaluation of the frequency response of ac transmission based offshore wind farms. *Wind Farm - Impact in Power System and Alternatives to Improve the Integration*, 2011. doi: 10.5772/17779.

Appendices

APPENDIX -A

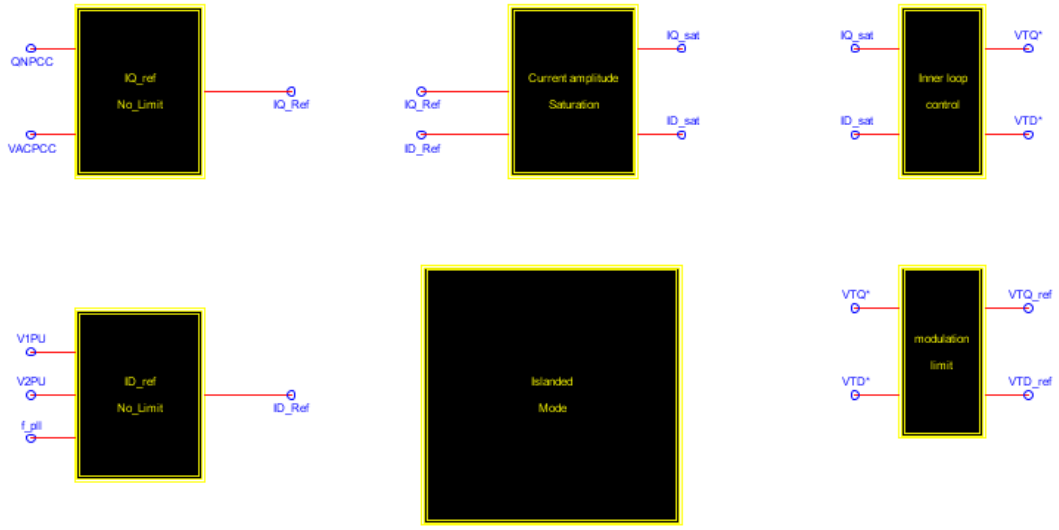

Figure 1: Grid Forming control as implemented on RSCAD

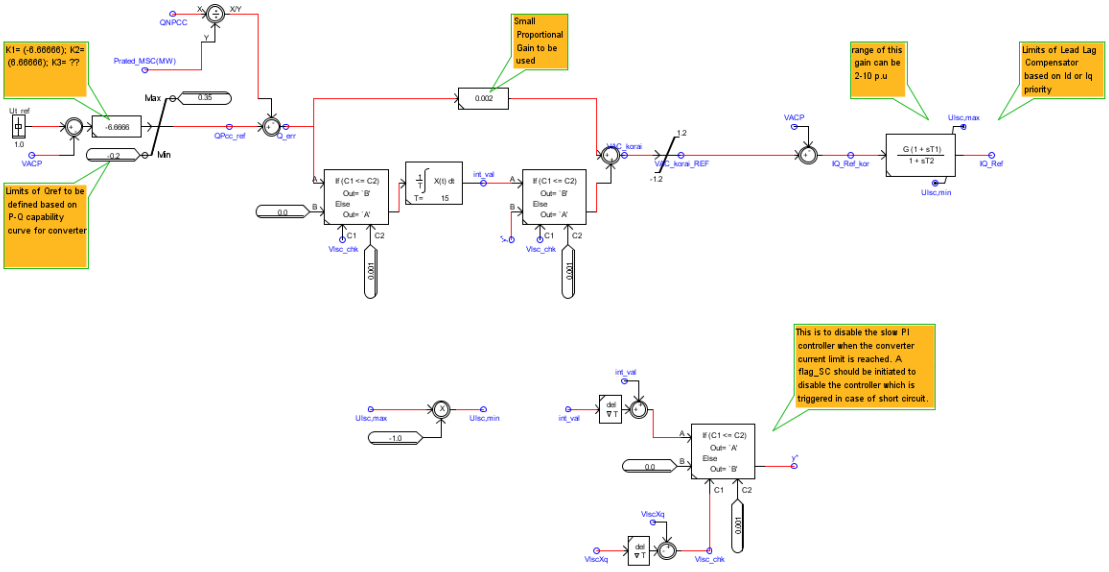

Figure 2: Controller implementation for generating i_q, ref

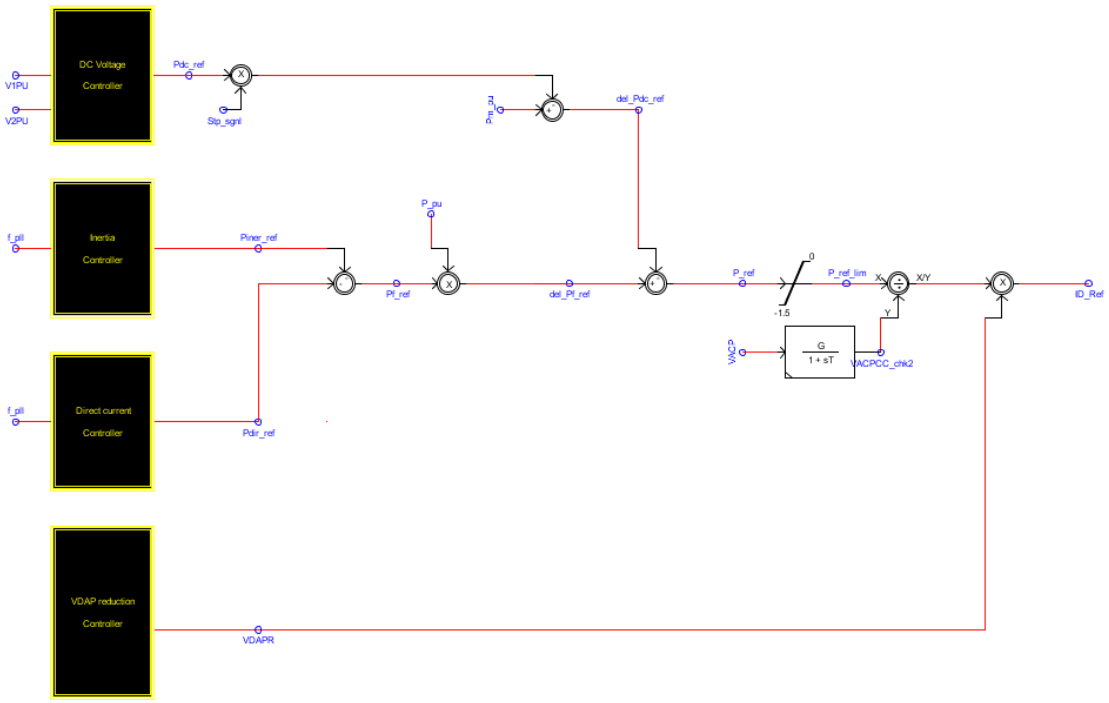

Figure 3: Controller implementation for generating i_d, ref

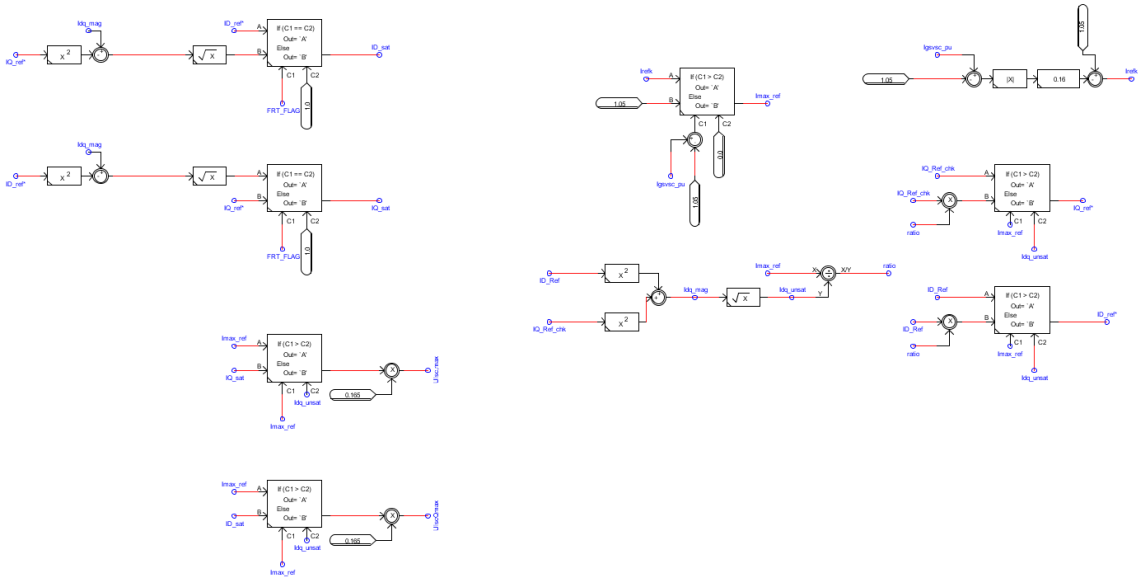

Figure 4: Current limitation block for limiting converter output current

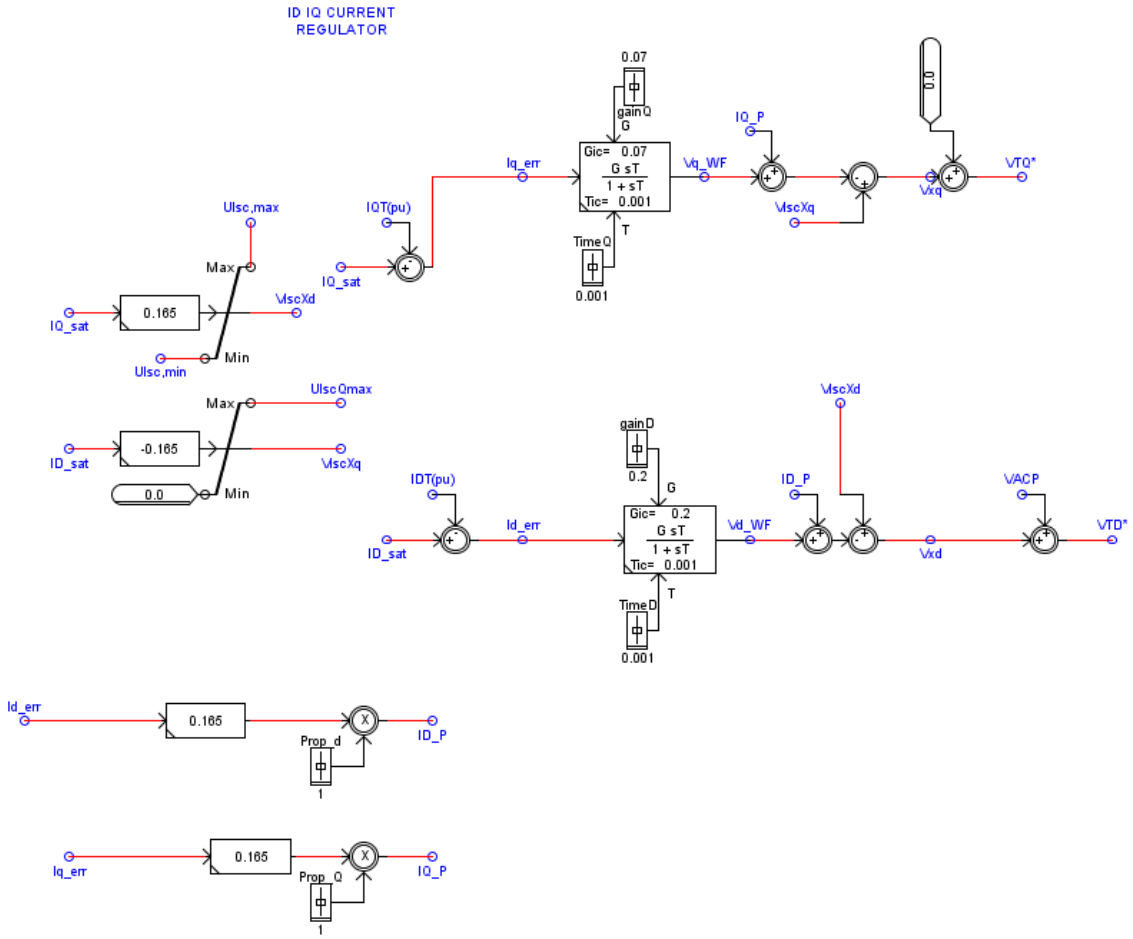

Figure 5: Inner control loop using washout filters

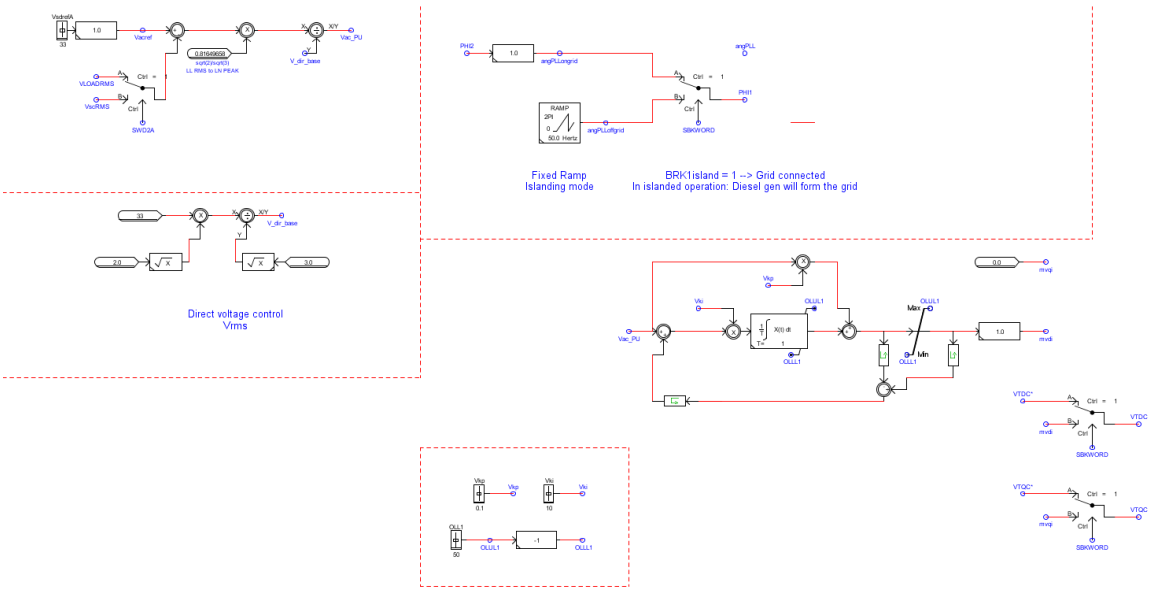

Figure 6: Control modification for Standalone Operation

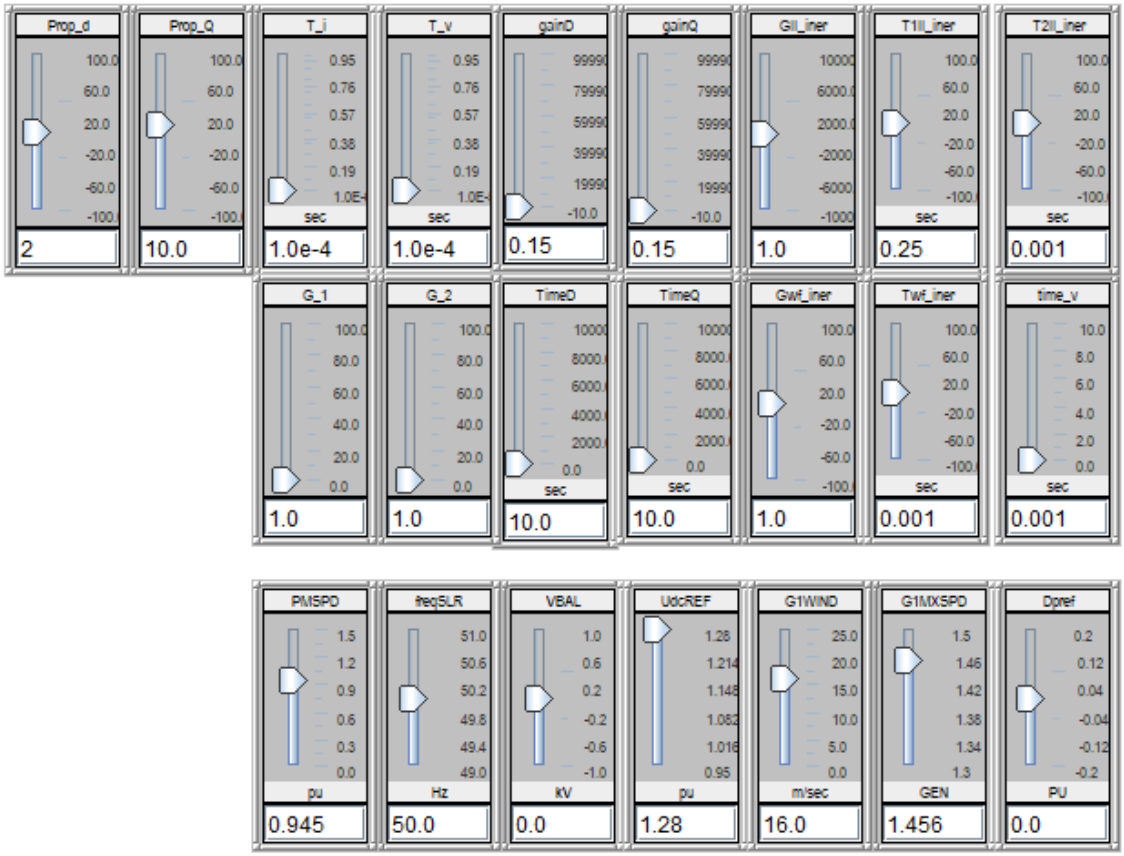

Figure 7: Runtime Screen for tuning the parameters of measurement filters as well as washout filters